

**NEUROINFLAMMATORY CONDITIONS MODULATE ARNT2 AND RME-8
EXPRESSION WITHIN THE CNS**

by

Adam Christopher Yu

B.MLSc., The University of British Columbia, 2014

A THESIS SUBMITTED IN PARTIAL FULFILLMENT OF
THE REQUIREMENTS FOR THE DEGREE OF

MASTER OF SCIENCE

in

THE FACULTY OF GRADUATE AND POSTDOCTORAL STUDIES
(Pathology and Laboratory Medicine)

THE UNIVERSITY OF BRITISH COLUMBIA

(Vancouver)

July 2016

© Adam Christopher Yu, 2016

Abstract

Microglia are the primary immune cells found within the central nervous system (CNS), playing a vital role in neuronal function, trophic support and also modulating immune or inflammatory responses to pathogens or damage during disease. Microglia are essential to repair processes influencing axonal health and remyelination. However, the study of microglia is limited as significant yields of microglia through tissue culture are difficult to obtain. We show that the addition of granulocyte macrophage colony-stimulating factor (GM-CSF) during the culture of embryonic microglia yields significantly greater cell numbers. GM-CSF cultured microglia exhibit a non-differentiated phenotype similar to *in vivo* microglia and represent a useful model for disease and reparative processes in the CNS.

Using our primary microglial model, we investigated two proteins, Aryl hydrocarbon receptor nuclear translocator 2 (ARNT2) and receptor-mediated endocytosis – 8 (RME-8). ARNT2, a transcription factor for several proteins but most notably for the neuronal growth factor, brain derived neurotrophic factor (BDNF), has been primarily studied in neurons. Our studies show regulation of ARNT2 in astrocytes and immune cells (microglia and splenocytes) under inflammatory conditions. In the experimental autoimmune encephalomyelitis (EAE) model, splenocytes exhibited lower ARNT2 expression than those from healthy controls.

Lipopolysaccharide and interferon- γ increased otherwise low ARNT2 expression in microglia.

RME-8 is a protein that is important in endosomal trafficking. Mutations in RME-8 have been linked to Parkinson's disease and essential tremor. However, RME-8 has yet to be characterized

within the CNS. Motor neurons, astrocytes and ependymal cells expressed RME-8 in healthy control mice; RME-8 was increased and co-localized with CD68 positive cells in immune infiltrates in EAE mice. Our results show the uptake of dextran in RME-8 mutant knock-in microglia is decreased, indicating the importance of this protein in phagocytic processes.

These results show that microglia can be effectively cultured from embryonic tissue with the addition of GM-CSF in comparison to previously established protocols and are similar to microglia *in vivo*. Furthermore, inflammatory mediators influence expression of ARNT2 and RME-8 and may highlight roles for each in neuroprotection or phagocytic function respectively, thereby influencing inflammatory neurodegenerative or reparative processes relevant to several diseases in the CNS.

Preface

A version of Chapter 2 has been submitted as: [Yu, AC]; Neil, SE; Quandt, JA (2016). High yield primary microglial cultures for functional studies related to reparative or pathological processes relevant to neurodegeneration. [Manuscript submitted]. I performed the cell culture, immunocytochemistry and cytokine ELISAs as well as the majority of the flow cytometry experiments and conducted data collection and analyses. I also developed and performed the phagocytosis assay and prepared the first draft of the manuscript. Ms. Neil performed some flow cytometry experiments on primary cultures and the microglial cell line and assisted with data analyses. Dr. Quandt conceived the culture approach, oversaw the experimental approach and design, reviewed data and analyses for interpretation of the data and oversaw the manuscript preparation, as well as conducting a critical review of the manuscript for technical and scientific accuracy. All authors have reviewed the manuscript in its entirety and are in agreement with the content of this work.

All methods were carried out in accordance with the Canadian Council on Animal Care regulations and all experimental protocols were approved by the University of British Columbia Animal Care Committee (Certificate number: A130281).

The projects outlined in this thesis were designed in collaboration with Dr. Jacqueline Quandt. I carried out and analyzed all experiments except for the EAE experiment where Dr. Quandt performed the EAE induction, animal scoring and care, euthanasia, and tissue collection.

Table of Contents

Abstract.....	ii
Preface.....	iv
Table of Contents	v
List of Tables	x
List of Figures.....	xi
List of Abbreviations	xiii
Acknowledgements	xvii
Dedication	xviii
Chapter 1: Introduction	1
1.1 Glial cells	1
1.1.1 Astrocytes	1
1.1.2 Microglia.....	2
1.2 Neurodegeneration of the CNS.....	4
1.2.1 The role of inflammation in CNS injury and disease	5
1.2.2 The role of inflammation in CNS repair.....	6
1.2.3 Multiple sclerosis.....	7
1.2.4 Experimental autoimmune encephalomyelitis (EAE)	10
1.3 Neurotrophic factors in neuronal health and development	11
1.4 Aryl-hydrocarbon nuclear translocator 2 (ARNT2)	12
1.5 Receptor mediated endocytosis – 8 (RME-8).....	13
1.6 Hypothesis.....	17

1.6.1	Microglia study	17
1.6.2	ARNT2 study	18
1.6.3	RME-8 study	18
Chapter 2: High yield primary microglial cultures for functional studies related to reparative or pathological processes relevant to neurodegeneration.....19		
2.1	Introduction.....	19
2.2	Materials and methods	22
2.2.1	Microglia cell culture and treatment	22
2.2.2	Microglial stimulation.....	23
2.2.3	Flow cytometry	24
2.2.4	Immunocytochemistry	25
2.2.5	Cytokine ELISA.....	26
2.2.6	Latex bead phagocytosis assay	26
2.2.7	Statistical analysis.....	26
2.3	Results.....	27
2.3.1	GM-CSF potentiates the proliferation and differentiation of embryonic cortical cells into microglia	27
2.3.2	Microglia undergoes a characteristic morphological change when treated with lipopolysaccharide (LPS).....	27
2.3.3	Microglia cultured in GM-CSF alone and in GM-CSF with IL-4 share similar myeloid and co-stimulatory marker profiles.....	30
2.3.4	IFN- γ upregulates marker of activation Iba-1 in GM-CSF cultured microglia	35
2.3.5	Inflammatory stimuli increase microglial cytokine production.....	38

2.3.6	LPS increases while IFN- γ decreases the phagocytic capabilities of primary microglia	41
2.4	Discussion	41
Chapter 3: Investigation of the regulation of ARNT2, a neuroprotective transcription factor, in models of inflammatory neurodegenerative disease		
46		
3.1	Introduction.....	46
3.2	Materials and methods	48
3.2.1	Primary microglia cultures and stimulation	48
3.2.2	Primary astrocyte cultures.....	49
3.2.3	Experimental autoimmune encephalomyelitis induction.....	49
3.2.4	Spleen lysates.....	50
3.2.5	Immunohistochemistry	50
3.2.6	Lysate preparation and protein quantification	53
3.2.7	SDS-PAGE and Western blot.....	54
3.2.8	Statistical analysis.....	54
3.3	Results.....	55
3.3.1	ARNT2 is upregulated in primary microglia when stimulated with LPS or IFN- γ ..	55
3.3.2	Splenocytes decrease ARNT2 expression in CFA-injected and EAE-induced mice	55
3.3.3	TNF- α and IFN- γ treatment does not alter ARNT2 expression in primary astrocytes.	55
3.3.4	ARNT2 is upregulated in GFAP positive astrocytes in EAE	59
3.4	Discussion	64
3.5	Limitations	66

3.6	Future directions	67
Chapter 4: Receptor Mediated Endocytosis – 8 expression within the CNS.....		70
4.1	Introduction.....	70
4.2	Materials and methods.....	72
4.2.1	Primary microglia and astrocyte cultures	72
4.2.2	Human cerebral microvascular endothelial cell line (hCMEC/D3) cultures	72
4.2.3	Primary mouse lung fibroblasts	72
4.2.4	Oregon Green® dextran phagocytosis assay	73
4.2.5	Flow cytometry.....	73
4.2.6	Spleen lysates.....	74
4.2.7	Lysate preparation and protein quantification	74
4.2.8	SDS-PAGE and Western blot.....	74
4.2.9	EAE induction.....	75
4.2.10	Immunohistochemistry	76
4.2.11	Statistical analysis.....	77
4.3	Results.....	77
4.3.1	RME-8 is highly expressed in primary microglia.....	77
4.3.2	Microglia derived from wild type and RME-8 mutant knock-in mice react similarly to treatment with LPS and IFN- γ	79
4.3.3	RME-8 deficient microglia have reduced ability to phagocytose Oregon Green® dextran.....	79
4.3.4	RME-8 expression remains constant in EAE-induced mouse spleens	82
4.3.5	Neither TNF- α nor IFN- γ affect RME-8 expression in astrocytes	82

4.3.6 RME-8 mutant mice tend to have less severe clinical disease when immunized for EAE	85
4.3.7 RME-8 is expressed in neurons, astrocytes, and ependymal cells in healthy spinal cord tissue and in CD68 positive immune infiltrates in EAE mice	85
4.4 Discussion	89
4.5 Limitations	92
4.6 Future directions	92
Chapter 5: Conclusion.....	95
5.1 Summary	95
5.2 Impact	96
References.....	99

List of Tables

Table 2.1 Primary microglia vs. cell line phenotype	32
Table 2.2 Primary GM-CSF microglial surface marker expression in response to LPS and IFN- γ	34
Table 2.3 BV-2 surface marker expression in response to LPS and IFN- γ	36
Table 3.1 EAE mouse clinical scoring guide (Quandt Lab, unpublished data).....	51

List of Figures

Figure 1.1 <i>Arnt2</i> and <i>Bdnf</i> gene expression over the course of EAE	14
Figure 1.2 ARNT2 expression is enhanced in the white matter of EAE spinal cords.....	15
Figure 2.1 GM-CSF addition enables the establishment of high yields of purified microglia from mouse.....	28
Figure 2.2 LPS treatment modifies microglial morphology	29
Figure 2.3 Phenotypic comparison of primary microglia vs. cell line.....	31
Figure 2.4 GM-CSF microglia differentially upregulate phenotypic and co-stimulatory markers when treated with IFN- γ and LPS.....	33
Figure 2.5 Primary microglia express the activation marker Iba-1	37
Figure 2.6 LPS significantly upregulates several cytokines in both primary cultures and cell lines	39
Figure 2.7 Inflammatory factors alter the phagocytic capacity of primary GM-CSF microglia ..	42
Figure 3.1 Primary microglia increase ARNT2 expression with exposure to inflammatory mediators.....	56
Figure 3.2 Inflammatory conditions decreased ARNT2 expression in spleens.....	57
Figure 3.3 TNF- α and IFN- γ did not affect ARNT2 expression in primary astrocytes.....	58
Figure 3.4 Average EAE score over 60 days.....	60
Figure 3.5 ARNT2 positivity and expression changes within white matter GFAP+ astrocytes ..	61
Figure 3.6 Astrocyte numbers increased in the grey matter of EAE mice	62
Figure 3.7 ARNT2 positive astrocytes accumulate in the grey matter of EAE mouse spinal cords	63

Figure 4.1 RME-8 is expressed in several CNS related cell types	78
Figure 4.2 Wild type and RME-8 mutant knock-in microglia exhibit no change in inflammatory marker expression patterns	80
Figure 4.3 RME-8 mutant microglia have decreased phagocytosis of Oregon Green® dextran .	81
Figure 4.4 No changes in RME-8 expression was seen between healthy, CFA only, and EAE mouse spleens	83
Figure 4.5 Inflammatory cytokines IFN- γ and TNF- α did not alter RME-8 expression in astrocytes.....	84
Figure 4.6 EAE disease scores were decreased in RME-8 mutant knock-in mice	86
Figure 4.7. Neurons, astrocytes, and ependymal cells express RME-8	87
Figure 4.8. CD68 positive cells express RME-8.....	88

List of Abbreviations

ADP	Adenosine diphosphate
AhR	Aryl hydrocarbon receptor
Arg	Arginine
ARNT2	Aryl hydrocarbon receptor nuclear translocator 2
ARTN	Artemin
ATP	Adenosine triphosphate
BDNF	Brain-derived neurotrophic factor
bHLH-PAS	Basic helix-loop-helix-PER-ARNT-SIM
cAMP	Cyclic adenosine monophosphate
CCL2	Chemokine (C-C motif) ligand 2
CD	Cluster of differentiation
CFA	Complete Freund's adjuvant
CNS	Central nervous system
CNTF	Ciliary neurotrophic factor
CSF	Colony stimulating factor
DAPI	4',6-diamidino-2-phenylindole
DIV	Day <i>in vitro</i>
DMEM	Dulbecco's modified eagle medium
EAE	Experimental autoimmune encephalomyelitis
ECL	Enhanced chemiluminescence

EGM	Endothelial cell growth medium
FACS	Fluorescence-activated cell sorting
FBS	Fetal bovine serum
FITC	Fluorescein isothiocyanate
GAPDH	Glyceraldehyde 3-phosphate dehydrogenase
GDNF	Glial cell-line derived neurotrophic factor
GFAP	Glial fibrillary acidic protein
Glu	Glutamic acid
GM-CSF	Granulocyte macrophage colony-stimulating factor
HAPI	Highly aggressively proliferating immortalized
HBSS	Hank's balanced salt solution
hCMEC/D3	Human cerebral microvascular endothelial cell
HIF-1 α	Hypoxia-inducible factor 1-alpha
HLA	Human leukocyte antigen
HRP	Horseradish peroxidase
Hsp40	Heat shock protein 40
Iba-1	Ionized calcium-binding adaptor molecule 1
IFN- γ	Interferon gamma
IgG	Immunoglobulin G
IL	Interleukin
IFA	Incomplete Freund's adjuvant
iNOS	Inducible nitric oxide synthase

IP	Intraperitoneal
LPS	Lipopolysaccharide
Lys	Lysine
MAP2	Microtubule-associated protein 2
MFI	Median fluorescence intensity
MBP	Myelin basic protein
MHC	Major histocompatibility complex
MOG	Myelin oligodendrocyte glycoprotein
MRI	Magnetic resonance imaging
MS	Multiple sclerosis
NRTN	Neurturin
NT-3	Neurotrophin-3
OCT	Optimal cutting temperature compound
PBMC	Peripheral blood mononuclear cell
PBS	Phosphate buffered saline
PLP	Myelin proteolipid protein
PSPN	Persephin
RIPA	Radioimmunoprecipitation assay
RME-8	Receptor-mediated endocytosis 8
RNS	Reactive nitrogen species
ROS	Reactive oxygen species
RPM	Revolutions per minute

SDS-PAGE	Sodium dodecyl sulphate polyacrylamide gel electrophoresis
SIM1	Single-minded homolog 1
TCDD	2,3,7,8-Tetrachlorodibenzo- <i>p</i> -dioxin
T _h 1	Type 1 T helper cell
T _h 2	Type 2 T helper cell
T _h 17	T helper 17 cell
TLR4	Toll-like receptor 4
TNF- α	Tumor necrosis factor alpha
Trk	Tropomyosin receptor kinase
Tyr	Tyrosine
WASH	Wiskott-Aldrich syndrome protein and SCAR homolog

Acknowledgements

I would like to acknowledge the current members of the Quandt lab (Tissa Rahim and Cheryl Whiting) and previous members (Sarah Neil, Negar Farzam-Kia, Katerina Othonos, Jolin Lu, and Andrew Leung) for their support and friendship throughout my degree. I would also like to acknowledge Drs. Matthew Farrer and Austen Milnerwood (University of British Columbia) for providing the mutant RME-8 knock-in mice and RME-8 antibody. I would also like to acknowledge Daisy Cao, for her continued technical support and assistance with tissue culturing. I would like to acknowledge Amanda Davison for editing my thesis and making it legible as well as for supporting me throughout my degree.

I would like to thank my supervisor Dr. Jacqueline Quandt and my supervisory committee members Dr. Neil Cashman, Dr. Marc Horwitz, and Dr. Wayne Moore, Dr. Susan Porter, for their mentorship, guidance, and continued support.

I would like to acknowledge stipend support from the UBC MS Renewal Program fund established by the Milan and Maureen Ilich Foundation, as well as partial support from an MS Society of Canada operating grant to Dr. Jacqueline Quandt to examine neuroprotective factors in models of MS.

Lastly, special thanks are owed to my family, where without their support and guidance, I would not be where I am today.

Dedication

To Sarah Elizabeth “Giant God of Time” Neil, you cunning, pliable, chestnut-haired sunfish.

You’ll forever be 15. Rest in peace.

Chapter 1: Introduction

1.1 Glial cells

The central nervous system (CNS) consists of a heterogeneous population of cells where glial cells outnumber neurons 50 to 1¹. Of these glial cells, astrocytes make up 20 to 40% of all glia while microglia make up 10-20% of all cells within the brain^{2,3}. Microglia are the main myeloid-derived immune cell found in the brain and spinal cord⁴. During embryogenesis, microglial progenitor cells infiltrate the brain from the yolk sac⁵. Microglia are important in supporting neuronal function and survival by clearing foreign pathogens and responding to insults within the CNS⁶. Astrocytes are essential in the maintenance and support of the blood-brain barrier and also provide trophic, metabolic, and structural support for neurons⁷. Oligodendrocytes are another type of glia with their main function being the myelination of axons within the CNS⁸. Consequently, oligodendrocytes are crucial to the functioning of the CNS by decreasing capacitance and increasing overall electrical resistance across the axolemma, necessary for adequate propagation of nerve impulses and saltatory conduction⁸. Other supporting glial cells include ependymal cells that are important in the movement and secretion of cerebrospinal fluid for the clearance of metabolic waste⁹. Ependymal cells line the central canal and the ventricular system⁹. The last glial cell of the CNS is the radial glial cell. Radial glial cells are bipolar in morphology and are the primary progenitor cells that can differentiate and give rise to neurons, astrocytes, and oligodendrocytes¹⁰.

1.1.1 Astrocytes

Astrocytes are able to regulate the blood-brain barrier by extending perivascular endfeet that surround the microvasculature forming the glial limitans¹¹. The glial limitans form a

physical barrier that prevents the entry of various molecules into the CNS and can upregulate the expression of tight junction proteins between endothelial cells during brain development¹². Neurons are able to communicate and connect with astrocytes where the release of neurotransmitters into the synaptic cleft can be taken up by astrocytes assisting with proper synaptic functioning by metabolizing neurotransmitters¹³. Astrocytes also have the ability to undergo glycogenesis. This allows them to create large stores of glycogen for later release as glucose to support neurons during periods that require high rates of glucose metabolism or periods of glucose shortage^{14,15}. Astrocytes further support the function of neurons by taking up excess potassium ions in the extracellular space to prevent inappropriate depolarization of neurons¹⁶. In several neuropathological conditions, astrocytes become activated and begin to rapidly proliferate which upregulates the synthesis of intermediate filaments such as glial fibrillary acidic protein (GFAP) in response to damage in the CNS¹⁷⁻²⁰. This allows for gliosis to take place: the formation of a glial scar where glial processes extend into regions of neurodegeneration after a pathological event¹⁷. Predominantly, astrocytes are identified histologically by GFAP expression. While not all types of astrocytes constitutively express GFAP, it remains the primary stain to identify or localize their presence in analyses of tissues in pathological analyses both in experimental as well as in clinical settings¹⁷.

1.1.2 Microglia

Microglia are the sensors of pathological events within the CNS. Microglia are able to undergo phenotypic changes under several CNS conditions and diseases, becoming intensely ramified and positive for the expression of ionized-calcium binding adaptor molecule 1 (Iba-1), a classic marker of microglial activation²¹. Microglia can be characterized by their state of

activation, reflected by changes in morphology and the production of inflammatory mediators. Amoeboid microglia are round in shape with small processes and are motile for scavenging debris for phagocytosis²². Quiescent ramified microglia have thin branching processes throughout the neuropil of the CNS. Quiescent ramified microglia will undergo a morphological change where their processes are retracted and thickened upon activation.

Changes within the extracellular matrix through the release of various factors including potassium and adenosine triphosphate (ATP) from damaged neurons are able to activate microglia²³. Once activated, microglia are able to secrete several inflammatory cytokines including interferon-gamma (IFN- γ), tumor necrosis factor-alpha (TNF- α), and interleukin 1-beta (IL-1 β), and reactive oxygen (ROS) and nitrogen species (RNS) such as hydroxyl radicals and nitric oxide^{24,25}. The subsequent release of these inflammatory mediators, just as in the periphery, plays an important role in regulating the reparative process of the CNS after injury. The phagocytosis of apoptotic cells, cellular debris, invading bacteria or viruses, or other foreign materials is crucial to allow the CNS to return back to healthy conditions²⁶.

Activated microglia have been found to play a role in plaque formation, dystrophic neurite growth, and excessive tau phosphorylation that worsens disease conditions in several neurodegenerative disorders²⁷. The sustained release of ROS results in oxidative stress where the excess formation of peroxides and free radicals can damage and disrupt cellular components. This includes proteins, lipids, and DNA which initially alter cell function but over time, causes neurodegeneration and ultimately cell death²⁸.

In order to understand and characterize the function of microglia, the ability to isolate and culture these cells is an area of great importance. The establishment of primary cultures that most accurately reflect the morphology and function seen *in vivo* is considered more pertinent than

immortal cell lines which have undergone significant mutation or selection via passaging in order to be immortalized. Current methods for the isolation of primary microglia require a relatively high volume of cerebral tissue relative to the number of microglia yielded.

Consequently, a method that reduces the amount of nervous tissues needed with a higher yield and purity of microglia is crucial to advance the research and further our understanding of the role of microglia in disease pathogenesis.

A potential method to improve the number of microglia yielded for *in vitro* studies can be achieved through growth factors such as colony stimulating factors (CSF) to stimulate proliferation and differentiation^{29,30}. Granulocyte macrophage colony stimulating factor (GM-CSF), a protein that belongs to the family of CSFs, promotes the proliferation of myeloid derived cells including granulocytes in the lymphoid organs, or in the CNS, microglia, and has been used previously to culture bone marrow-derived dendritic cells^{31,32}.

1.2 Neurodegeneration of the CNS

There are several different factors as well as processes that contribute to neurodegeneration within the CNS, such as protein misfolding, mitochondrial dysfunction, genetic predisposition, and aging³³. Protein misfolding results in several different proteopathic neurodegenerative diseases such as Alzheimer's, Parkinson's, amyotrophic lateral sclerosis, and prion disease³⁴. In several of these conditions the accumulation and aggregation of misfolded proteins such as α -synuclein, tau, and β -amyloid within neurons can cause toxicity³⁴. Misfolded α -synuclein can cause neuronal toxicity through the damaging of the cell membrane causing vesiculation and membrane curvature³⁵.

Mitochondrial dysfunction has also been linked to neurodegeneration where dysfunction can result in the excess formation of intracellular ROS and subsequent oxidative stress²⁸. Oxidative stress can then go on to damage intracellular organelles resulting in cell death by the induction of apoptotic pathways through an influx of calcium into the cytoplasm of the cell^{28,36,37}. Mitochondrial dysfunction has also been linked to energy imbalances where glutamate excitotoxicity depletes cellular ATP resulting in the induction of cellular necrosis³⁸. Glutamate excitotoxicity is thought to play a role in multiple sclerosis (MS) pathogenesis^{39,40}.

The alteration and disruption of axonal transport can also result in neurodegeneration. The disruption of axonal transport proteins kinesin, dynein, and microtubule-associated proteins can result in the accumulation of vesicles and organelles and can be caused by tau accumulation^{41,42}. Disruption to axonal transport can also result in Wallerian degeneration⁴³. Wallerian degeneration occurs when the axon is cut and is separated from the cell body causing the endoplasmic reticulum and neurofilaments to degrade, swelling of the mitochondria, and fragmentation of the remaining axon for phagocytosis⁴³.

1.2.1 The role of inflammation in CNS injury and disease

Several of these functions of both astrocytes and microglia arise as a response during neuroinflammatory and neurodegenerative conditions, including viral and bacterial infections, traumatic brain injury, or autoimmunity⁴⁴⁻⁴⁶. Microglia undergo a phenotypic change and become activated in response to invading pathogens or tissue damage resulting in the release of soluble inflammatory mediators such as inducible nitric oxide (iNOS), TNF- α , IL-1 β , IFN- γ , and CCL2^{47,48}. Although the inflammatory response is initiated to help protect and repair the CNS in traumatic or infectious conditions, the continued activation of microglia and astrocytes and the

consequent overproduction and accumulation of pro-inflammatory mediators such as ROS can ultimately lead to neurotoxicity. The accumulation of pro-inflammatory cytokines such as TNF- α has been shown to induce apoptosis of neurons through the binding of the p55 receptor⁴⁹. Sustained inflammation also results in increased complement deposition and complement-mediated damage to which neurons are highly susceptible⁴⁹⁻⁵¹. Activated microglia are major contributors to this cytokine release and subsequent direct and indirect types of damage.

RNS such as nitric oxide and peroxynitrite produced by microglia cause DNA, protein, and lipid damage that disrupt neuronal function, resulting in cell death²⁵. The presence of ROS, RNS, and also the release of cytokines can contribute to alterations and ultimately a breakdown of the blood-brain barrier⁵². These factors increase its permeability, as well as cause the upregulation of adhesion molecules that are important in leukocyte-endothelial cell migration⁵². This allows for the infiltration by other immune cells such as T cells, B cells, and macrophages, which can exacerbate certain inflammatory neurodegenerative diseases such as in multiple sclerosis (MS)⁵³⁻⁵⁵.

1.2.2 The role of inflammation in CNS repair

Although inflammation in the CNS can result in the development of several neurodegenerative processes, inflammation is also beneficial and imperative for the repair and restoration of the CNS. In response to a brain insult, astrocytes become activated, extending their processes into the site of tissue damage, releasing cytokines¹⁷. Astrocytes also contribute to the formation of the glial scar¹⁷. Although the formation of the glial scar inhibits axonal regeneration and remyelination, neuronal loss is increased when this process is inhibited, suggesting that glial

scars are somewhat neurotrophic⁵⁶. Glial scarring also allows for the repair of the blood-brain barrier and axonal remyelination⁵⁶.

Microglia have been shown to be important in the repair of the CNS. The phagocytosis of cellular debris at the site of tissue damage plays a fundamental role in the reorganization of neuronal circuits and the initiation of neuronal repair²⁶. Microglia are also able to secrete cytokines and chemokines that are important in the recruitment of oligodendrocyte precursor cells to the site of axonal damage enhancing remyelination⁵⁷.

1.2.3 Multiple sclerosis

MS is a disease of the CNS that can result in motor, vision, and speech impairment, cognitive dysfunction, ataxia, and paralysis and is a classic example of inflammatory neurodegeneration⁵⁸. Canada has the highest incidence of MS worldwide⁵⁹; women are three times more likely to develop MS than their male counterparts⁶⁰. The cause of MS is still unknown. However, there are several factors that are thought to contribute to the onset of the disease, such as geographical location and infections involving the Epstein Barr virus⁶¹. Other factors include genetic susceptibility where human leukocyte antigen – antigen D Related (HLA-DR) variants have been associated with MS that can be influenced by various environmental factors such as smoking, stress, and exposure to toxins⁶²⁻⁶⁵. The hyperactivity of the immune system is thought to drive the pathogenesis of the disease, where autoreactive myelin-specific T cells mediate inflammation⁵⁸. T cells are thought to invade the CNS through disruptions in the blood-brain barrier and are able to recognize myelin protein as a foreign pathogen, resulting in the release of cytokines and the recruitment of other immune cells⁵⁸. Such cytokines include IFN- γ and TNF- α , which are both found in abundance in MS lesions^{66,67}. Inflammatory cells are

thought to be key contributors to oxidative stress, demyelination, and neuronal cytotoxicity^{68,69}. The activation of the iNOS pathway and the formation of nitric oxides are expressed primarily by activated microglia and macrophages, causing oxidative stress and neuronal damage²⁵. The resulting demyelination exposes the axon to these inflammatory mediators, causing axonal damage and loss, giving rise to the clinical symptoms seen in the disease⁷⁰.

The pathogenic hallmarks of MS include inflammatory infiltrates, demyelination of axons, loss of oligodendrocytes, and axonal damage and loss, resulting in the formation of plaques⁷¹. Within these MS plaques, microglia and macrophages contain phagocytosed myelin⁷². As well, a higher concentration of IFN- γ is seen within these plaques with astrocytes and microglia expressing the antigen presentation molecule MHC class II⁷³. IFN- γ is able to upregulate the expression of MHC class II and T cell co-stimulatory molecules CD80 and CD86 needed for T cell activation in microglia^{74,75}.

Currently there is no cure for MS. However, there are several treatments that slow the progression of the disease. Current therapeutics include the administering of interferon- β 1a/1b (Betaseron®), which is thought to help balance the expression of pro- and anti-inflammatory mediators and by reducing the amount of immune cells that are able to cross the blood-brain barrier^{76,77}. Glatiramer acetate, a polymer of four amino acids (Glu, Lys, Ala, and Tyr) found in myelin basic protein (MBP), is another treatment that is thought to divert the immune response and the conversion of pro-inflammatory Type 1 T helper (T_h1) cells to anti-inflammatory Type 2 T helper cell (T_h2)⁷⁸. Glatiramer acetate also downregulates IL-17 within the CNS, reducing the amount of T cells that are polarized to the pro-inflammatory and autoimmune-linked T helper 17 cell (T_h17) phenotype⁷⁹. Betaseron® and glatiramer acetate are first line therapies and have been shown to reduce relapses by 29-34%, slowing down disability progression moderately⁷⁶.

Second line therapies include natalizumab, fingolimod, and mitoxantrone. Natalizumab is a humanized monoclonal antibody against α 4-integrin and is thought to work by preventing inflammatory immune cells from adhering to the brain microvasculature^{80,81}. Natalizumab decreased the rate of relapse by 65% and reduced the risk of disability progression to 42% over two years⁸². Fingolimod decreased relapse rates by 50% over the course of a year while mitoxantrone was able to reduce the progression of disability and relapse^{83,84}. However, several of these immunomodulatory drugs have greater side effects. Natalizumab and Betaseron® have been associated with an increased risk in progressive multifocal leukoencephalopathy, while mitoxantrone use can result in cardiac toxicity and increased risk of leukemia^{85,86}.

There are several emerging monoclonal antibody therapies in the treatment of MS. Recent studies have shown that ocrelizumab, a humanized monoclonal anti-CD20 antibody that targets B cells, is effective at greatly reducing the amount of lesions seen by MRI in patients with relapsing-remitting MS and was just identified by the FDA in 2015 as the first disease modifying therapeutic indicated for progressive MS⁸⁷. Alemtuzumab is an anti-CD52 monoclonal antibody that targets lymphocytes⁸⁸. Alemtuzumab showed a reduction in relapse rates and an increase in patients who were relapse-free after 2 years in comparison to Betaseron®⁸⁹.

The majority of these therapies and treatments are currently limited to modulating and suppressing the immune system. However, there is a lack of therapies that target and improve neuroprotection, allowing for the potential remyelination, regeneration, and repair of damaged axons. Current approaches to afford neuroprotection include sodium channel blockers, nitric oxide blockers, and glutamate agonists. However, several of these compounds can cause severe toxicity^{90,91}.

1.2.4 Experimental autoimmune encephalomyelitis (EAE)

The most common model of multiple sclerosis is EAE. EAE can be induced passively or through active immunization^{92,93}. In the active immunization model EAE, mice are injected with a mixture of heat-killed *mycobacterium tuberculosis* along with myelin proteins (myelin basic protein (MBP), myelin oligodendrocyte glycoprotein (MOG), or myelin proteolipid protein (PLP)) in mineral oil, a mixture described by Jules Freund known as complete Freund's adjuvant (CFA)⁹⁴. Additional injections of pertussis toxin is used to help permeabilize the vasculature of the blood-brain barrier to allow for immune cell access to the CNS⁹⁴. Incomplete Freund's adjuvant (IFA) contains the antigen emulsified in mineral oil and water without the addition of *mycobacterium tuberculosis*.

The clinical course of disease seen in the EAE model is dependent on several factors that include the strain or type of animal and the type of myelin protein used⁹⁴. In C57BL/6 mice that have been induced for EAE with MOG is characterized by ascending paralysis with the majority of lesions seen in the spinal cord⁹².

The pathogenesis of EAE is driven by the phagocytosis of myelin protein by antigen presentation cells (APCs) such as macrophages and dendritic cells⁹⁵. These APCs present the myelin antigen to T cells forming encephalitogenic T cells by MHC class II and CD4 binding and co-stimulation by CD80 and CD86⁹⁵. These activated T cells migrate and infiltrate the CNS by the increased permeability of the blood-brain barrier by the pertussis toxin and the upregulation of cellular adhesion molecules⁹⁵. T cells encounter their cognate antigen in the CNS, and initiate an inflammatory cascade which leads to demyelination: axons are damaged by cytokine release, direct cell-to-cell cytotoxicity, and myelin-specific antibodies through T cell mediated cytotoxicity, and B cell and macrophage recruitment⁹⁵.

Histopathologically, EAE spinal cords show lesions with immune infiltrates, demyelination, and neuronal loss secondary to the activation of T cells autoreactive to the myelin peptide used during immunization⁹⁶. Consequently, this makes EAE useful for modelling neurodegenerative disease mechanisms mediated by (autoimmune) inflammatory conditions.

The similarities between EAE and MS include similar histopathology (immune infiltrates, demyelination, axonal damage and loss), T cell activation, and early spinal cord neuronal loss⁹⁷. Differences between EAE and MS include a paucity of active disease or inflammation in the brain of EAE mice, as well the active role of T and B cells in disease initiation, and the requirement of vaccination for disease induction^{90,95,98}. Another difference is the different T cell mediated pathology where principally CD4+ T cells have been shown to drive disease in EAE while CD8+ T cells are greater contributors to disease in MS^{99,100}.

1.3 Neurotrophic factors in neuronal health and development

Neurotrophins are a family of proteins that act as neurotrophic factors to support neuronal survival, growth, and differentiation¹⁰¹. Key members include the proteins nerve growth factor (NGF), brain-derived neurotrophic factor (BDNF), and neurotrophin-3 (NT-3)¹⁰¹. NGF is imperative for the maintenance and survival of sympathetic and sensory neurons and signals through tropomyosin receptor kinase (Trk) A¹⁰². NT-3 is highly expressed in the immature developing regions of the CNS during embryogenesis, signalling through receptors TrkC and TrkB¹⁰¹. This is in contrast to BDNF, where expression is lower in developing regions of the CNS and is increased as these regions mature¹⁰¹.

The glial cell line-derived neurotrophic factor (GDNF) family of ligands is another group of neurotrophic factors that include the proteins glial cell line-derived neurotrophic factor

(GDNF), neurturin (NRTN), artemin (ARTN), and persephin (PSPN). GDNF treatment of midbrain cultures increased survival and promoted differentiation of dopaminergic neurons¹⁰³. GDNF and NRTN increased the survival of sympathetic neurons, as well as of sensory neurons of the inferior vagus and dorsal root ganglia¹⁰⁴.

Ciliary neurotrophic factor (CNTF) is highly expressed in sciatic nerves, myelinating Schwann cells, and astrocytes¹⁰⁵. CNTF supports the survival and differentiation of sensory, sympathetic, and motor neurons¹⁰⁵. Motor neuron transection-related degeneration was prevented with the treatment of CNTF¹⁰⁶.

1.4 Aryl-hydrocarbon nuclear translocator 2 (ARNT2)

The release of growth factors by glial cells that act on neurons for the promotion of neurogenesis also plays an important role in improving neuronal survival¹⁰⁷. ARNT2 belongs to the basic-helix-loop-helix-Per-Arnt-Sim (bHLH-PAS) family of transcription factors and acts as a binding partner with other bHLH-PAS proteins, forming heterodimers^{108,109}. These heterodimers bind to DNA regulatory sequences responsive to different stimuli, resulting in the active transcription of various proteins. This includes the neuronal growth factor, BDNF^{110,111}. BDNF is expressed by T cells, macrophages, microglia, astrocytes, and neurons¹¹². EAE mice lacking immune cell-derived BDNF have enhanced axonal loss, while mice deficient in astrocyte-derived BDNF had an increase in disease severity and axonal damage and loss¹¹³. BDNF has also been shown to be able to repair axons after axonal transection¹¹³. Previous studies of ARNT2 have been focused primarily on neurons and its role in neurodevelopment as ARNT2 expression is mainly localized to the CNS with some expression seen in the kidneys and thymus¹¹⁴. ARNT2 knockouts have shown lethality in perinatal mice and induced apoptosis in

the PC12 cell line¹¹⁵. This suggests a role for ARNT2 as a survival factor. ARNT2 and HIF1 α heterodimerize under hypoxic conditions in the CNS, resulting in the transcription of genes encoding for proteins responsible for angiogenesis and erythropoiesis¹¹⁶

Our laboratory has shown a decrease in ARNT2 expression over the course of disease in mice immunized for EAE; transcription of *Arnt2* mRNA is downregulated at peak disease (day 18) in EAE mice when the greatest amount of inflammatory infiltrates and axonal damage is observed (Figure 1.1; Quandt Lab, unpublished data). A decrease in *Bdnf* mRNA was also seen when *Arnt2* mRNA was decreased. ARNT2 expression appeared to be enhanced in astrocytes with some ARNT2 staining appearing within the subarachnoid space of EAE spinal cords (Figure 1.2; Quandt Lab, unpublished data) suggestive of ARNT2 staining within immune cells.

Characterizing the expression of ARNT2 in microglia and astrocytes and how expression is regulated are key to understanding disease development. With the characterization of ARNT2 for its association with neuronal and axonal health, we can assess its suitability as a potential novel target in helping prevent and limit the course of inflammatory-mediated neurodegenerative diseases through glial-mediated neuroprotection.

1.5 Receptor mediated endocytosis – 8 (RME-8)

Microglia have been shown to be crucial regulators in the initiation and maintenance of both developmental and pathological processes in the CNS. They are key contributors to shaping

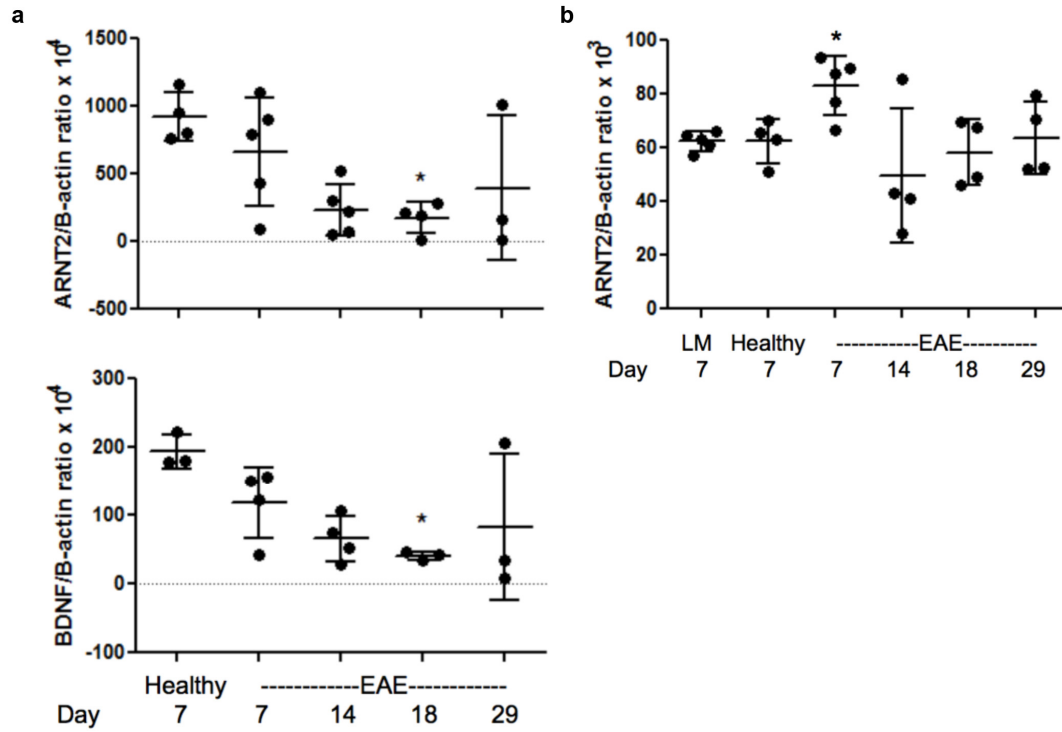


Figure 1.1 *Arnt2* and *Bdnf* gene expression over the course of EAE. (a) *Arnt2* and *Bdnf* decrease in gene expression significantly by day 18 within the spinal cord of EAE mice ($p < 0.05$). (b) *Arnt2* expression increases significantly at day 7 (pre-onset of disease) within the brain of EAE mice ($p < 0.05$). Mean with standard deviation. Mann Whitney t-test. (Quandt et al., unpublished data).

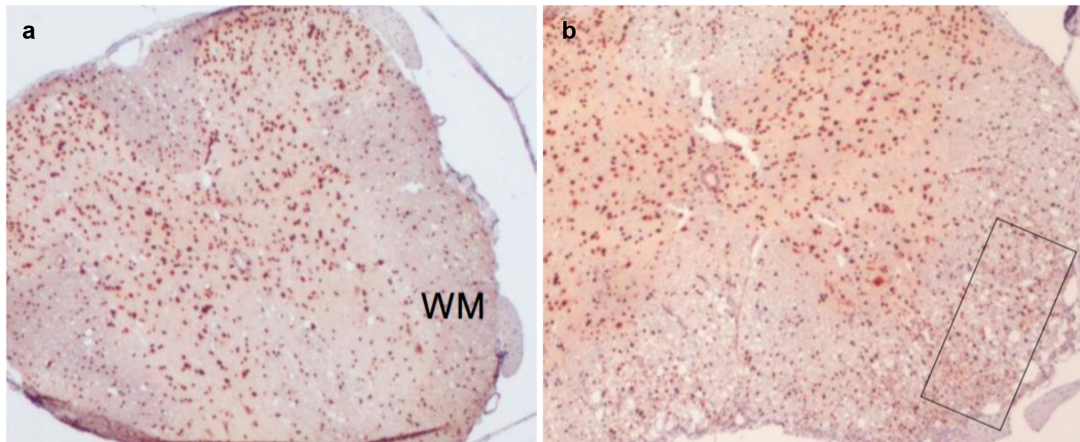


Figure 1.2 ARNT2 expression is enhanced in the white matter of EAE spinal cords. (a) Healthy control spinal cords show ARNT2 expression throughout the grey matter, with a few cells within the white matter staining positive for ARNT2. (b) EAE mice at peak disease show an increase in ARNT2 positive cells within the white matter (black rectangle), with the possible increase in expression coming from glia or immune cells (Quandt et al., unpublished data).

neuronal function and are early mediators in damage and repair settings, such as the remyelination process of axons in demyelinating diseases^{57,117}. The clearance of cell and myelin debris from areas of inflammation by microglia is important in the repair process and suggests a crucial role for proteins that mediate clathrin-mediated receptors and endocytosis processes^{26,118}. This includes receptor mediated endocytosis – 8 (RME-8), a protein involved in endosomal trafficking¹¹⁹.

RME-8 plays an important role in vesicular trafficking by uncoating clathrin-coated vesicles and in the regulation of receptor trafficking in early endosomes. RME-8 has been linked to the CNS with a possible role in neurodegeneration where a mutation in the protein is thought to have caused hereditary adult onset autosomal dominant Parkinson's disease¹²⁰. Mutations in RME-8 have also been associated with essential tremor¹²¹. This suggests that RME-8 plays an important role in the function of the CNS with a possible role in neuronal health and function. In studies using the fibroblast-like COS7 cell line that was transfected with a copy of the mutated RME-8 gene, cells had fewer internalized vesicles after stimulation of the transferrin receptor in comparison to COS7 cells that carried the wild type version. This suggested that the mutated copy of RME-8 correlated with a relative loss in function affecting the endosomal pathway. RME-8 interacts with retromer proteins and the Wiskott-Aldrich syndrome protein and SCAR homolog (WASH) complex, two group of proteins that when mutated have been associated with neurodegenerative diseases^{122,123}. This suggests that the role of these proteins is key to neuronal health, survival, and function. The knockdown of RME-8 disrupts the epidermal growth factor receptor and mannose-6-phosphate receptor mediated endocytosis shown by irregular perinuclear clusters of the receptors as well as a decrease in the ligands bound by these receptors¹²². RME-8 is expressed in macrophage-like coelomocytes in *Caenorhabditis elegans*, where it co-localizes

to the membrane of large endosomes with endocytosis markers¹²⁴. This suggests a possible function of RME-8 in phagocytic leukocytes.

The characterization of RME-8 expression within the CNS and its functional relevance to specific cell types such as microglia would further the understanding of endosomal trafficking within the CNS and how the change in expression of this protein may contribute to disease.

1.6 Hypothesis

1.6.1 Microglia study

We hypothesized that GM-CSF will potentiate the growth of quiescent, non-activated microglia exhibiting a similar phenotype to microglia *in vivo* while maintaining their function. This would result in an effective method to easily generate cultures that mimic microglia *in vivo*.

To test our hypothesis, we had three aims that were to:

1. Establish primary cellular models of murine microglia.
2. Characterize the expression of inflammatory markers and the morphological changes of the primary microglia cell culture after exposure to lipopolysaccharide (LPS), a bacterial cell wall component, and the pro-inflammatory cytokine IFN- γ and how this compares to other microglial models.
3. Characterize the functional relevance of cultured primary microglia by confirming their ability to carry out phagocytosis and secrete cytokines.

1.6.2 ARNT2 study

Next, we hypothesized that inflammatory mediators regulate ARNT2 expression in microglia and astrocytes. To characterize ARNT2 for its involvement in inflammatory neurodegeneration, our aims for a second study were to:

1. Examine the ability of cytokines (LPS and IFN- γ) and excitatory stimulants (potassium chloride) to influence the expression of ARNT2 in primary microglia and astrocyte cultures.
2. Identify the spatial and temporal expression of ARNT2 and its regulation in inflammatory neurodegenerative disease using the EAE mouse model.

1.6.3 RME-8 study

Lastly, we hypothesized that RME-8 will be expressed by several cells of the CNS including neurons, astrocytes and microglia and will play a role in microglia phagocytosis. To characterize and to understand the functional relevance of RME-8 within the CNS under healthy and neurodegenerative conditions, our aims for a third study were to:

1. Examine the ability of cytokines (TNF- α and IFN- γ) to influence expression of RME-8 in primary astrocyte cultures.
2. Assess RME-8 function in primary microglia by the phagocytosis of dextran in wild type and RME-8 mutant microglia.
3. Evaluate the effects of heterozygous and homozygous RME-8 mutations on the development of clinical disease in the MS model EAE.
4. Identify the spatial and temporal expression of RME-8 and its regulation in inflammatory neurodegenerative disease by using the EAE mouse model.

Chapter 2: High yield primary microglial cultures for functional studies related to reparative or pathological processes relevant to neurodegeneration

2.1 Introduction

Glial interactions within the neurovascular niche have become an area of increased research due to their importance in our understanding of disease pathogenesis. The central nervous system (CNS) consists of a heterogeneous population of cells where microglial cells make up roughly 10% of the cell population³. Microglia are the main myeloid-derived immune cell found in the CNS and are important in development and the neuromodulatory, neurotrophic, and neuroimmune responses to insult or disease^{7,125-127}. During embryogenesis, microglial progenitor cells infiltrate the brain from the yolk sac⁵. Microglia survey and scavenge the CNS for potential pathogens and play an important role supporting neurons by synaptic pruning and the engulfing of synaptic material^{128,129}.

Insults, such as spinal cord injury, can result in changes to the microenvironment that change the phenotype in microglia from resting to activated and have been thought to play a role in the neuropathogenesis of several neurodegenerative diseases¹³⁰. This change in microglial phenotype has been linked to neurodegenerative disorders such as Parkinson's and Alzheimer's disease as well as amyotrophic lateral sclerosis¹³¹⁻¹³³. Through several neurodegenerative and neuroinflammatory conditions and diseases, microglia undergo a phenotypic change, becoming intensely ramified and positive for the expression of ionized-calcium binding adaptor molecule 1 (Iba-1), a classic marker of microglial activation²¹. Microglia exist in several states of activity, reflected by changes in morphology. Amoeboid microglia are round in shape with small processes and are motile for scavenging debris for phagocytosis²². Quiescent ramified microglia

have thin branching processes found throughout the CNS. However, unlike amoeboid microglia, the cell body is static while the processes are constantly extending and retracting to perform surveillance in the CNS¹³⁴. Quiescent ramified microglia when activated will undergo a morphological change where their processes are retracted and thickened. Activation of microglia can result in antigen presentation and secretion of cytokines such as IL-1 β , IFN- γ , and TNF- α , as well as secretion of several proteases and reactive oxygen species^{6,135}. Therefore, understanding the function of glial cells in disease onset and progression and how they interact with other cells as well as within the neurovascular niche is crucial to better understand their contributions to damage and repair and how they may be targeted for potential novel therapeutics.

In vitro models are among the most straightforward means to establish factors and conditions, which can influence the phenotype and function of these cells. Fundamentally, the best *in vitro* models are established using minimal manipulation, preservation of the *in vivo* characteristics of a given cell type, and all at a high yield and purity to enable the clearest interpretation and extrapolation of results. The establishment of primary cultures to most accurately reflect morphology and function seen *in vivo* is considered more pertinent than cell lines which through either passaging, transformation, or immortalization are all altered to some extent; where some cell lines undergo significant mutation in order to become immortal. A commonly used model of *in vivo* microglia is the murine BV-2 cell line or the rat-derived highly aggressive proliferating immortalized (HAPI) cells. The BV-2 cell line have been immortalized by infecting primary microglia with the J2 retrovirus carrying the oncogenes *v-raf* and *v-myc*¹³⁶. The HAPI cell line was developed spontaneously through a mutation of a primary microglial enriched culture¹³⁷. However, the suitability of these cell lines as an appropriate model of *in vivo* microglia has been questioned. Studies have shown that neither the BV-2 nor HAPI cell lines

respond similarly to relevant stimuli in terms of TNF- α , IL-1 β , IL-6, and CCL2 production^{138,139}. It has also been found that the BV-2 and HAPI cell lines have differential expression of Iba-1, cytokines, chemokines, nitric oxide production, and altered migratory capacity compared to primary microglia¹⁴⁰. This suggests that there is a significant limitation in what can be extrapolated from the data generated using these cell lines, which were typically used given as to how difficult it can be to obtain primary microglia in sufficient numbers for study.

Perhaps the most accepted and widely used method utilized for the isolation of primary microglia is the dissociation of newborn murine cerebral cortical tissue followed by plating for several days. Vigorous shaking is applied to suspend loosely adherent microglia from the astrocyte “feeder” layer, and the non-adherent cells are passaged to improve microglial purity¹⁴¹. This method requires 7 days in culture before microglia can be harvested, and the cell yield is typically low despite the extended culture time. Another method dissociates murine brains that have been separated into their various cell types through discontinuous Percoll gradients¹⁴². However, microglia are only a small proportion of the cells within the brain so a relatively low yield is expected from the start.

Colony stimulating factors are a group of secreted cytokines that result in the differentiation and proliferation of precursor cells into cells of myeloid lineage¹⁴³⁻¹⁴⁵. Granulocyte macrophage colony stimulating factor (GM-CSF) promotes the proliferation of myeloid derived cells such as microglia. In cell culture, GM-CSF has been used alone^{31,32} and in conjunction with IL-4^{146,147} to generate primary bone marrow-derived dendritic cells from myeloid precursors.

This study presents a relatively simple protocol to culture microglia from embryonic day 18 (E18) primary cerebral cortical neural progenitor cells of mouse origin through GM-CSF

stimulation resulting in higher yield and purity than can be expected from current methods. Microglial phenotypic and inflammatory marker expression was characterized following their exposure to LPS and IFN- γ , and compared to similarly exposed BV-2 cells. The expression profiles of microglia cultured in the presence of GM-CSF with and without the addition of the anti-inflammatory cytokine IL-4 was compared to healthy adult microglia to determine the suitability of GM-CSF cultured microglia as an *in vitro* model.

2.2 Materials and methods

2.2.1 Microglia cell culture and treatment

Glial cultures were prepared from E18 C57BL/6 mouse cerebral cortices according to a previously established protocol¹⁴⁸. Briefly, whole brains were isolated from E18 pups. The cerebral cortices were removed and the hippocampus and striatum were dissected out. Isolated cortices were washed in Hank's balanced salt solution (HBSS) (Invitrogen, Carlsbad, CA) and trypsinized with 0.05% trypsin (Sigma, St. Louis, MO) before mechanical dissociation by pipetting up and down into a single cell suspension. Following the counting of viable cells determined by trypan blue dye exclusion, cells were seeded at 100,000 cells/cm² in plating media [Dulbecco's modified eagle medium (DMEM) (Invitrogen)], completed with 0.5% wt/vol glucose (Bio Basic Inc., Markham ON), 100 μ g/mL Penicillin and 100 U/mL streptomycin (Sigma), 10% horse serum (Invitrogen) on a 25 or 75 cm² poly-L-lysine (Sigma)-coated flasks (Corning Inc., Corning, NY). The cells were incubated at 37°C with 5% CO₂.

Plating media was changed the next day followed by the addition of 50 ng/mL murine GM-CSF (Peprotech, Rocky Hill, NJ). Some plates also received 25 ng/mL of murine IL-4 (Peprotech). Developing microglia appear as lightly tethered amoeboid cells above a mixed

astroglial and neuronal cell monolayer and expand until day *in vitro* (DIV) 21 when the microglia reached peak confluency. Microglia were harvested by gentle pipetting to dislodge non- and loosely adherent microglia allowing for isolation. The cells were then washed, pelleted and resuspended in plating media and seeded into poly-L-lysine-coated tissue culture plates at 50,000 cells/cm².

For comparison of our proposed method for isolating primary microglia, primary microglia were also prepared using a common protocol for culturing microglia *in vitro*¹⁴¹. Briefly, E18 mixed cerebral cortical cells were seeded into 75 cm² flasks (Corning) at 300,000 cells/cm². At day 10, loosely adherent microglia were shaken off overnight on an orbital shaker at 180 rpm and collected the next day before plating into another flask. Adherent microglia were trypsinized and resuspended for further experiments. Whole murine brain single cell suspensions were isolated by passing minced mouse brain through a 70 µm filter and washing with HBSS. Cells were separated from myelin and other cells and cellular debris using a 30% Percoll gradient and after washing in PBS with 2% fetal bovine serum (FBS), were stained for flow cytometry (detailed in 2.2.3).

The BV-2 cell line was cultured according to previous studies¹³⁶ in DMEM media supplemented with 10% heat-inactivated FBS (Invitrogen), 100 µg/mL Penicillin and 100 U/mL streptomycin (Sigma), and L-glutamine (4 mM)(Gibco). Cells were passaged weekly at a confluency of 90-95% by trypsinization and reseeded at a density of 10,000 cells/cm².

2.2.2 Microglial stimulation

To model immune or inflammatory activation *in vivo*, harvested primary microglia and BV-2 cells were treated with either 50 ng/mL of ultrapure LPS isolated from *E. coli* E12

(specific to toll-like receptor 4 (TLR4)) (InvivoGen, San Diego, CA) or 200 U/mL of murine IFN- γ (R&D Systems, Minneapolis, MN). Prior to treatment, primary microglia were harvested by pipetting up and down gently to collect non-adherent cells. The harvested cells were centrifuged, washed, resuspended, and seeded for experiments at a density of 50,000 cells/cm². The BV-2 cells were collected by trypsinization and seeded similarly into cell culture plates for treatment. LPS and IFN- γ were added to the BV-2 cultures when cultures reached 70% confluency.

2.2.3 Flow cytometry

Cells were examined for expression of immune and inflammatory markers relevant to phenotype and function by flow cytometry. Cells were harvested as indicated above (Chapter 2.2.2) and were either stained immediately for direct characterization or seeded in 6-well plates. Seeded cells were either treated with LPS or IFN- γ or left untreated, and the treatment groups were analyzed and compared to untreated cells 24 and 48 hours later to study cell activation. Cells were resuspended and washed twice in staining buffer (1% FBS plus 0.05% sodium azide in PBS) prior to Fc receptor blocking (Pharmlingen by BD Biosciences, San Diego, CA) and staining in a 96-well V-bottom plate (Corning). 0.5 μ L Fc block (Pharmlingen) in 50 μ L staining buffer was added to each well and incubated on ice for 10 minutes prior to the addition of primary antibodies. Murine microglia were incubated with anti-mouse CD45 (VioBlue)(eBioscience), CD11b (APC) (eBioscience), CD11c (PE)(Pharmlingen), MHC class I (H2D^b)(FITC) (eBioscience), MHC class II (IA^d-IE^d)(FITC)(Pharmlingen), CD40 (PE Cy7) (BioLegend), CD80 (FITC)(Pharmlingen), CD86 (PE)(Pharmlingen), and CD39 (PE Cy7)(eBioscience) or with immunoglobulin matched isotype controls (eBioscience). After

staining, wells were topped up with staining buffer and washed twice. Flow cytometry analysis was performed using a MACSQuant flow cytometer (laser capability, seven color) (Miltenyi, Auburn, CA) and analyzed using FlowJo software (Version 7.6.5; Treestar, Ashland, OR). Viable cells were selected based on forward and side scatter; staining prior to flow cytometry revealed greater than 95% of cells excluded trypan blue demonstrating their viability. Protein expressed was qualitatively assessed as negligible, low, intermediate, or high based on log shifts in the intensity of the detected fluorophore compared to isotype controls for each antibody/stain. Negligible coincided with intensities comparable to isotype antibodies, and low intermediate or high intensity staining related to one, two or three log shifts from negligible staining levels.

2.2.4 Immunocytochemistry

Cells were washed with PBS then fixed with 4% paraformaldehyde for 15 minutes at room temperature and washed again with PBS. Cells were permeabilized using 0.1% triton x-100 for 10 minutes and blocked with 10% normal horse serum for 30 minutes. The cell markers Iba-1 (microglia; Abcam, Cambridge, UK), glial fibrillary acidic protein (astrocytes; Millipore), and microtubule-associated protein 2 (neurons; Sigma Aldrich) were used to identify different cell types within the microglial cultures by immunofluorescence. All primary antibodies were incubated overnight followed by one-hour RT incubation with an affinity purified donkey anti-goat, Alexafluor® 568 conjugated (Thermo Fisher Scientific, Waltham, MA) secondary antibody. Normal goat IgG (Santa Cruz Biotechnology, Dallas, TX) and chicken IgG (Santa Cruz Biotechnology) antibodies were used as isotype controls. Images were acquired using fluorescent and phase contrast microscopy with a Zeiss Axio Observer Z1 microscope with Zen 2 acquisition and analysis software (Version2.0.0.0, Oberkochen, DE).

2.2.5 Cytokine ELISA

Primary microglia and BV-2 cells were treated with LPS and IFN- γ . Supernatants were collected at 4, 12, and 24 hours from the treated plates and immediately frozen and stored at -80°C until assayed for cytokine production. TNF- α , CCL2, IL-1 β , IL-6, and IL-10 production was determined using R&D Duoset ELISA kits as per the manufacturer's protocol.

2.2.6 Latex bead phagocytosis assay

Microglia were treated for 24 hours in a 6-well plate. Fluorescent FITC latex beads (Sigma) were then added to the wells at a final concentration of 0.0125% for 1 hour as per previous protocols^{149,150}. After 1 hour of incubation, microglia were trypsinized, centrifuged, washed with PBS, and resuspended in staining buffer. Flow cytometry was used for the assessment of latex bead uptake.

2.2.7 Statistical analysis

Flow cytometry data were analyzed using a Repeated Measures ANOVA on Ranks test with a Tukey's Multiple Comparisons test comparing median fluorescence intensity (MFI) of different markers. Statistical significance was determined as a p value of less than 0.05. A One-way ANOVA was used to analyze the Iba-1 immunofluorescence, ELISA, and phagocytosis assay data with a Tukey's Multiple Comparisons test. All statistical analysis was done using GraphPad Prism 4 (GraphPad Software, Inc., San Diego, CA, USA).

2.3 Results

2.3.1 GM-CSF potentiates the proliferation and differentiation of embryonic cortical cells into microglia

The addition of GM-CSF significantly enhanced the yield of primary microglia using our methods. Microglia began to appear on day 14 (Figure 2.1a). Microglia grown with GM-CSF showed a considerable increase in cell numbers in comparison to microglia grown without GM-CSF up until day 21-23 in culture (Figure 2.1b). Microglia appeared as refractile amoeboid cells that were non-adherent or lightly tethered to the monolayer of astrocytes and neurons (Figure 2.1c). The addition of IL-4 did not change the relative appearance of microglia; however, the degree of expansion was considerably lower than what was observed with GM-CSF alone (Figure 2.1d, Figure 2.1e). Single wells of a 6-well plate seeded with 950,000 cells from a mixed cortical suspension yielded 4.2×10^5 microglia when cultured using the previously established protocol for cultured microglia. GM-CSF cultured microglia yielded 2.2×10^6 cells whereas GM-CSF and IL-4 cultured microglia yielded 2.2×10^5 cells (Figure 1f).

2.3.2 Microglia undergoes a characteristic morphological change when treated with lipopolysaccharide (LPS)

Harvested microglia from the astroglial and neuronal monolayer remained largely non-adherent and refractile with an amoeboid morphology (Figure 2.2). Microglia exhibited many small processes but were typically non-ramified and non-branched through 2-3 days in culture after reseeding. The addition of LPS increased adherence and a stellate morphology with a greater number of processes that were in turn more branched following LPS treatment over 48 hours.

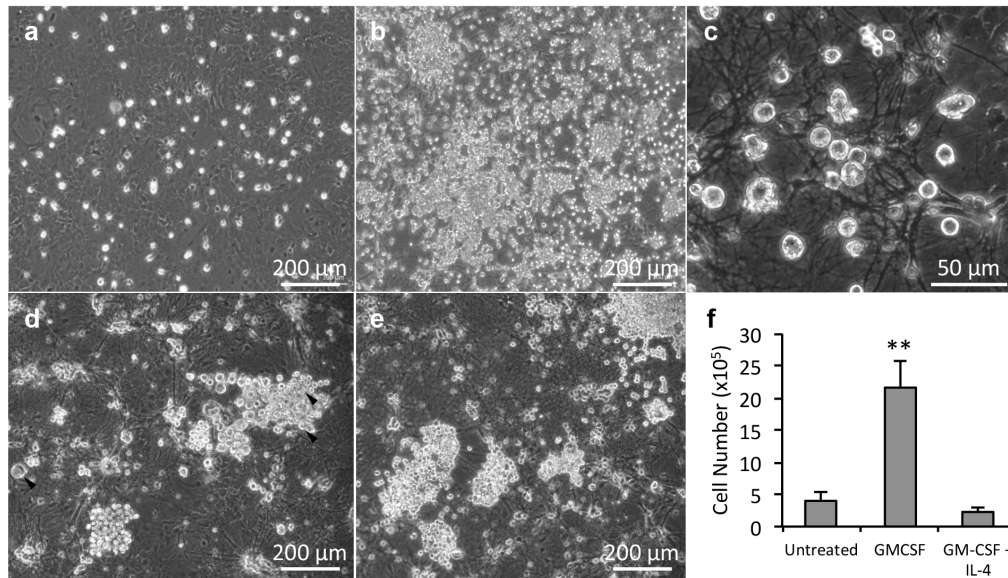


Figure 2.1 GM-CSF addition enables the establishment of high yields of purified microglia from mouse.

Microglia exhibiting an amoeboid morphology underwent rapid expansion between (a) days *in vitro* (DIV) 14 and (b) DIV 21 as shown by the round refractile spheres resting on the non-refractile astrocyte feeder layer. (c) Higher magnification view of individual microglia (DIV 21) showed the majority of the microglial cells as amoeboid. Microglia cultured with GM-CSF and IL-4 at DIV 17 (d) had occasional larger granular microglia (black arrows) as well as smaller amoeboid microglia that are seen in cultures with (e) GM-CSF only at DIV 17. (f) GM-CSF provided 5-6 fold more microglia when added throughout the culture period in comparison to untreated, and GM-CSF with IL-4 cultured microglia on DIV 21. Average with standard deviation. One-way ANOVA with Tukey's post comparison test)(n=3).

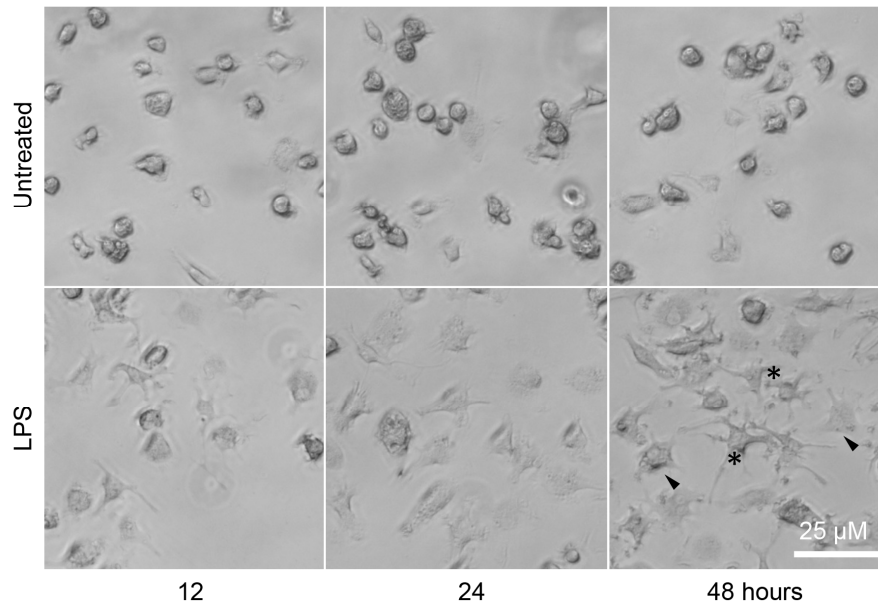


Figure 2.2 LPS treatment modifies microglial morphology. Untreated cells displayed little change in the 48 hours after replating. Cells became increasingly ramified (black asterisks) with larger cell bodies (black arrows) after longer exposure times to LPS. Representative images from 1 of 4 experiments.

2.3.3 Microglia cultured in GM-CSF alone and in GM-CSF with IL-4 share similar myeloid and co-stimulatory marker profiles

Cultured microglia were characterized and compared to *ex vivo* microglia isolated from adult mouse brain tissue and the BV-2 cell line. Microglia were phenotyped using CD45 (leukocyte cell marker), CD11b (myeloid cell marker), and CD11c (dendritic cell marker). Inflammatory markers MHC class I and II (antigen presentation molecules), T cell co-stimulatory molecules CD40, CD80, and CD86, and ectoATPase CD39 were also used. GM-CSF cultured microglia had a CD45^{low}, CD11b⁺, CD11c⁻, MHC I⁺, MHC II⁻, CD86⁻, CD80⁻, and CD39⁺ phenotype (Figure 2.3; Table 2.1).

The addition of IL-4 altered some of the expression of phenotypic markers seen in comparison to microglia cultured in GM-CSF alone. MHC I expression was consistently significantly reduced in comparison to GM-CSF-only cultured microglia.

The adult brain microglia analyzed *ex vivo* expressed a similar phenotypic profile to our cultured microglia *in vitro*. Both were CD45^{low}, CD11b⁺, CD11c⁻, CD80⁻, and CD86⁻. BV-2 cells also shared a CD45^{low}, CD11b⁺, CD11c⁻, MHC I⁺, MHC II⁻, and CD39⁺ phenotype but were consistently higher in its constitutive expression of CD86⁺.

Microglia were activated by the addition of LPS or IFN- γ for 24 and 48 hours in comparison to untreated microglia. LPS treated microglia cultured solely with GM-CSF had significantly upregulated the expression of CD11b and CD86 after treatment for 48 hours ($p < 0.05$) (Figure 2.4; Table 2.2). IFN- γ treated microglia significantly upregulated CD40, CD45, CD80, and MHC I after 48 hours of treatment ($p < 0.05$). CD39 was downregulated in LPS treated microglia while IFN- γ upregulated expression. The BV-2 cells showed a similar response profile

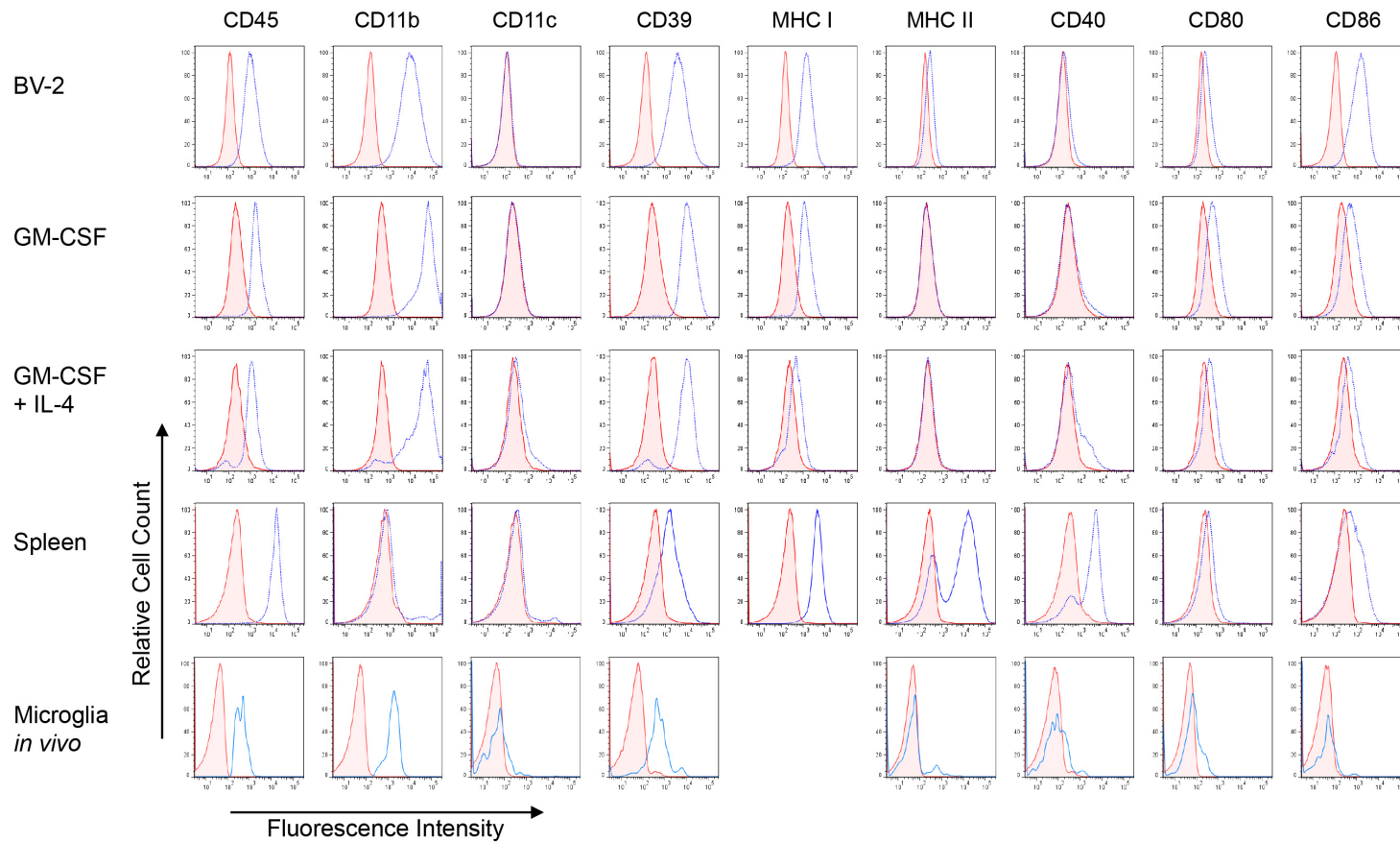


Figure 2.3 Phenotypic comparison of primary microglia vs. cell line. GM-CSF microglia had a similar phenotype to GM-CSF plus IL-4 cultured microglia and the BV-2 microglial cell line. Primary microglia were CD45^{intermediate}, CD11b⁺, CD11c⁻, CD39⁺, MHC I⁺, MHC II^{negligible}, CD80^{lo} and CD86^{lo}; BV-2 showed a higher constitutive expression of CD86 than primary cultures. The GM-CSF and IL-4 cultured microglia differed only in their lower expression of MHC class I. (n=7 for GM-CSF, GM-CSF/IL-4, Spleen; n=3 for BV-2; n=4 for microglia analyzed *ex vivo*).

	BV-2	GM-CSF	GM-CSF and IL-4	<i>In vivo</i>
CD45	Intermediate	Intermediate	Intermediate	Intermediate
CD11b	High	High	High	Intermediate
CD11c	Negligible	Negligible	Negligible	Negligible
CD39	Intermediate	Intermediate	Intermediate	Intermediate
MHC I	Low	Low	Negligible	N/A
MHC II	Negligible	Negligible	Negligible	Negligible
CD40	Negligible	Negligible	Negligible	Negligible
CD80	Negligible	Negligible	Negligible	Negligible
CD86	Intermediate	Negligible	Negligible	Negligible

Table 2.1 Primary microglia vs. cell line phenotype. Primary microglia cultured in GM-CSF with and without IL-4 had a similar phenotype in comparison to microglia *in vivo* and the BV-2 cell line. The BV-2 cell line showed a higher constitutive expression of CD86 overall in comparison to the other microglia culture methods. GM-CSF with IL-4 showed a lower overall expression in MHC I in comparison to microglia cultured in GM-CSF alone.

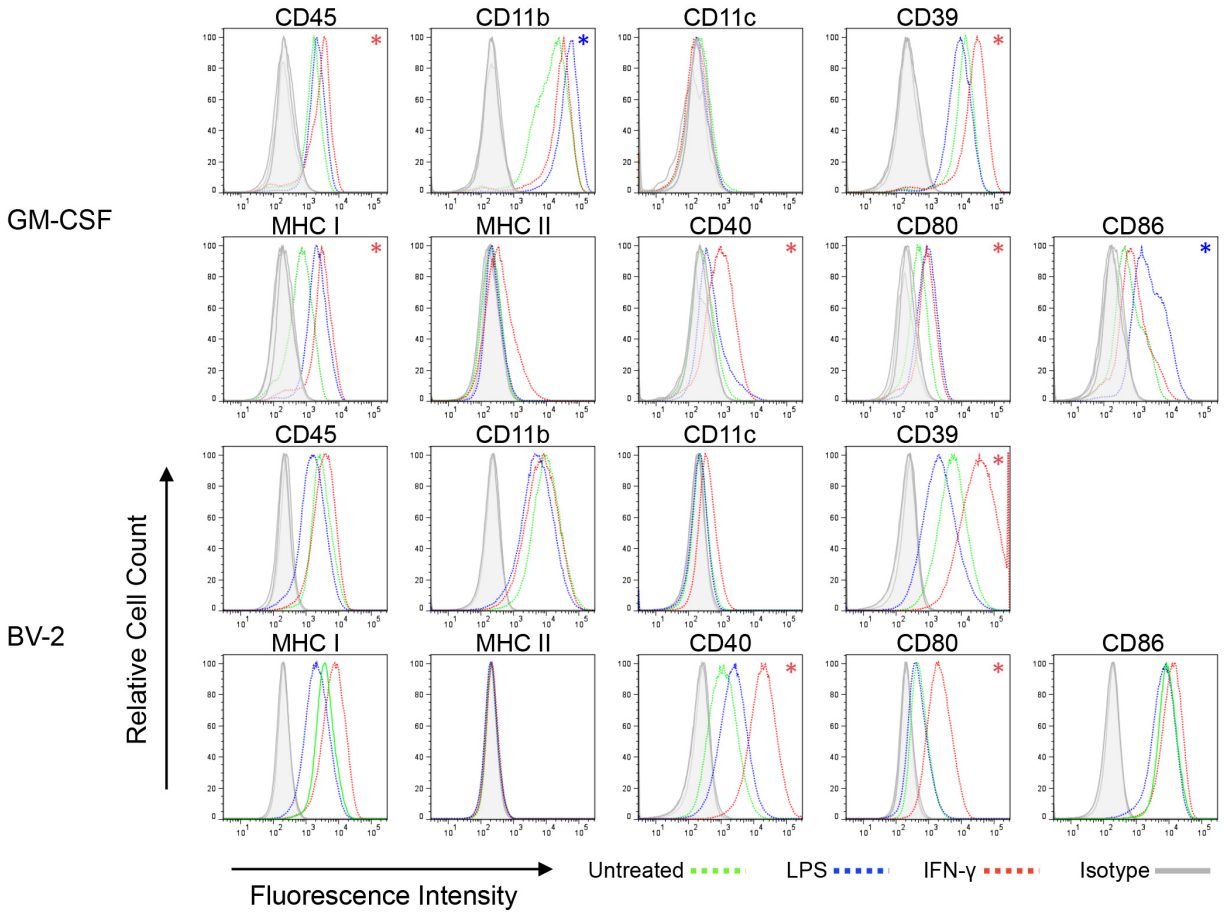


Figure 2.4 GM-CSF microglia differentially upregulate phenotypic and co-stimulatory markers when treated with IFN- γ and LPS. BV-2 and GM-CSF cultured microglia showed similar expression patterns when treated with inflammatory mediators, notably the upregulation of CD39, CD40, and CD80. Blue and red and asterisks indicate significance in LPS or IFN- γ treatments compared to untreated controls respectively. (n=5 GM-CSF, n=2 BV-2)

	Untreated	LPS	IFN- γ
CD45	1287.3 \pm 122.3	1985.0 \pm 76.8	3091.0 \pm 1014.1*
CD11c	32.3 \pm 34.6	36.8 \pm 29.9	121.8 \pm 122.3
CD11b	18172.0 \pm 6893.2	49841.8 \pm 12465.5*	32637 \pm 7946
CD40	84.0 \pm 49.7	283.5 \pm 164.8	1138.0 \pm 567.5*
CD80	632.5 \pm 517.0	712.0 \pm 145.4	1961.0 \pm 921.3*
MHC I	963.3 \pm 463.1	3237.0 \pm 1526.7	5987.8 \pm 2170.6*
CD86	229.3 \pm 105.2	1196.5 \pm 830.9*	571.8 \pm 276.4
MHC II	-52.0 \pm 120.0	-89.0 \pm 194.3	176.0 \pm 193.4
CD39	10698.6 \pm 1662.3	7957.2 \pm 1729.3	25460.0 \pm 3798.4*

Table 2.2 Primary GM-CSF microglial surface marker expression in response to LPS and IFN- γ . LPS

significantly upregulated CD11b and CD86 while IFN- γ significantly upregulated CD40, CD45, CD80, MHC I, and CD39 expression after 48 hours of treatment. Values represent mean fluorescence intensity \pm standard deviation.

Bolded values represent those *P<0.050, Repeated Measures ANOVA on Ranks test with a Tukey Post Comparison Test. (n=5)

as the primary microglia (Figure 2.4; Table 2.3). CD45 and CD11b were both upregulated following IFN- γ or LPS treatment. Baseline CD40 expression was higher in BV-2 cells than primary microglia; CD40 expression was further increased following treatment with LPS and significantly by IFN- γ ($p < 0.05$). High constitutive expression of CD86 by BV-2 cells was not increased by treatment with the factors examined as was observed with GM-CSF cultured microglia. The divergent trends of LPS and IFN- γ on CD39 expression were also observed in the BV-2 cell line where IFN- γ increased CD39 expression ($p < 0.05$). IFN- γ also upregulated CD80 significantly ($p < 0.05$).

2.3.4 IFN- γ upregulates marker of activation Iba-1 in GM-CSF cultured microglia

Primary microglia cultured with GM-CSF were characterized immunocytochemically. Cells were negative for MAP2 and GFAP expression, which confirmed the absence of neuronal or astroglial contamination respectively. Primary microglia were assessed for the expression of the classic microglial activation marker Iba-1 using immunofluorescence and changes in its regulation by treatment with IFN- γ or LPS. Treatment of microglia with IFN- γ resulted in flat and round cells with a relatively large cell body in contrast to LPS treated cells that showed extensive ramification and numerous processes. Both untreated and LPS-treated microglia remained negative for Iba-1 for the first 48 hours of treatment (Figure 2.5). IFN- γ significantly increased the percentage of Iba-1 positive cells ($p < 0.01$), with Iba-1 localized throughout the cytoplasm of the majority of cells treated with IFN- γ .

	Untreated	LPS	IFN- γ
CD45	749.1 \pm 296.3	588.5 \pm 84.6	1338.6 \pm 571.8
CD11c	-21.6 \pm 14.8	-79.4 \pm 119.2	-70.6 \pm 48.7
CD11b	1664.7 \pm 1163.0	1687.6 \pm 830.0	1145.1 \pm 523.3
CD40	264.6 \pm 284.7	1734.3 \pm 1200.9	6933.0 \pm 3315.9*
CD80	296.3 \pm 168.2	357.7 \pm 399.9	1462.7 \pm 879.2*
MHC I	672.3 \pm 273.3	584.9 \pm 428.1	2543.0 \pm 1252.9
CD86	3576.6 \pm 4105.7	3991.0 \pm 4565.2	9444.2 \pm 13489.5
MHC II	-43.3 \pm 120.6	-116.3 \pm 240.3	-112.3 \pm 218.1
CD39	1814.9 \pm 1889.7	957.5 \pm 956.0	15514.9 \pm 1716.7*

Table 2.3 BV-2 surface marker expression in response to LPS and IFN- γ . IFN- γ significantly upregulated CD40, CD80, and CD39 expression by 48 hours of treatment. Values represent mean fluorescence intensity \pm standard deviation from 4 experiments. Bolded values represent those *P<0.050, One-way ANOVA with a Tukey Post Comparison Test. (n=3)

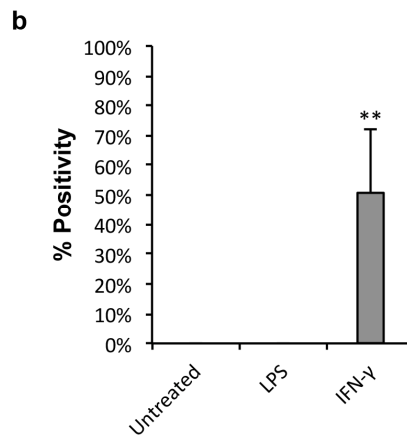
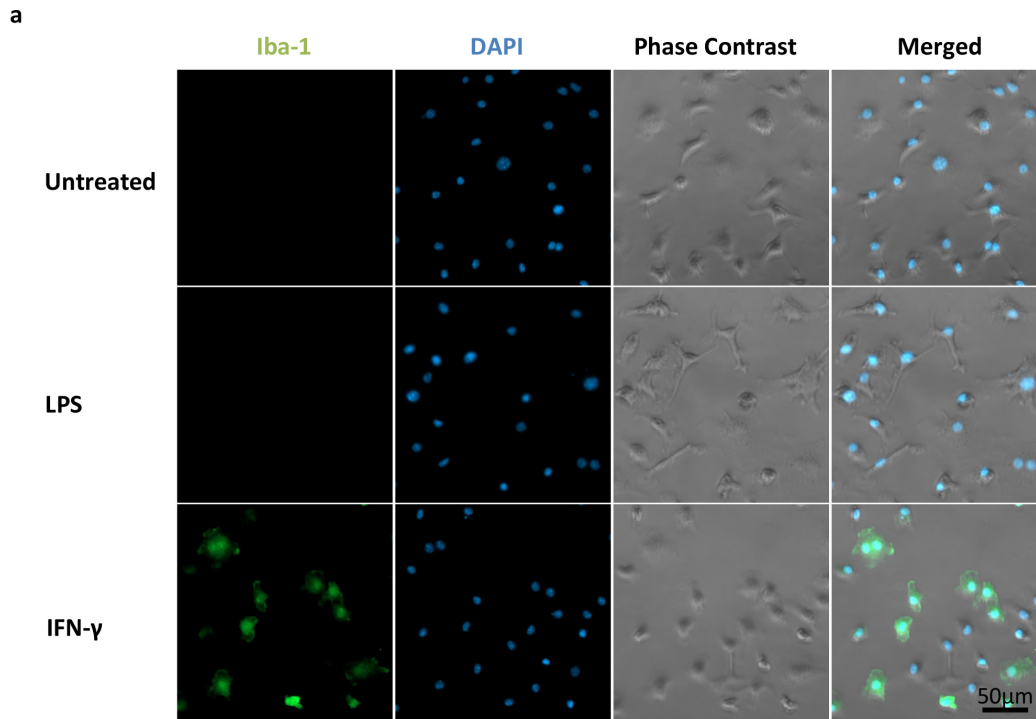


Figure 2.5 Primary microglia express the activation marker Iba-1. (a) Untreated and LPS treated microglia had negligible expression of Iba-1. (b) IFN- γ significantly upregulated Iba-1 expression in primary GM-CSF cultured microglia ($p < 0.01$; One-way ANOVA with Tukey's post comparison test). Average with standard deviation. ($n = 3$)

2.3.5 Inflammatory stimuli increase microglial cytokine production

Microglial secretion of CCL2, TNF- α , IL-10, IL-6, and IL-1 β was detected by ELISA analysis of supernatants after various treatments. All microglia, regardless of treatment or lack thereof, showed constitutively high levels of CCL2 in cell supernatants. Untreated and IFN- γ treated microglia had similar levels of CCL2 at all three time points (4, 12, and 24 hours). CCL2 production was significantly higher in LPS-treated GM-CSF cultured microglia in comparison to untreated and IFN- γ -treated cells with 4.06, 7.30, and 8.07 ng/mL of CCL2 at 4, 12, and 24 hours respectively.

Untreated microglia secreted 0.32 ng/mL of TNF- α during the first 4 hours of reseeding to a 96-well plate (Figure 2.6a). TNF- α levels decreased over time whereby at 24 hours only 0.02 ng/mL could be detected. Similarly, IFN- γ -treated cells secreted 0.43 ng/mL at 4 hours and dropped to 0.20 ng/mL by 24 hours. In contrast, LPS-treated microglia increased TNF- α levels significantly by 4 hours to 3.42 ng/mL, an approximate 10-fold increase compared to untreated controls.

Both untreated and IFN- γ -treated cells had low secretion of IL-10 at 4 hours that were comparable at 12 and 24 hours. At 4 hours, LPS-treated primary microglia had 4.83 ng/mL of IL-10 secretion that was unchanged at 12 and 24 hours.

A negligible amount of IL-6 was detected in untreated and IFN- γ -treated microglia over the 24 hours examined. In contrast, LPS treatment raised IL-6 levels to 5.95 ng/mL by 4 hours and resulted in an increase of detectable IL-6 levels to 8.83 ng/mL and 9.41 ng/mL at 12 and 24 hours respectively. No detectable amounts of IL-1 β were found in the supernatants of either untreated or treated cells (data not shown).

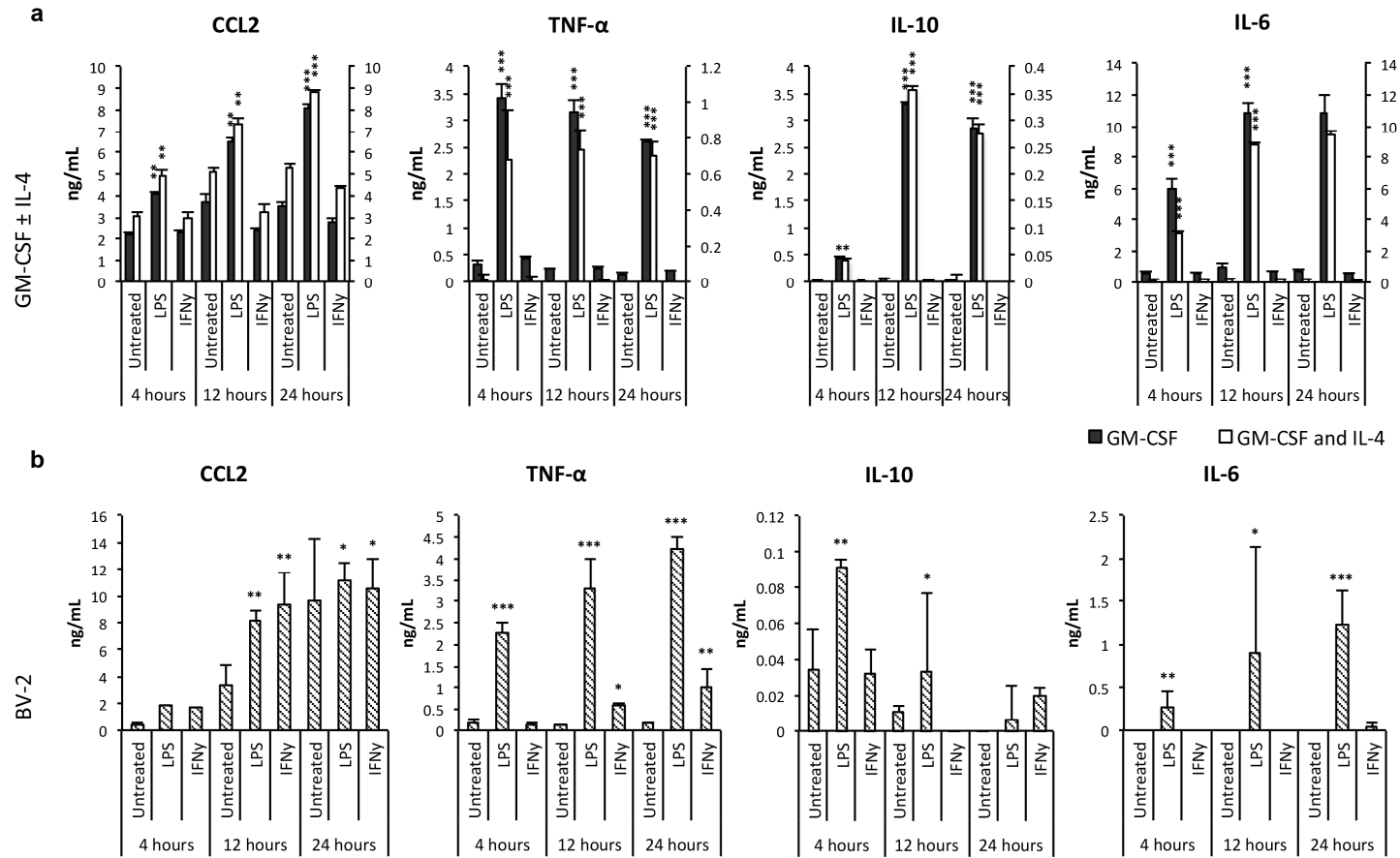


Figure 2.6 LPS significantly upregulates several cytokines in both primary cultures and cell lines. (a) IL-10, CCL2, IL-6, and TNF- α were increased by 4, 12, and through 24 hours; IFN- γ treatment resulted in no changes. (b) BV-2 cell line had significantly lower IL-6 and IL-10 production in comparison to primary GM-CSF microglia. Bars represent the mean cytokine production +/- standard deviation (* $P < 0.050$, ** $P < 0.001$, *** $P < 0.0001$ One-way ANOVA with Tukey's post comparison test). Average with standard deviation. (n=3 for GM-CSF, n=2 for GM-CSF with IL-4, n=2 for BV-2).

Compared to our primary method of culturing which involved the addition of GM-CSF alone, GM-CSF with IL-4 cultured microglia exhibited the same relative amounts and expression trends in secretion of the cytokines CCL2 and IL-6 (Figure 2.6a). Notably, the production of TNF- α and IL-10 were several fold lower when IL-4 had been part of the culture process to generate microglia.

Analysis of the BV-2 cell line showed that it responded similarly to our GM-CSF microglial cultures. Similarly to the GM-CSF with and without IL-4 cultured microglia, CCL2 production increased with time in untreated and treated BV-2 cells. No marked changes were observed until 12 and 24 hours post-treatment. LPS-treated BV-2 cells had 8.18 ng/mL of CCL2 at 12 hours, roughly 2.5-fold higher than untreated. IFN- γ -treated cells had 9.28 ng/mL of CCL2 at 12 hours, which was a significant 3-fold higher than untreated cells.

The BV-2 cell line followed a similar trend in TNF- α production. A significant increase was observed at 4, 12, and 24 hours post addition of LPS (Figure 2.6b). Unlike the GM-CSF cultured microglia, a significant upregulation was seen with IFN- γ -treatment: BV-2 cells increased TNF- α secretion; 0.13 ng/mL was detectable at 4 hours, and secretion was significantly increased to 1.03 ng/mL by 24 hours.

Untreated and IFN- γ -treated BV-2 cells had roughly equal amounts of detectable IL-10 at all time points. Approximately 0.03 ng/mL IL-10 was observed at 4 hours and there was no significant change seen at 12 and 24 hours. LPS increased IL-10 levels slightly. Approximately 0.09 ng/mL of IL-10 was present at 4 hours, which was about 3-fold higher than the untreated cells. However, IL-10 production in LPS-treated cells dropped off at later time points: 0.03 ng/mL at 12 hours, and 0.01 ng/mL at 24 hours. Notably these levels were nearly 10-fold lower than those observed in treated cultures of primary GM-CSF microglia.

Negligible IL-6 was detected in untreated and IFN- γ -treated BV-2 cells. However, LPS treatment significantly upregulated detectable IL-6 at all three time points. IL-6 levels were 0.27 ng/mL at 4 hours, and increased to 0.91 ng/mL at 12 hours and 1.22 ng/mL at 24 hours. Notably, this increase in IL-6 secretion was roughly 6-fold lower than what was observed in the GM-CSF cultured microglia.

2.3.6 LPS increases while IFN- γ decreases the phagocytic capabilities of primary microglia

To examine inflammatory factors that alter the functional activity of our primary microglia, phagocytic activity was assessed by the uptake of fluorescently labelled latex beads. A heterogeneous population of microglia seemed to be present in our cultures as approximately half of the cells had uptake of the latex beads. The percent positivity and median fluorescence intensity (MFI) was determined by the cells in gate A (figure 2.7a). Several of the microglia took up very little to no latex beads in comparison to another subset of microglia that took up a considerable amount that appeared to be altered by the presence of inflammatory mediators. Untreated microglia had a MFI of 43,466.7 with 77.6% of the cell population having uptake of the latex beads (figure 2.7c). Contrarily, IFN- γ treated microglia had a significant decrease in phagocytic activity with a MFI of 27,100.0 ($p < 0.05$) averaged through the 67% of cells that were positive ($p < 0.01$) for the FITC conjugated latex beads.

2.4 Discussion

In this study we provided a simple and effective method for isolating a high purity population of primary microglia from E18 mice that enabled us to model inflammatory

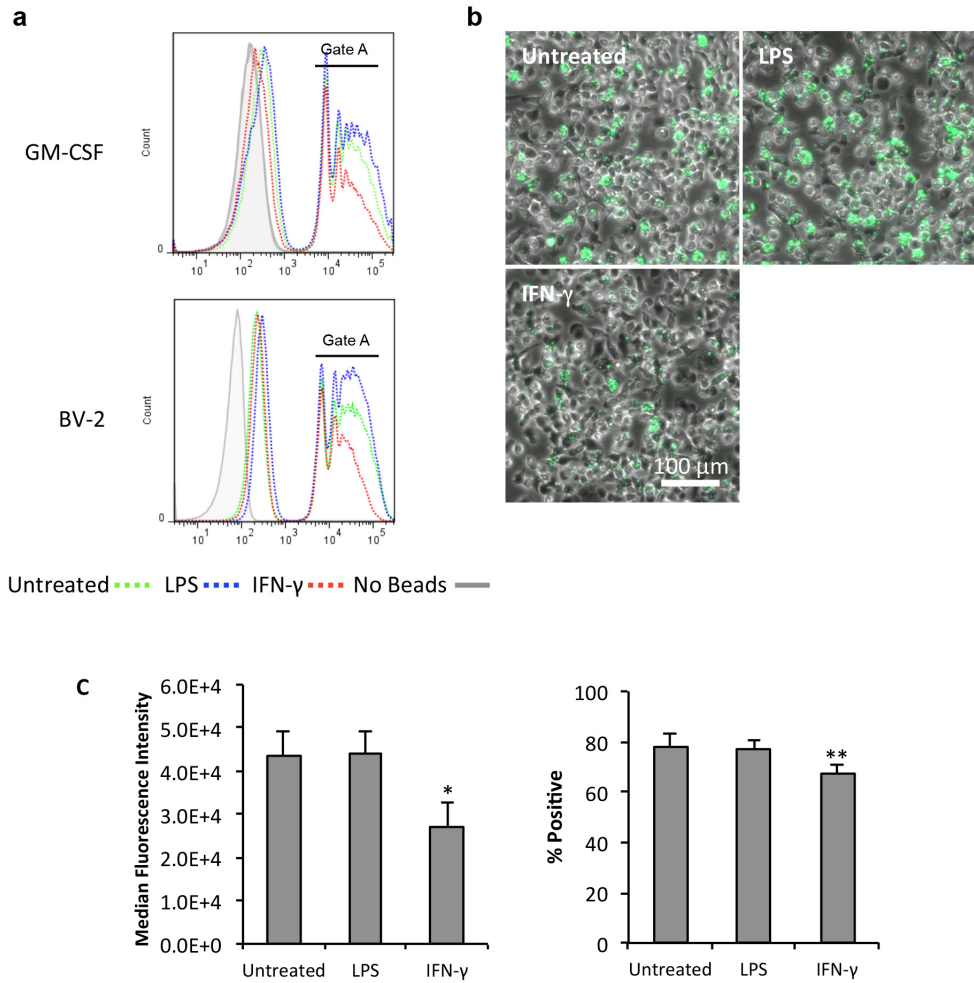


Figure 2.7 Inflammatory factors alter the phagocytic capacity of primary GM-CSF microglia. (a) IFN- γ down regulated phagocytosis of FITC labeled latex beads in comparison to untreated microglia in both BV-2 and GM-CSF cultured cells (upper vs. lower panel) within gate A. (b) Phase-contrast micrograph of GM-CSF cultured microglia showed latex beads (green) within untreated, LPS, and IFN- γ treated cells. (c) GM-CSF cultured microglia treated with IFN- γ had a significant decrease in the median fluorescence intensity ($p < 0.05$) and the percentage of FITC positive cells ($p < 0.01$; One-way ANOVA with Tukey's post comparison test). Average with standard deviation. (n=3).

conditions and microglial activation. Uniquely, this method took advantage of the growth-stimulating effects of GM-CSF to help increase the total number of microglia from embryonic nervous tissue. The addition of GM-CSF to the media is crucial to the rapid growth and proliferation of microglia as cultures without GM-CSF had significantly fewer cells.

Our GM-CSF microglial cultures had an intermediate expression of CD45, were positive for CD11b, and did not express the dendritic marker CD11c. This expression profile is consistent with a microglial phenotype per our own *ex vivo* analysis and those of others^{151,152}. It has been suggested that the inclusion of GM-CSF may alter properties of these cells due to the inflammatory nature of GM-CSF and its effects upon other myeloid cells such as macrophages or dendritic cells^{153,154}. However, we showed that our cultures were predominantly similar to those isolated and examined *ex vivo*. Both our GM-CSF cultured microglia and *ex vivo* microglia demonstrated negligible expression of CD40, CD80, CD86, and MHC class I and II. This further supports that the activation profiles of our GM-CSF microglia are similar to that of microglia seen *in vivo*.

IFN- γ and LPS differentially regulated microglial changes. LPS and IFN- γ both increased the expression of MHC I while only IFN- γ was able to increase MHC II expression. This suggests that our cultured microglia are able to process and present antigen. CD45 and CD11b expression increased after both LPS and IFN- γ treatments, which is consistent with previous studies where microglia have been shown to upregulate these proteins when activated with LPS or IFN- γ ¹⁵⁵⁻¹⁵⁷. The BV-2 cell line showed similar patterns when exposed to LPS or IFN- γ , suggesting that said responses are likely to be characteristic of microglial cell lines as well as primary cultures.

Consistent with previous studies, IFN- γ increased CD80 expression within the BV-2 cell line¹⁵⁸. Our primary GM-CSF-cultured microglia treated with IFN- γ slightly upregulated CD86 and increased CD80 significantly, which was consistent with other studies in primary human microglia⁷⁴. Notably, GM-CSF-cultured microglia had an overall lower baseline expression of CD86 in comparison to the BV-2 cell line. This suggests that the BV-2 cell line is already at a more pro-inflammatory state, similar to that described for the M1 “pro-inflammatory” designation applied to microglia¹⁵⁹, in comparison to a more reparative or M2 phenotype. This increased CD86 expression may also be attributable to the viral transfection of the cells during the immortalization process, as similar increases of CD86 expression had been previously described in B lymphocytes and dendritic cells post viral infection^{160,161}. The differences seen in CD86 expression may have also been related to other differences between these primary cultures and the BV-2 cell line. IL-10 secretion was considerably lower than our GM-CSF cultured microglia. Consequently, the inability of the BV-2 cell line to produce IL-10 may be correlated to the high expression of CD86. BV-2 cells treated with IL-10 has been found to suppress the expression of CD86¹⁵⁸ as well as in other myeloid derived cells¹⁶².

LPS and IFN- γ each differentially regulated the otherwise constitutive expression of the ectoATPase CD39 in both the BV-2 cell line and our GM-CSF cultured microglia. In both primary cultures and cell lines, LPS-treated microglia downregulated the expression of CD39 while IFN- γ treatment resulted in an increase of expression. This emphasizes that there are differences in the various states of activation of microglia, dependent on the source of stimuli. This has already been shown in other immune cells where CD39 was expressed on activated NK cells, B cells, and T cells but was absent when cells were in a resting state¹⁶³. Within the CNS, microglia and endothelial cells and smooth muscle cells of the vasculature expressed CD39

while neurons were absent of CD39 expression¹⁶⁴. CD39, a purinoreceptor, plays a role in purinergic-mediated microglial migration¹⁶⁵ where it hydrolyzes ATP to AMP¹⁶⁶. It is this release of ATP by dying cells that functions as a chemoattractant in microglia. This suggests a role for CD39 in disease pathogenesis as ATP does not exist in high concentration within the extracellular space unless released exocytotically or from damaged and dying cells in the CNS^{167,168}. This would make microglial or endothelial exposure to ATP more likely due to degenerative conditions. ATP signaling through purinoreceptors in microglia could mediate cytokine release and nitric oxide production while increasing potassium conductance¹⁶⁹. However, the role of inflammatory mediators and their effects on CD39 expression and microglial migration has not been clearly defined in microglia.

The majority of protocols for culturing primary microglia required a substantial amount of neuronal tissue yet failed to return a proportional microglia yield. The addition of GM-CSF to our primary microglia cultures increased the microglia yield without altering surface marker profiles, confirmed by comparison to adult microglia analyzed *ex vivo*. The BV-2 cell line, although commonly employed as a model of microglia, deviated considerably from their primary *in vitro* counterparts in our direct comparison of cell surface markers and cytokine production profiles. This highlights the importance of using primary microglial cultures to investigate *in vitro* functions in order to be able to confidently extend observations to their potential roles in processes of pathogenesis and repair *in vivo*.

Chapter 3: Investigation of the regulation of ARNT2, a neuroprotective transcription factor, in models of inflammatory neurodegenerative disease

3.1 Introduction

Aryl hydrocarbon receptor nuclear translocator 2 (ARNT2) belongs to the basic-helix-loop-helix-PER-ARNT-SIM (bHLH-PAS) family of transcription factors¹⁰⁹. ARNT2 is able to heterodimerize with several other transcription factors within the bHLH-PAS family that results in its subsequent binding to DNA regulatory sequences which leads to an alteration of gene transcription¹⁰⁸. ARNT2 is able to bind to aryl hydrocarbon receptor (AhR), a ligand-activated transcription factor that functions by inducing the transcription of xenobiotic metabolizing enzymes to remove foreign toxic chemicals such as dioxins and 2,3,7,8-tetrachlorodibenzo-*p*-dioxin (TCDD)¹⁷⁰. AhR ligation increases the production of T_h17 differentiated T cells, a subset of T cells that is associated with autoimmune diseases^{171,172}.

ARNT2 has been found to play an important role in embryogenesis. It is expressed within the nervous system (spinal cord, brain, and eye) and the kidney (adrenal medulla and developing tubules within the cortex of the kidney), both of which are developed from the neuroectoderm^{114,173}. ARNT2 expression has also been found within the thymus¹¹⁴. ARNT2 has a role in the development of the hypothalamus, determined by its binding of another bHLH-PAS transcription factor, single minded homolog 1 (SIM1)¹⁷⁴. In addition, ARNT2 plays an important part in hypoxia within the CNS by binding HIF1 α , a transcription factor that is responsible for the transcription of genes encoding for proteins responsible for angiogenesis and erythropoiesis¹¹⁶. ARNT2 is also thought to play a role in cell survival. When the adrenal gland cell line PC12 cells which share the same lineage as neurons are exposed to oxidative stress, cell

death is seen following a decrease in ARNT2 expression. Conversely, impairing the progression of the PC12 cell cycle enhanced ARNT2 expression¹¹⁵. This suggests that ARNT2 is involved in regulating cell cycle progression and preventing cell death. ARNT2 has also been identified as a binding partner for the transcription of BDNF, a neuronal growth factor^{110,111}.

The study of ARNT2 thus far has been primarily focused on its function in neurons with no characterization in other cell types. Consequently, ARNT2 and its expression profiles have yet to be characterized in glia (astrocytes or microglia) or cells of the immune system that may enter the CNS during insult or injury. With the role of AhR as a mediator in the metabolism of exogenous and endogenous toxic compounds, its role in T cell polarization, and its binding of ARNT2 for gene transcription suggests that immune cells could express ARNT2 and be regulated by inflammatory mediators. Such immune cells include microglia that have been shown to be crucial regulators in the initiation and maintenance of both developmental and pathological processes in the CNS. They are key contributors to neuronal function and are early mediators in damage and reparative settings such as the remyelination process of axons in demyelinating animal models of disease²⁶.

Previous studies from our lab have shown that the transcription of *Arnt2* mRNA is upregulated at pre-onset disease (day 7) in the brain and is downregulated at peak disease (day 18) in EAE mice when the greatest amount of inflammatory infiltrates and axonal damage is observed (Quandt Lab, unpublished data)(Figure 1.1). The downregulation in *Arnt2* mRNA was also seen with a downregulation in *Bdnf* mRNA in the spinal cord. Within the spinal cord, ARNT2 expression appeared to be enhanced by astrocytes with some ARNT2 staining appearing within the subarachnoid space (Quandt Lab, unpublished data)(Figure 1.2). This suggests the possible expression of ARNT2 within immune cells.

This study examined the expression and regulation of ARNT2 within microglia and GFAP staining astrocytes by stimulating appropriate cells with LPS, IFN- γ , TNF- α , and potassium chloride. Treatment with LPS, IFN- γ , and TNF- α were used to mimic inflammatory conditions including infection and acute/chronic inflammation respectively. Potassium chloride was used to address whether ARNT2 expression is regulated by excitatory conditions. With preliminary data showing ARNT2 expression within the white matter and subarachnoid space in the EAE mouse model, continued in depth analysis of ARNT2 expression was further characterized within the spinal cord and compared between spleens from healthy mice or mice immunized to develop EAE.

Specifically, in this study we aim to:

1. Examine the role of cytokines (LPS and IFN- γ) and excitatory stimulants (potassium chloride) and their influence on the expression of ARNT2 in primary microglia and astrocyte cultures.
2. Identify the spatial and temporal expression of ARNT2 and its regulation in inflammatory neurodegenerative disease using experimental autoimmune encephalomyelitis as a model.

3.2 Materials and methods

3.2.1 Primary microglia cultures and stimulation

Primary murine microglia were cultured using the same protocol as described in chapter 2. Briefly, a mixed cortical suspension from E18 mice was seeded with the addition of GM-CSF at DIV 2. Microglia were harvested at DIV 21 and reseeded in 12-well plates. To model immune or inflammatory activation *in vivo*, harvested primary microglia were treated with 50 ng/mL of

ultrapure (TLR-4 agonist only) LPS (InvivoGen) or 200 U/mL IFN- γ (R&D Systems). Microglia were stimulated with 25 mM of potassium chloride to model excitatory conditions.

3.2.2 Primary astrocyte cultures

Astrocyte cultures were prepared similarly to primary microglia cultures. A mixed cortical cell suspension was prepared from E18 mice and seeded (Chapter 2.2.1) using the same plating media as listed above (Chapter 2.2.1). Media was changed every 2-3 days and astrocyte cultures were gently agitated to dislodge and remove any loosely adherent glia and neuronal debris to further purify the culture. By day 5, small patches of clustered astrocytes were seen throughout the well. By day 14, the culture was 80-90% confluent and was subsequently used for experiments. Astrocytes were treated with 200 U/mL of murine IFN- γ (R&D Systems) or 200 U/mL TNF- α (R&D Systems) for 24 and 48 hours.

3.2.3 Experimental autoimmune encephalomyelitis induction

All methods were carried out in accordance with the Canadian Council on Animal Care regulations and all experimental protocols were approved by the University of British Columbia Animal Care Committee. The EAE mouse model was chosen to mimic the inflammatory neurodegenerative disease processes. EAE was induced in male C57BL/6 mice that were 12-13 weeks old by 50 μ L subcutaneous injections of a myelin oligodendrocyte glycoprotein (MOG 35-55) (MEVGWYRSPFSRVVHLYRNGK; Stanford Pan Facility, Stanford, CA) peptide and complete Freund's adjuvant (CFA) emulsion in four different locations on their back and rear flanks, for a total of 200 μ L. Each 200 μ L of the emulsion contained 200 μ g of MOG, 100 μ L of 8 mg/mL working solution of CFA, and 100 μ L of PBS. CFA was made with 8 mg/mL of

H37Ra *Mycobacterium tuberculosis* (Difco Laboratories, Detroit, MI) emulsified in incomplete Freund's adjuvant. Mice were then injected intraperitoneally with 200 ng of pertussis toxin (List Biologicals, Campbell, CA), on days 0 and 2 days later. Mice were weighed, monitored, and scored daily for their clinical symptoms until day 90, where the mice were euthanized, flushed with PBS, and perfused with formalin. Mice were scored daily from 0-5 based on their level of disability (Table 3.1; Quandt Lab unpublished data). Their spleens, brains, and spinal cords were then removed. Age- matched littermates were not induced for EAE and were used as healthy controls.

EAE was also induced in 8-week old female C57BL/6 (Jackson Laboratory, Bar Harbor, ME) mice using the same method.

3.2.4 Spleen lysates

Spleens were harvested at day 45 from healthy female C57BL/6 adult mice or mice that were induced for EAE or received CFA only without the MOG peptide. The harvested spleens were minced into radioimmunoprecipitation assay (RIPA) buffer with 0.05% protease inhibitor cocktail (Roche). The spleen sample was then lysed in the RIPA buffer by passing the tissue up and down through a 21-gauge needle 20 times on ice. The samples were then centrifuged at 15,000 rpm and the supernatant was pipetted into a fresh, pre-chilled tube and immediately frozen at -20°C.

3.2.5 Immunohistochemistry

C57BL/6 mice spinal columns and brains were isolated from healthy mice and EAE mice by flushing with PBS, and subsequent perfusion and fixing with buffered formalin. Tissues were

Score	Clinical symptoms
0-0.5	0 no disease; 0.5 distal limp tail
1	Limp tail
2	Weakness in one or 2.5 in both hind limbs/ slippin on bars
3	Paralysis in one or 3.5 both hind limbs
4	(3.0) plus weakness in one or 4.5 in both forelimbs
5	Moribund

Table 3.1 EAE mouse clinical scoring guide (Quandt Lab, unpublished data)

fixed in 4% paraformaldehyde for 3-5 days and were subsequently washed in PBS before being submerged in a 30% sucrose solution for cryosectioning. Spinal cords were soaked in sucrose for a minimum of one week to allow for adequate permeation. Spinal cords were extracted from their columns by removing the vertebral column with forceps before being placed in 30% sucrose. Spinal cords were cut in four equal quarters and were embedded in optimal cutting temperature compound (OCT) (VWR, Radnor, PA) and frozen using an isopentane and dry ice slurry. Spinal cords were cut into 8 μm thick sections sampling three different regions (cervical/thoracic, lumbar, and sacral).

Sectioned tissues were blocked with 2% normal goat or horse serum for 1 hour and permeabilized with 0.05% triton. Tissues were incubated with antibodies to CD68 (BioRad), MAP2 (Sigma), CD68 (BioRad), GFAP (Abcam), or ARNT2 (Santa Cruz) antibody overnight. MAP2 was used to stain for neurons, GFAP for astrocytes, and CD68 for macrophages. After incubation, tissues were washed with TBST followed by a one-hour incubation with Alexafluor® 488, 568, or 648 conjugated (Thermo Fisher Scientific) secondary antibody at room temperature. Normal goat, chicken, rat, mouse, and rabbit IgG (Santa Cruz Biotechnology) antibodies were used as an isotype control. The specificity of the ARNT2 antibody was confirmed by the lack of ARNT2 staining by immunocytochemistry and by western blotting of primary cortical neurons after qPCR-confirmed knockdown with 3 separate ARNT2-targeting siRNA constructs by nanoparticle delivery (Precision NanoSystems Inc., Vancouver, BC) compared to scramble controls (data not shown).

Analysis was carried out with Zen 2 analysis software (Version 2.0.0.0, Oberkochen, DE). For each spinal cord, a section from the thoracic, lumbar, and sacral regions were analyzed. A binary mask was created for the grey matter using the fluorescent signal from MAP2 positive

neurons of the grey matter. The spinal cord image was divided in half sagittally and the total amount of GFAP positive astrocytes was electronically counted by having the software detect and count the fluorescent signal from GFAP positive cells and was then reconfirmed manually which was roughly 200-500 cells in total. Within each GFAP staining astrocyte, a binary mask was created from the DAPI fluorescence. The mask was then used to take the total fluorescent intensity of ARNT2. Similarly, a binary mask of the white matter was created using the fluorescent signal from GFAP positive astrocytes within the white matter. The total fluorescence intensity of ARNT2 in each DAPI positive nucleus was then quantified using a DAPI mask. The values of all of the cells within one sagittal half of a spinal cord were averaged. The values for each spinal cord section within the same mouse were then averaged, representing one mouse. The average value generated from each mouse was then pooled and averaged for analysis.

3.2.6 Lysate preparation and protein quantification

Treated cells were washed once in PBS and then immediately lysed with RIPA buffer and protease inhibitor cocktail on ice. Wells were scraped using mini cell scrapers. The cell lysate was then pipetted into a pre-chilled 1.5 mL microcentrifuge tube and centrifuged at 12,000xg for 10 minutes at 4°C. After centrifugation, the lysate was transferred to a new pre-chilled microcentrifuge tube and stored at -20°C.

A bicinchoninic acid (BCA) protein assay (Sigma B9643-1L) was used to quantify the concentration of protein within lysates. A standard curve was generated from a known concentration of bovine serum albumin (Thermo Fisher), with samples prepared in duplicate. 5 µL of each sample was added to a 96-well plate with 95 µL of a BCA and copper (II) sulphate

solution. Plates were then incubated at 37°C for 30 minutes with an absorbance of 570nm measured on a SpectraMax M2 microplate reader (Sunnyvale, CA).

3.2.7 SDS-PAGE and Western blot

Lysates were mixed with loading buffer and dithiothreitol and heated to 95°C for 5 minutes. Samples were separated on a 10% SDS precast gel (BioRad) and wet transferred to nitrocellulose membrane. The nitrocellulose membranes were incubated with primary antibodies against ARNT2 (Santa Cruz) at a 1 in 400 dilution. Glyceraldehyde 3-phosphate dehydrogenase (GAPDH) was also detected using a monoclonal primary antibody (Thermo Scientific) at a 1 in 2,000 dilution to serve as a loading control. Horseradish peroxidase conjugated goat anti-mouse and goat anti-rabbit (Jackson) secondary antibodies that were used to detect GAPDH and ARNT2 respectively. The BioRad Western ECL Substrate Kit (BioRad) was used for the visualization of the proteins. A BioRad ChemiDoc was used to image Western Blots and BioRad Image Lab (Version 5.0) was used to quantify protein for quantitative densitometry.

3.2.8 Statistical analysis

Western blot data from the spleens were analyzed using an unpaired t test. Treated astrocytes were analyzed by a one-way ANOVA with a Tukey's multiple comparisons test. An unpaired t test was used for the analysis of the immunohistochemistry. Statistical significance was determined as a p value of less than 0.05. All statistical analysis was done using GraphPad Prism 4 (GraphPad Software, Inc., San Diego, CA, USA).

3.3 Results

3.3.1 ARNT2 is upregulated in primary microglia when stimulated with LPS or IFN- γ

After 48 hours of treatment with LPS or IFN- γ , microglia were found to upregulate ARNT2 expression 4-fold higher than the expression seen in untreated microglia (Figure 3.1). Under excitatory conditions, potassium chloride was found to have no effect on the expression of ARNT2 with the expression value staying the same as untreated microglia (data not shown).

3.3.2 Splenocytes decrease ARNT2 expression in CFA-injected and EAE-induced mice

Two ARNT2 bands were detected in the spleen, one slightly above and another below the ARNT2 band seen in neurons at 79 kDa. This suggests a possible alternative splice variation or posttranslational modification of ARNT2 within immune cells in contrast to neurons. Spleens taken from our EAE mice at peak disease had a 4-fold decrease in expression compared to healthy controls ($p < 0.01$) (Figure 3.2). Similarly, our CFA-only control mice showed a significant reduction in ARNT2 expression when compared to healthy controls.

3.3.3 TNF- α and IFN- γ treatment does not alter ARNT2 expression in primary astrocytes

No significant change in ARNT2 expression was seen after 24 and 48 hours of stimulation with TNF- α and IFN- γ in primary astrocytes (Figure 3.3). At 24 hours, primary untreated astrocytes and TNF- α and IFN- γ treated astrocytes had similar ARNT2 expression. Similarly, at 48 hours both untreated and IFN- γ and TNF- α treated astrocytes had the same expression of ARNT2.

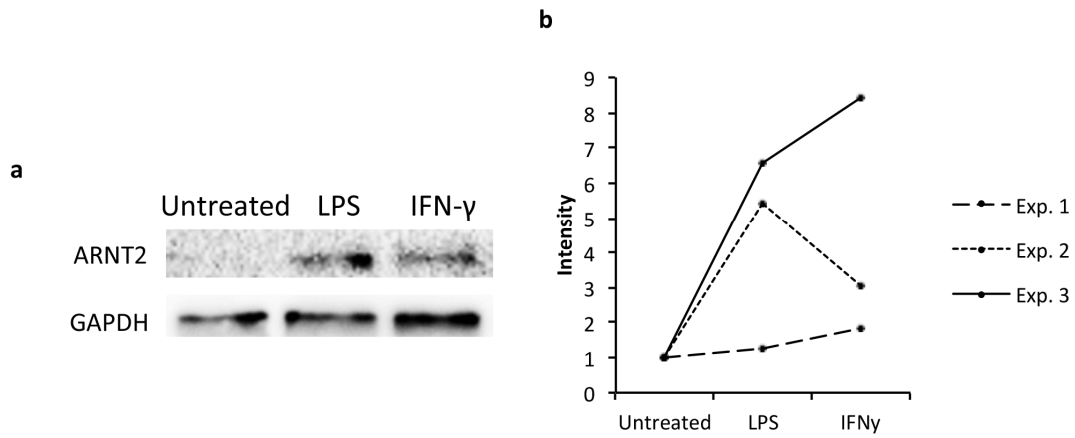


Figure 3.1 Primary microglia increase ARNT2 expression with exposure to inflammatory mediators. (a)

Primary microglia treatment with LPS and IFN- γ suggests an upregulation in ARNT2 expression. (b) LPS and IFN- γ treated microglia were both 4-fold greater in ARNT2 expression than untreated microglia (individual experiments, biological replicates). Average with standard deviation. One-way ANOVA with Tukey's multiple comparisons test (n=3).

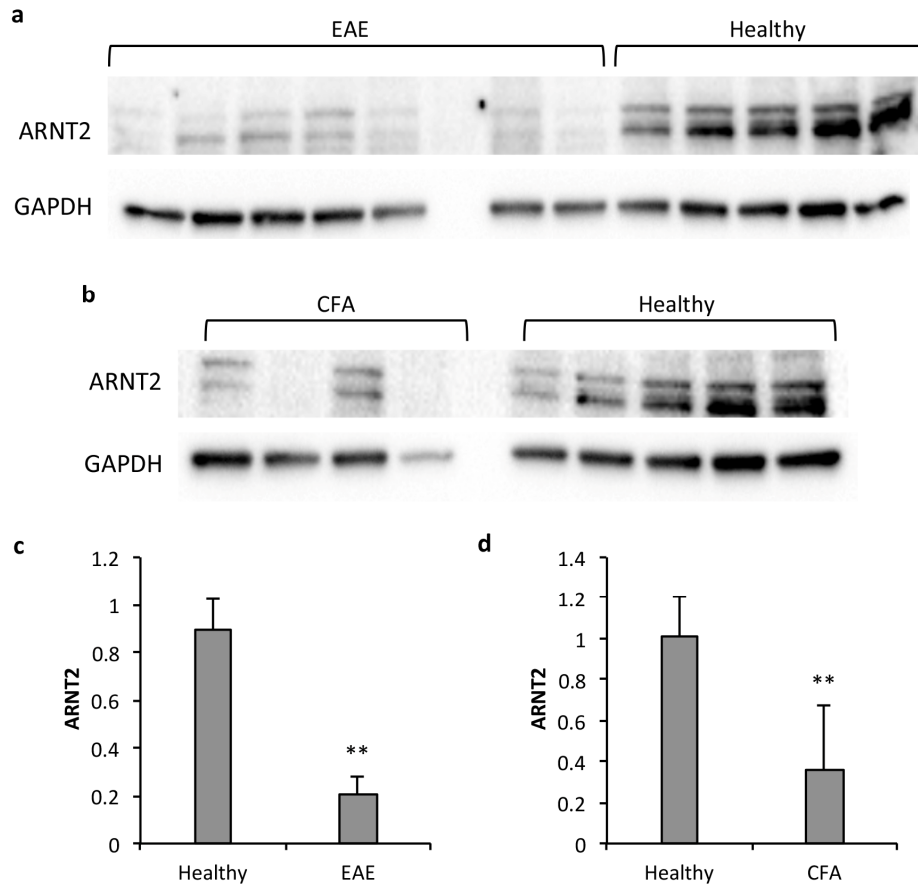


Figure 3.2 Inflammatory conditions decreased ARNT2 expression in spleens. (a and c) Relative ARNT2 expression was significantly decreased in EAE ($p=0.0025$) and (b and d) CFA ($p=0.0317$) spleens compared to healthy spleens from WT mice (Mann-Whitney test). ARNT2 expression normalized to GAPDH in EAE spleens was 4-fold lower than the healthy control. CFA spleens had a relative expression nearly 3-fold lower than healthy controls. Unpaired T-test. Average with standard deviation. ($n=5$ for healthy, $n=7$ for EAE, and $n=4$ for CFA spleens).

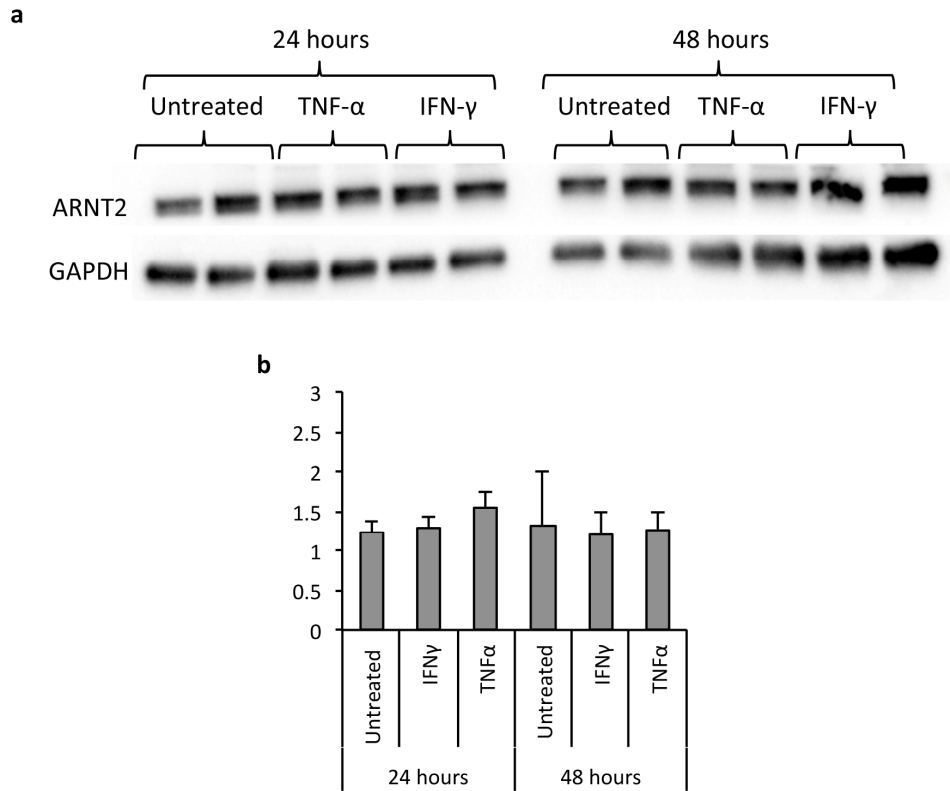


Figure 3.3 TNF- α and IFN- γ did not affect ARNT2 expression in primary astrocytes. (a) No changes in ARNT2 expression were seen between primary astrocytes treated with (b) IFN- γ or TNF- α in comparison to the untreated controls at 24 and 48 hours. One-Way ANOVA with Tukey Multiple Comparison Test. Average with standard deviation. (n=3).

3.3.4 ARNT2 is upregulated in GFAP positive astrocytes in EAE

EAE mice were monitored over the course of 60 days (Figure 3.4). Peak disease was observed at day 17 with an average score of 3.83 ± 0.05 with mice having limp tails, weakness in both hind limbs, and some forelimb weakness. Little to no recovery was observed in the EAE mice, remaining consistent in EAE score for the duration of the disease. Mice were culled and the tissues were harvested at day 60 with an average EAE score of 3.33 ± 0.14 . GFAP staining astrocytes were mainly seen towards the outer edge of the white matter of the spinal cord in healthy mice (Figure 3.5a). EAE mice had an increase in GFAP positive astrocytes within the white matter of the spinal cord in comparison to healthy controls (Figure 3.5c). In the white matter of healthy control mice, 39.6% of GFAP staining astrocytes were positive for ARNT2 with several astrocytes showing negligible expression (Figure 3.5b and e). In the white matter of EAE mice, 64.4% of all GFAP positive astrocytes expressed ARNT2, showing a near 3-fold increase in comparison to the healthy controls. White matter GFAP staining astrocytes had increased ARNT2 expression in EAE mice in comparison to the expression seen in astrocytes within the white matter of healthy mice ($p < 0.05$) (Figure 3.5b and d).

Within the grey matter of healthy mice, there were few GFAP positive astrocytes sparsely scattered throughout (Figure 3.6a) with the majority of the GFAP positive cells located near the central canal (Figure 3.6b). 5.2% of all cells within the grey matter of healthy mice were astrocytes staining positive for GFAP (Figure 3.6c). Within the grey matter of EAE mice, the amount of GFAP positive astrocytes significantly increased to 37.7% and were scattered throughout, and not primarily limited to the central canal (Figure 3.7b). The amount of astrocytes that were positive for ARNT2 was roughly 99% and was not significantly different between

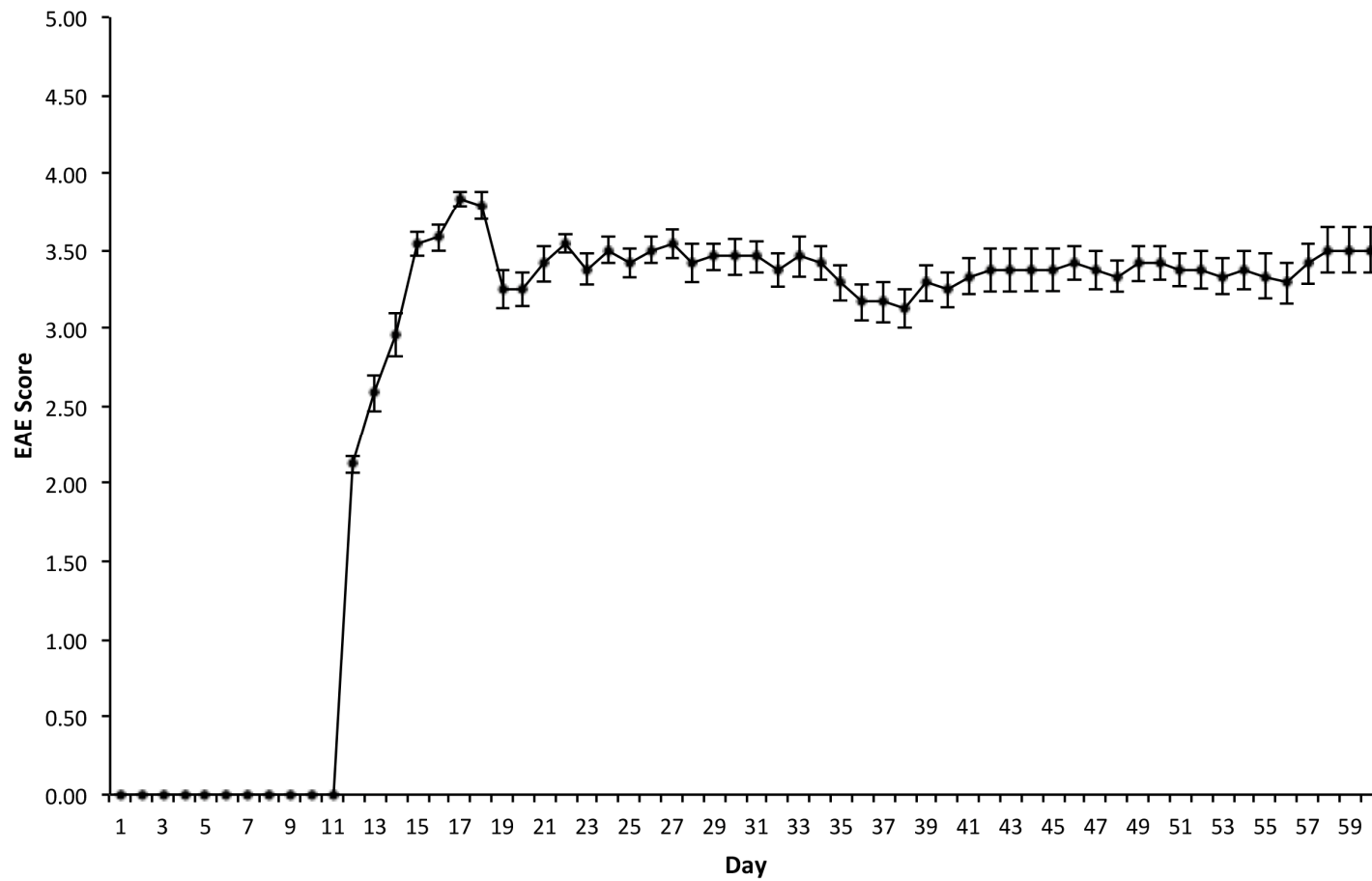


Figure 3.4 Average EAE score over 60 days. Peak disease was observed at day 17 with an average score of 3.83 ± 0.05 with mice having limp tails, weakness in both hind limbs, and some forelimb weakness. Little recovery in disease score was seen in the mice over the duration of the study. Mice were culled at day 60 with an average EAE score of 3.33 ± 0.14 . Average \pm Standard error of the mean. (n=5).

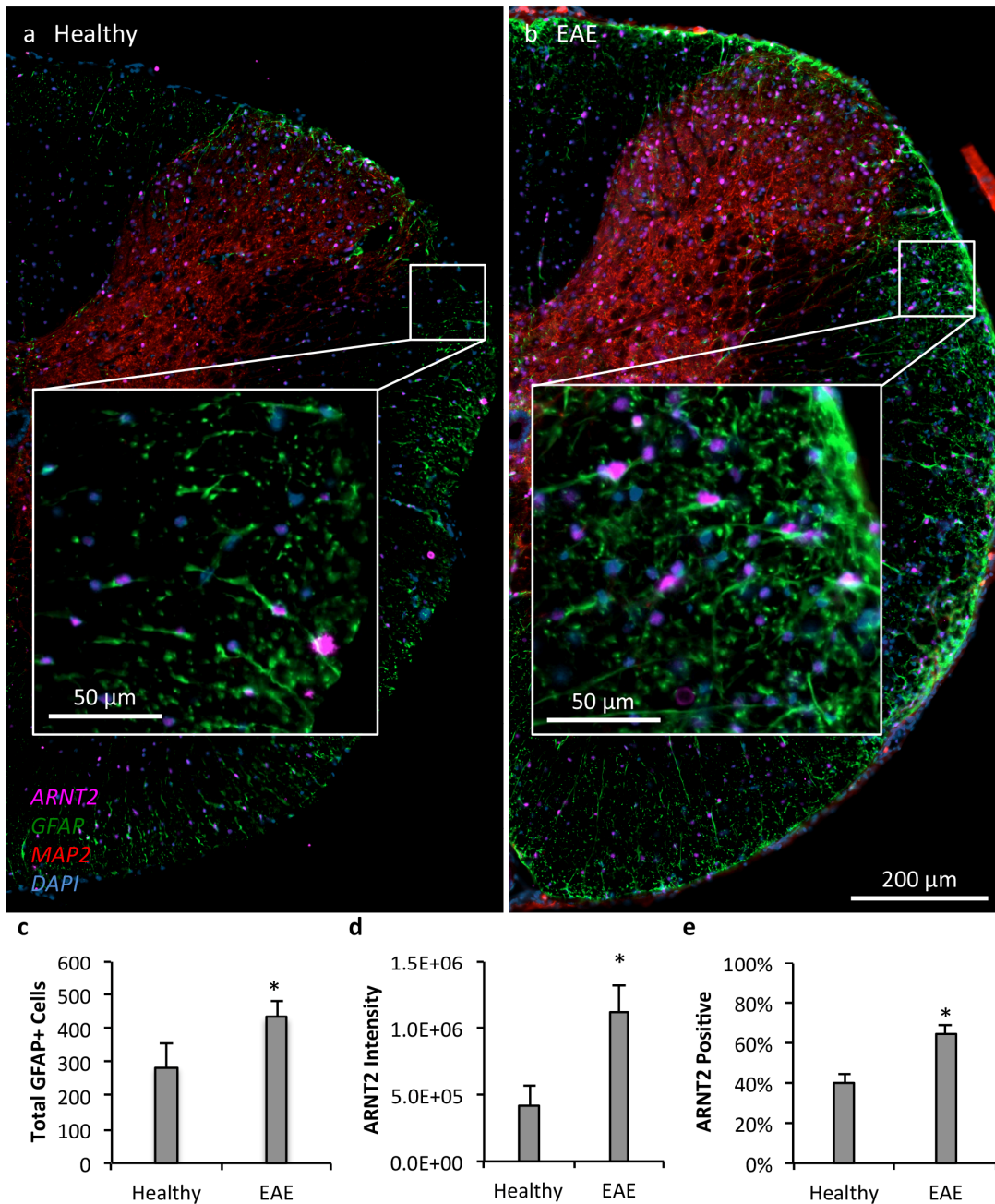


Figure 3.5 ARNT2 positivity and expression changes within white matter GFAP+ astrocytes. (a) White matter GFAP+ astrocytes in control spinal cord in comparison to (b) EAE induced mice. (c) ARNT2 and GFAP+ astrocytes increased significantly in the white matter of spinal cords in EAE induced mice ($p < 0.05$). (d) GFAP+ Astrocytes within the white matter of EAE induced mice had a significant increase in ARNT2 expression and (e) increased overall in ARNT2 positivity in comparison to control spinal cords. Unpaired T-test. Average with standard deviation. (n=4 for EAE; n=2 for healthy controls).

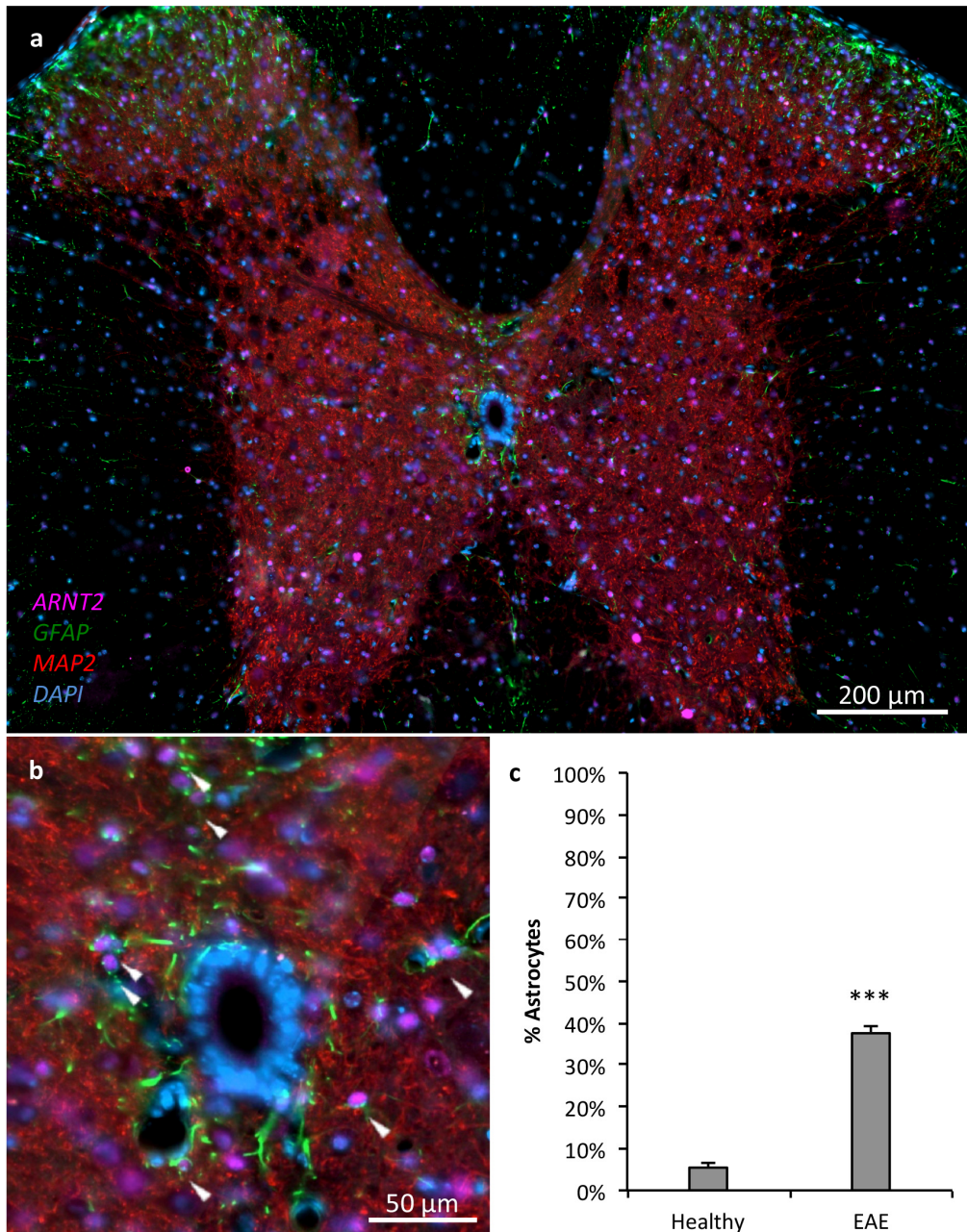


Figure 3.6 Astrocyte numbers increased in the grey matter of EAE mice. (a) GFAP+ astrocytes localized primarily around the central canal in healthy spinal cords with fewer GFAP+ astrocytes being found throughout the grey matter. (b) GFAP+ astrocytes throughout the grey matter (including those around the central canal) were 99.0% positive for ARNT2. (c) 5.3% of cells within the grey matter were GFAP+ astrocytes in healthy spinal cords, and significantly increased to 37.8% in EAE spinal cords ($p < 0.001$). Unpaired T-test. Average with standard deviation. (n=4 for EAE; n=2 for healthy controls).

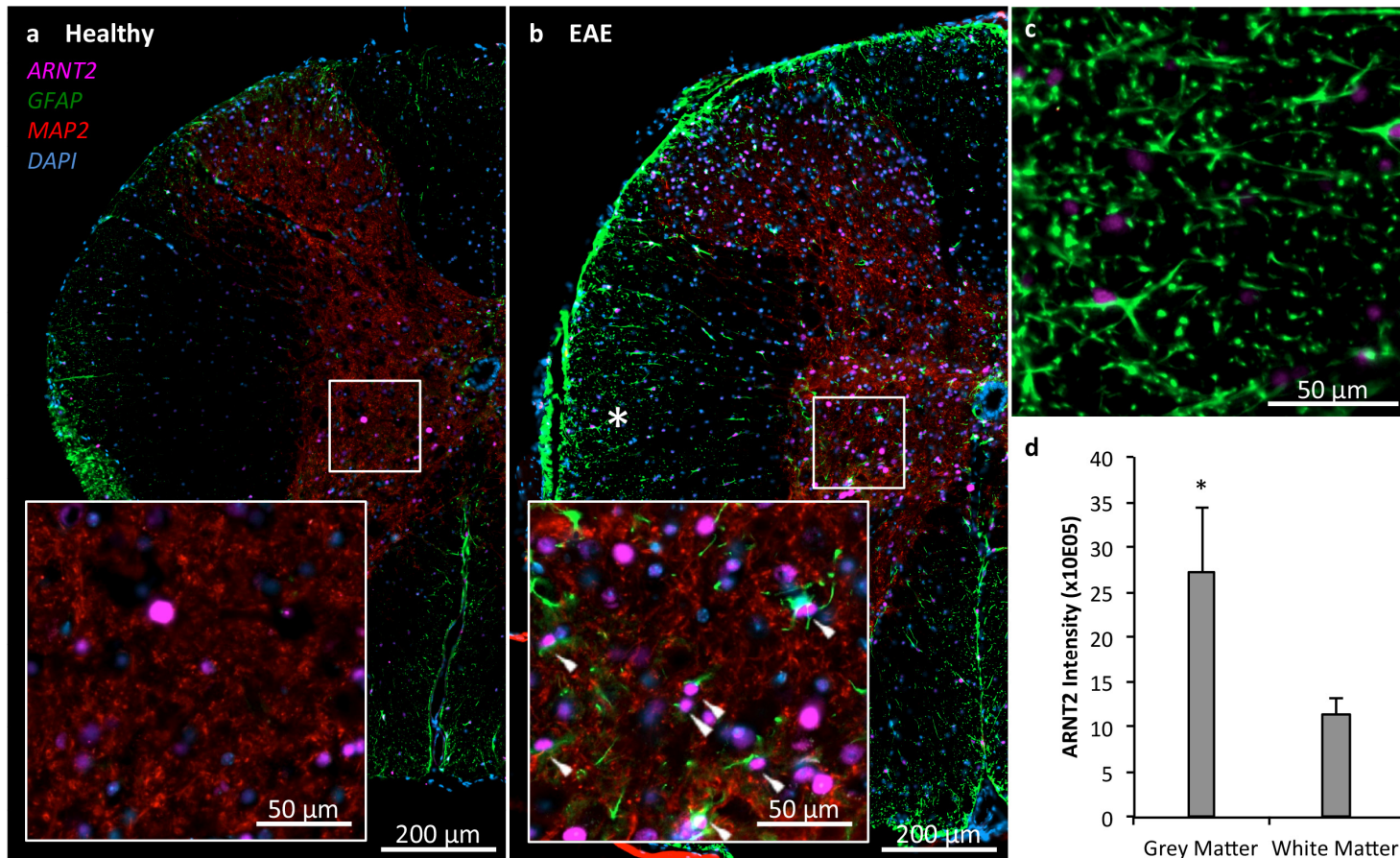


Figure 3.7 ARNT2 positive astrocytes accumulate in the grey matter of EAE mouse spinal cords. (a) Healthy spinal cords were devoid of GFAP+ astrocytes in the grey matter while (b) astrocytes (white arrows) appeared in the grey matter of EAE mice with the expression of ARNT2. (c) Higher magnification view of astrocytes (white asterisk) within a region of the white matter (b). (d) Astrocytes within the white matter of EAE mice had significantly lower ARNT2 expression than astrocytes located within the grey matter ($p < 0.05$). Unpaired T-test. Average with standard deviation. (n=4 for EAE mice; n=2 for healthy controls).

healthy and EAE mice. The expression of ARNT2 was not significantly different between grey matter astrocytes in healthy and EAE mice.

ARNT2 expression within the grey matter of EAE mice was significantly increased in GFAP positive astrocytes in comparison to ARNT2 expressing astrocytes within the white matter of both healthy and EAE mice ($p < 0.05$).

Preliminary studies were performed to characterize ARNT2 expression in CD68 positive immune cells within the immune infiltrates of EAE mice. Some CD68 positive macrophages were observed to be positive for ARNT2 expression (additional analyses are ongoing, including the assessment of ARNT2 expression in Iba-1 positive microglia).

3.4 Discussion

In this study, we characterized the expression of ARNT2 in immune cells *in vitro* and under inflammatory neurodegenerative disease conditions *in vivo*. In previous studies, analysis of ARNT2 expression has been focused primarily on neurons. However, our study shows that several cells of the immune system, along with glia, were found to be positive for ARNT2 expression. ARNT2 was expressed in splenocytes and microglia. This novel finding suggests a potential functional role for ARNT2 in immune cells, likely regulating transcription processes.

Primary microglia showed a significant upregulation in ARNT2 expression after stimulation with LPS or IFN- γ . This suggests that ARNT2 is important in the modulation of the inflammatory response by microglia as they become activated, and that inflammatory mediators play a role in regulating ARNT2 expression. Microglia are extremely sensitive to changes in extracellular potassium, which is indicated by their very specific and unique set of potassium channels that can detect excess potassium (possibly due to a pathological event that could result

in CNS damage). However, ARNT2 did not change expression with exposure to potassium chloride, suggesting that ARNT2 is not regulated under excitatory conditions, but only under inflammatory conditions in microglia.

The immunomodulatory role of ARNT2 is further supported by the downregulation of ARNT2 in spleens collected from EAE-induced and CFA-injected mice. This suggests that the activation of the immune system with pertussis and *Mycobacterium tuberculosis* in CFA was sufficient to downregulate ARNT2 expression, without the needed addition of MOG peptide and the presence of chronic inflammatory disease. The downregulation of ARNT2 within the spleen suggests what may be a differential regulation or function of ARNT2 in one or more of the cell types within the spleen (B cells, T cells, splenic macrophages, and dendritic cells) in comparison to microglia, where LPS and IFN- γ stimulation suggested an upregulation of ARNT2 *in vitro*. A cell specific analysis such as flow cytometer would better address ARNT2 expression in distinct populations which may be changing in numbers, rather than relative expression changing within a cell subset.

In contrast, the expression of ARNT2 within primary astrocytes was not altered after treatment with TNF- α or IFN- γ . This indicates that ARNT2 may not be regulated by inflammatory conditions within primary astrocytes, and may not be the drivers behind altered ARNT2 expression in EAE. This differed from what was seen with the primary microglia. This could be due to a functional difference of ARNT2 depending on its location and role. Conversely, in the EAE model, GFAP positive astrocytes were found to significantly change their expression of ARNT2 in comparison to healthy controls. ARNT2 was increased overall in GFAP positive astrocytes but expression was the greatest in the astrocytes located in the grey matter. This suggests a differential regulation of ARNT2, where the presence of degenerating

neurons or factors that are present in the grey matter and less so in the white matter mediates ARNT2 expression. While GFAP-negative astrocytes have indeed been localized to the spinal cord, they were not included in our analyses¹⁷⁵.

To our knowledge, this is the first study to characterize ARNT2 expression within astrocytes and to describe its modulation *in vivo*. One study examined GFAP positive cells within the substantia nigra and found that they did not express ARNT2¹⁷⁶. Another study examined ARNT2 expression in astrocytes *in vitro* and found low levels in mixed cortical populations. However, the regulation and function were not explored¹⁷⁷.

This study presents the novel finding that ARNT2 is expressed in GFAP staining astrocytes *in vivo* and that expression is increased within these cells in EAE mice during chronic inflammatory disease. This study is also the first to characterize ARNT2 expression within microglia. The characterization of ARNT2 in both astrocytes and microglia under inflammatory and neurodegenerative disease conditions suggests a protective role for the protein that could be potentially targeted by novel therapeutics to alter disease onset and progression.

3.5 Limitations

This study looked at primary astrocytes and microglia and their expression of ARNT2 at two time points (24 and 48 hours) *in vitro*. However, earlier time points should be considered to see when the expression of ARNT2 actually begins to increase. As well, TNF- α stimulation was only looked at in astrocytes but not in microglia. Similarly, only microglia were treated with LPS while astrocytes were not. For continuity in the characterization of ARNT2 expression within astrocytes and microglia, both need to be treated with LPS and TNF- α respectively. Another

cytokine that is increased under neurodegenerative conditions includes IL-1 β ⁷⁰. IL-1 β could be used to treat both astrocytes and microglia to characterize its effect on ARNT2 expression.

Our *in vivo* study only looked at ARNT2 expression in EAE mice late in disease. It would be beneficial to see ARNT2 expression immunohistochemically in EAE mice that are culled at peak or acute disease to see which cells are expressing ARNT2. This would strengthen the correlation found between the upregulation of *Arnt2* mRNA at peak disease with protein expression (Unpublished data, Quandt Lab).

Another limitation of the *in vivo* study is that only GFAP positive astrocytes were taken into consideration for analyses. The grey matter of the spinal cord consists of several protoplasmic astrocytes¹⁷⁸. However, these astrocytes did not stain positively for GFAP. These astrocytes could be included for analysis by using different markers in future studies. In future studies, SOX9 could be used in combination with GFAP to allow better distinction of astrocyte staining, as GFAP is primarily found within the cytoplasm while SOX9 is a nuclear marker of astrocytes. This would allow for the co-localization of the expression of ARNT2 within astrocytes.

Although this study shows the upregulation of ARNT2 in astrocytes *in vivo* and microglia *in vitro*, the functions and targets of ARNT2 as a transcription factor has not been characterized in these cells.

3.6 Future directions

Although the upregulation of ARNT2 was seen under inflammatory conditions, further studies need to be conducted to look at how these conditions affect ARNT2 target proteins. As there was no prior description of ARNT2 expression within astrocytes, the potential transcription

targets have yet to be identified. Potential binding partners for ARNT2 in astrocytes (outside of potential homodimers) have not been identified to date. One likely downstream product based on ARNT2 expression in neurons and an ARNT2 binding region in BDNF, is the growth factor BDNF. This could be addressed by looking at the expression of BDNF by Western blot, qPCR, or ELISA when microglia are treated with either LPS or IFN- γ . BDNF expression could be correlated with ARNT2 expression by the silencing and overexpression of ARNT2 in both astrocyte and microglial cultures to test the effects on BDNF transcription and translation. Silencing the expression could be achieved by a knockdown with nanoparticles, viral transfection, electroporation, or lipofectamine to deliver ARNT2-targeting siRNA. Overexpression of ARNT2 could be achieved by the transfection of microglia with a vector carrying the ARNT2 gene.

Our *in vivo* studies showed that ARNT2 expression could be modulated within astrocytes. Consequently, other factors need to be tested in primary astrocytes to determine their ability to influence ARNT2 expression. This includes factors that have been shown to drive the activation of astrocytes that are apparent as stellation increases, such as isoproterenol, dibutyryl-cAMP, ADP, and ATP^{179,180}.

Previous studies have shown that ARNT2-knockout mice result in perinatal lethality¹⁸¹. However, conditional knockout mice for ARNT2 could be generated where ARNT2 can be temporally regulated using Cre-lox that has been combined with an estrogen receptor. This would allow for temporal regulation through the injection of tamoxifen that would bind to the estrogen receptor. This results in the translocation of the Cre-lox protein to the nucleus where the *Arnt2* gene will be cleaved, preventing expression. The functional role of ARNT2 in specific cells such as astrocytes and neurons could also be furthered studied by using conditional

knockout mice for ARNT2 by crossing a loxP-flanked *Arnt2* mouse with another mouse where Cre recombinase is inserted at a cell-specific promoter such as GFAP in astrocytes.

Chapter 4: Receptor Mediated Endocytosis – 8 expression within the CNS

4.1 Introduction

Receptor mediated endocytosis-8 (RME-8), also known as Hsp40 homolog, subfamily C, member 13 (DNAJ13), is a protein involved in vesicular trafficking. It uncoats clathrin-coated vesicles and regulates receptor trafficking in early endosomes¹¹⁹. Silencing of RME-8 results in the disruption of epidermal growth factor receptor and mannose-6-phosphate receptor mediated endocytosis shown by irregular perinuclear clusters of the receptors as well as a decrease in the ligands bound by these receptors¹²². In *Caenorhabditis elegans* RME-8 was found in macrophage-like coelomocytes, where it co-localizes to the membrane of large endosomes with endocytosis markers suggesting a possible function of RME-8 in phagocytic leukocytes¹²⁴.

In a subset of hereditary adult-onset autosomal dominant Parkinson's Disease, RME-8 was found to be the common mutated gene (p.(N855S)) between the individuals screened¹²⁰. This suggests that RME-8 may have a greater role in neurodegenerative diseases. RME-8 interacts with retromer proteins and the Wiskott-Aldrich syndrome protein and SCAR homolog (WASH) complex, two group of proteins that when mutated have been associated with neurodegenerative diseases^{122,123}. This suggests that the role of these proteins is key to axonal survival and function. A loss in RME-8 results in an increase in unsorted protein-containing branched endosomal tubules further suggesting the importance of RME-8 in endosomal trafficking¹⁸². The fibroblast-like COS7 cell line when transfected with the mutated copy of RME-8 and treated with transferrin, a ligand dependent on receptor mediated endocytosis for uptake, resulted in fewer internalized vesicles in comparison to cells with the wild type copy. This indicates that the mutated copy of RME-8 resulted in a functional alteration that affected the endosomal pathway. Notch – a protein important in cell fate, proliferation, and differentiation –

can induce pathological cell signalling when RME-8 is depleted¹⁸³. The Notch signalling pathway has been found to play an important role in the differentiation of progenitor cells into astrocytes¹⁸⁴⁻¹⁸⁶. The mutation of RME-8 has also been linked to essential tremor¹²¹. This further suggests a role of RME-8 in neurological function. No previous studies of RME-8 have been conducted within cells of the CNS to characterize its normal function or role in neurodegenerative pathologies that are mediated by inflammation.

The study outlined below is a preliminary characterization of RME-8 expression by cells of the CNS and also the functional role of RME-8 in primary murine microglia. Microglia were treated with LPS or IFN- γ to assess the effects of pro-inflammatory stimuli on RME-8 expression. Microglial function was assessed by their ability to phagocytose particles. The role of RME-8 in neurodegenerative disease was assessed in the complex *in vivo* setting of EAE, the prototypical autoimmune demyelinating model of MS. Specifically, our study aims include to:

1. Examine whether the cytokines (TNF- α and IFN- γ) influence the expression of RME-8 in primary astrocyte cultures.
2. Assess RME-8 function in primary microglia by the phagocytosis of dextran in wild type and RME-8 mutant microglia.
3. Characterize EAE in wild type, heterozygous, and homozygous RME-8 mutant knock-in mice for changes in the severity of clinical disease attributable to mutations.
4. Identify the spatial and temporal expression of RME-8 and its regulation in inflammatory neurodegenerative disease using the EAE mouse model.

4.2 Materials and methods

4.2.1 Primary microglia and astrocyte cultures

Primary microglia and astrocytes were cultured as previously described in chapter 2 and 3. CL57BL/6 mice that were heterozygous or homozygous for the p.(N855S) mutation in RME-8 (generously provided by Dr. Milnerwood) were used to supply RME-8 deficient microglia for our primary cultures. The specificity of the RME-8 antibody was determined by the knockdown of RME-8 expression using siRNA (Milnerwood Lab, unpublished data) that was confirmed by the decrease in RME-8 expression in the COS7 cell line transfected with RME-8 by Western blot.

4.2.2 Human cerebral microvascular endothelial cell line (hCMEC/D3) cultures

The hCMEC/D3 cell line was cultured according to previous studies¹⁸⁷. The hCMEC/D3 cell line was seeded and cultured on type I collagen-coated plates in endothelial cell growth medium-2 (EGM-2)(Lonza Group, Basel, CH), completed with 5% FBS (GE Healthcare, Little Chalfont, UK), ascorbic acid (Sigma), penicillin-streptomycin (Gibco), hydrocortisone (Sigma), chemically defined lipid concentrate, (Gibco) and HEPES (Sigma). The culture was grown until cells were 90-95% confluent.

4.2.3 Primary mouse lung fibroblasts

Previous studies have shown RME-8 expression in fibroblasts¹¹⁹. Mr. Anthony Tam generously provided a primary mouse lung fibroblast lysate established from explants for use as a positive control in western blotting experiments.

4.2.4 Oregon Green® dextran phagocytosis assay

A 10,000 molecular weight Oregon Green® conjugated dextran (Thermo Fisher) was added at a concentration of 100 µg/mL to microglia that were used untreated or following pretreatment with IFN- γ or LPS for 24 hours. Treatments were seeded in triplicate and cells were incubated with the dextran for 6, 12, or 24 hours. The uptake of the fluorescently tagged dextran was quantified using a Molecular Devices SpectraMax M2 microplate reader (Sunnyvale, CA) that was used in chapter 3.

4.2.5 Flow cytometry

Microglia were analyzed for expression of phenotypic markers CD11b, CD11c, CD45, inflammatory molecules MHC class I and II, CD39, CD40, CD80, and CD86 as previously described in chapter 2. Briefly, microglia were reseeded to 6-well plates and stimulated for 24 and 48 hours with LPS or IFN- γ . Adherent microglia were then trypsinized and pooled with non-adherent microglia. The pooled samples were centrifuged and washed twice with PBS before being resuspended in staining buffer (1% FBS plus 0.05% sodium azide in PBS). Cells were then incubated with Fc block for 15 minutes before being incubated with fluorescently tagged antibodies as described in chapter 2.2.3. Flow cytometry analysis was performed using a MACSQuant flow cytometer (laser capability, seven color) (Miltenyi, Auburn, CA) and analyzed using FlowJo software (Version 7.6.5; Treestar, Ashland, OR). Cells were gated on the basis of size with forward and side scatter, excluding cell debris to establish the populations for analysis.

4.2.6 Spleen lysates

Spleen lysates were prepared as previously described in chapter 3. Briefly, spleens were harvested from healthy C57BL/6 adult mice or mice that were induced for EAE. Minced spleens were further lysed in RIPA buffer and 0.05% protease inhibitor cocktail by passing the tissue up and down through a 21-gauge needle 20 times on ice. Subsequent samples were centrifuged, the supernatant was decanted and collected in another tube, and immediately frozen at -20°C.

4.2.7 Lysate preparation and protein quantification

Primary cell lysates were prepared and quantified as previously described in chapter 3. Briefly, treated cells were washed once in PBS and were immediately incubated with RIPA buffer and 0.05% protease inhibitor cocktail. The wells were placed on ice and scraped using mini cell scrapers. The lysates were collected and further lysed by pipetting up and down 15 times. Samples were centrifuged and the supernatant was collected and frozen at -20°C.

A BCA protein assay was used to quantify sample protein concentrations. In duplicate, 5µL of each sample or BSA standard of known concentration was added to a 96-well plate with 95 µL of a bicinchoninic acid and copper (II) sulphate solution. Plates were then incubated at 37°C for 30 minutes. A SpectraMax M2 microplate reader was used to measure the absorbances at 570nm.

4.2.8 SDS-PAGE and Western blot

SDS-PAGE and Western blot were conducted as previously described in chapter 3. For every experiment, an equal amount of protein was loaded onto the gel. Lysates were mixed with loading buffer and DTT and heated to 95°C for 5 minutes before being loaded into a 10% SDS

gel and transferred to nitrocellulose membrane. The membranes were incubated with primary antibodies against RME-8 (generously given to us by Dr. Milnerwood) at a 1 in 400 dilution or GAPDH at a 1 in 2000 dilution. After incubation with the primary antibodies, the membranes were washed and incubated with an HRP-conjugated secondary antibody (Jackson ImmunoResearch Labs, Baltimore Pike, PA). The blots were then incubated with BioRad Western ECL Substrate Kit.

4.2.9 EAE induction

Drs. Austen Milnerwood and Matthew Farrer generously provided RME-8 mutant knock-in transgenic mice. Briefly, mutant RME-8 knock-in mice were generated using FLP-FRT recombination. An FRT-flanked neomycin cassette containing the human RME-8 gene was inserted on chromosome 9 in C57BL/6 template mice between exons 22 and 23. A cassette containing the human N855S mutated RME-8 gene was introduced into exon 24. Using Cre-lox recombinase, wild type exons 23-56 were deleted. The human *Rme-8* gene is 82% homologous to the *Rme-8* gene found in mice¹⁸⁸. With the *Rme-8* gene being similar in sequence between both mouse and human, we expect the functionality of the protein to be the same between species. The RME-8 mutant mice were used to characterize the functional role of the protein under inflammatory neurodegenerative disease conditions using the RME-8 mutation to represent a loss of function. The RME-8 mutation has been previously shown to have a loss of function by the accumulation of intracellular vesicles in RME-8 mutant cortical neurons (Milnerwood lab, Unpublished data).

EAE was induced in 12-13 week old male C57BL/6 mice that were either wild type, heterozygous or homozygous for the RME-8 mutation. Mice received 50 μ L subcutaneous

injections of a myelin oligodendrocyte glycoprotein peptide 35-55(MOG 35-55) (MEVGWYRSPFSRVVHLYRNGK; Stanford Pan Facility, Stanford, CA) and complete Freund's adjuvant (CFA) emulsion in four different locations on their back and rear flanks, for a total of 200 μ L. Each 200 μ L of the emulsion contained 200 μ g of MOG in 100 μ L of PBS and 100 μ L of 8 mg/mL H37Ra *Mycobacterium tuberculosis* (Difco Laboratories, Detroit, MI) emulsified in incomplete Freund's adjuvant. Mice were then injected intraperitoneally with 200 ng of pertussis toxin (List Biologicals, Campbell, CA) and again 2 days later. Clinical disease was monitored over 90 days with daily scoring of motor symptoms related primarily to ascending paralysis. The examiner was blinded to the phenotype of the mice until the end of the study.

4.2.10 Immunohistochemistry

Immunohistochemistry was done as previously described in chapter 3.2.5. Healthy non-immunized mice and EAE mice were culled 90 days post EAE induction. Mice were perfused and fixed with formalin. Spinal cords were isolated from healthy and EAE induced mice and the vertebrae were removed before being washed and transferred into 30% sucrose. The spinal cords were cut into four equal quarters. Spinal cords were cryosectioned at 8 μ m in thickness and were stained for RME-8, MAP2, CD68, and GFAP. MAP2 was used to stain for neurons, CD68 for macrophages, and GFAP for astrocytes.

Three regions of the spinal cord (cervical/thoracic, lumbar, and sacral) were qualitatively analyzed from four EAE mice and two healthy controls. Images were acquired using fluorescent and phase contrast microscopy with a Zeiss Axio Observer Z1 microscope with Zen 2 acquisition and analysis software (Version2.0.0.0, Oberkochen, DE). The entire spinal cord from each of the

three regions of the spinal cord from two healthy and four EAE mice were analyzed to discern whether RME-8 was observed in GFAP positive astrocytes, MAP2 positive neurons, CD68 positive macrophages, or ependymal cells lining the central canal or in non-characterized cells associated with inflammatory infiltrates. Where RME-8 staining was detected in a specific cell type or region, positivity was reported as present or absent. Individual filter channels were analyzed for the localization of RME-8 expression with cell specific markers.

4.2.11 Statistical analysis

Both the phagocytosis assay data and Western blot data were analyzed using an unpaired t test. RME-8 expression by astrocytes was analyzed by a one-way ANOVA with a Tukey's multiple comparisons test. The EAE cumulative scores were analyzed using a one-way ANOVA with a Tukey's multiple comparisons test. Statistical significance was determined as a p value of less than 0.05. All statistical analysis was done using GraphPad Prism 4 (GraphPad Software, Inc., San Diego, CA, USA).

4.3 Results

4.3.1 RME-8 is highly expressed in primary microglia

Preliminary Western blot analysis of primary cell cultures showed that microglia had constitutively the highest relative expression of RME-8 in comparison to primary astrocytes, cortical neurons, and the hCMEC/D3 cell line (Figure 4.1a). Microglial expression was 1.8-fold higher than astrocytes, which were the second highest RME-8 expressing cell (Figure 4.1b). The hCMEC/D3 cell line and murine cortical neurons had 1.3 and 4.1-fold less RME-8 expression than microglia respectively. Previous studies have shown high levels of RME-8 expression in

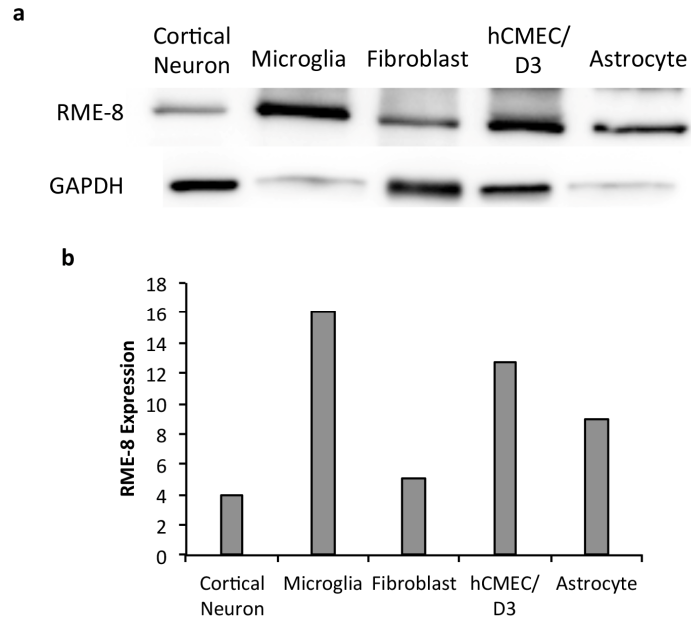


Figure 4.1 RME-8 is expressed in several CNS related cell types. (a) Preliminary data suggests primary mouse cortical neurons, microglia, and astrocytes, and the hCMEC/D3 cell line all express RME-8 in comparison to the fibroblast positive control. (b) Microglia had the highest expression of RME-8, followed by the hCMEC/D3 cell line and astrocytes. The cortical neurons had the lowest expression. Equal protein was loaded for each cell type with RME-8 being normalized to GAPDH expression for each cell type in 4.1(b). (n=1).

fibroblasts-like cells therefore primary mouse lung fibroblasts were used as a positive control for our study¹²⁰.

4.3.2 Microglia derived from wild type and RME-8 mutant knock-in mice react similarly to treatment with LPS and IFN- γ

Primary microglia cultured from homozygous RME-8 mutant knock-in mice and wild type mice were treated with either LPS or IFN- γ for 24 and 48 hours (Figure 4.2) to model responses to mediators that are typically described as drivers of microglia activation in infectious or inflammatory disease settings. Preliminary data suggest that phenotypic markers CD11b, CD11c, and CD45 did not differ in expression in untreated and treated cells 24 and 48 hours post treatment. Inflammatory markers CD39, CD40, CD80, CD86, MHC class I and II also did not differ in expression between the RME-8 mutant knock-in and wild type microglia after 24 and 48 hours of stimulation. Stimulus specific CD40, CD80, and CD86 were similarly increased accordingly in RME-8 mutant knock-in microglia, as observed in microglia established from wild type animals (particularly as observed in chapter 2.3.3 after treatment with IFN- γ)

4.3.3 RME-8 deficient microglia have reduced ability to phagocytose Oregon Green® dextran

Homozygous RME-8 mutant knock-in microglia showed a significant reduction in the uptake of Oregon Green® dextran in comparison to wild type microglia (Figure 4.3). At 6 and 12 hours of treatment with dextran, there were no significant changes seen in dextran uptake across all treatment groups. Dextran uptake peaked at 24 hours for wild type microglia while

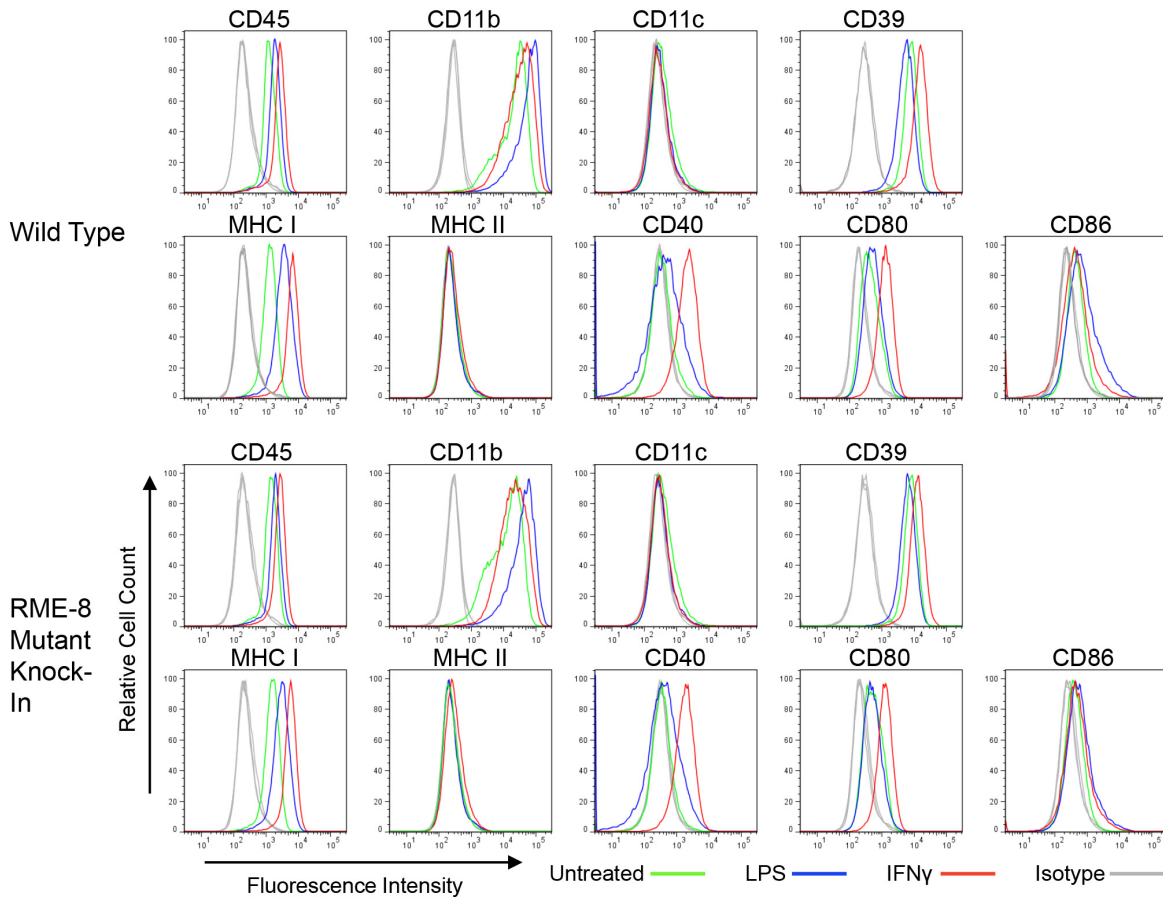


Figure 4.2 Wild type and RME-8 mutant knock-in microglia exhibit no change in inflammatory marker expression patterns. Preliminary data show wild type and homozygous RME-8 mutant microglia specifically upregulated phenotypic and inflammatory markers after stimulation with LPS or IFN- γ after 24 and 48 hours of exposure. Upregulation in markers were similar to what was seen in chapter 2.3.3. (n=1)

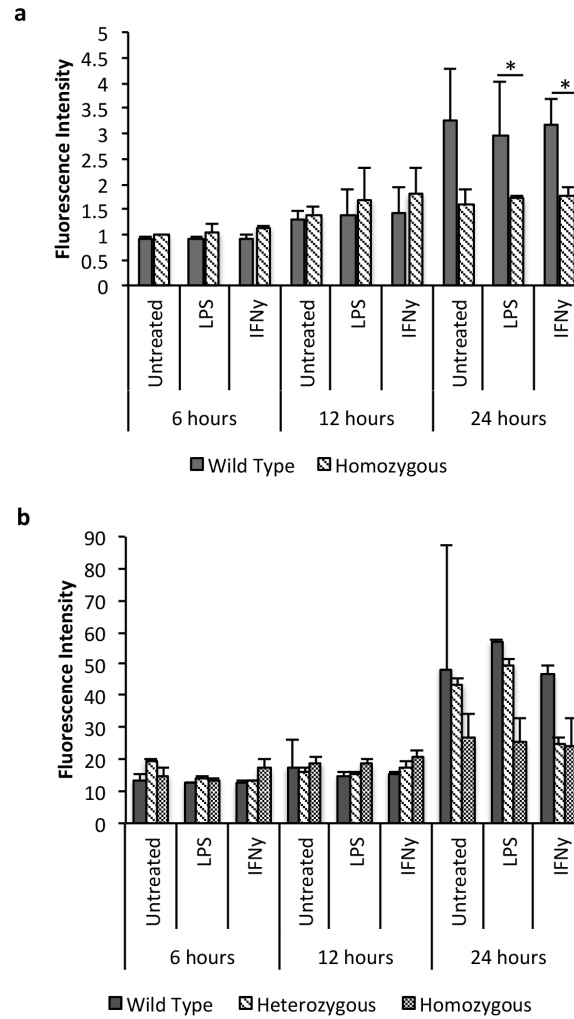


Figure 4.3 RME-8 mutant microglia have decreased phagocytosis of Oregon Green® dextran. (a) RME-8 mutant mice had a significant increase in internalized dextran independent of treatment with LPS or IFN- γ in comparison to wild type microglia by 24 hours of exposure ($p < 0.05$). Unpaired T-test. Standard deviation. ($n=2$). (b) Preliminary data show that RME-8 heterozygous mutant microglia have intermediate fluorescence intensity with fluorescence being highest in wild type microglia and lowest in homozygous mutant microglia. Standard deviation between triplicates. ($n=1$)

homozygous RME-8 mutant microglia showed similar uptake from 6 to 24 hours. Untreated wild type microglia had a fluorescence intensity that was 2-fold higher in comparison to RME-8 mutant microglia at 24 hours. Preliminary data suggests the reduction in dextran uptake in heterozygous RME-8 mutant knock-in microglia. Microglia treated with LPS or IFN- γ did not have a significant change in baseline dextran uptake. However, a significant decrease in uptake was still observed between homozygous mutant RME-8 knock-in microglia in comparison to wild type independent of treatment with LPS or IFN- γ . LPS-treated wild type microglia had a fluorescence intensity that was nearly 2-fold higher in comparison to RME-8 mutant microglia. Similarly, IFN- γ treated wild type microglia had a fluorescent intensity that was nearly 2-fold higher than RME-8 mutant microglia.

4.3.4 RME-8 expression remains constant in EAE-induced mouse spleens

Western blotting of splenic lysates collected from EAE-induced mice at peak disease showed no significant change in RME-8 expression in comparison to healthy controls (Figure 4.4). Similarly, CFA treated mouse spleens had no significant change in RME-8 expression in comparison to healthy control spleens.

4.3.5 Neither TNF- α nor IFN- γ affect RME-8 expression in astrocytes

Primary astrocytes were treated with TNF- α or IFN- γ and were analyzed for RME-8 expression by Western Blot (Figure 4.5). There was no significant change in RME-8 expression seen after 24 or 48 hours of stimulation with either cytokine in comparison to untreated astrocytes.

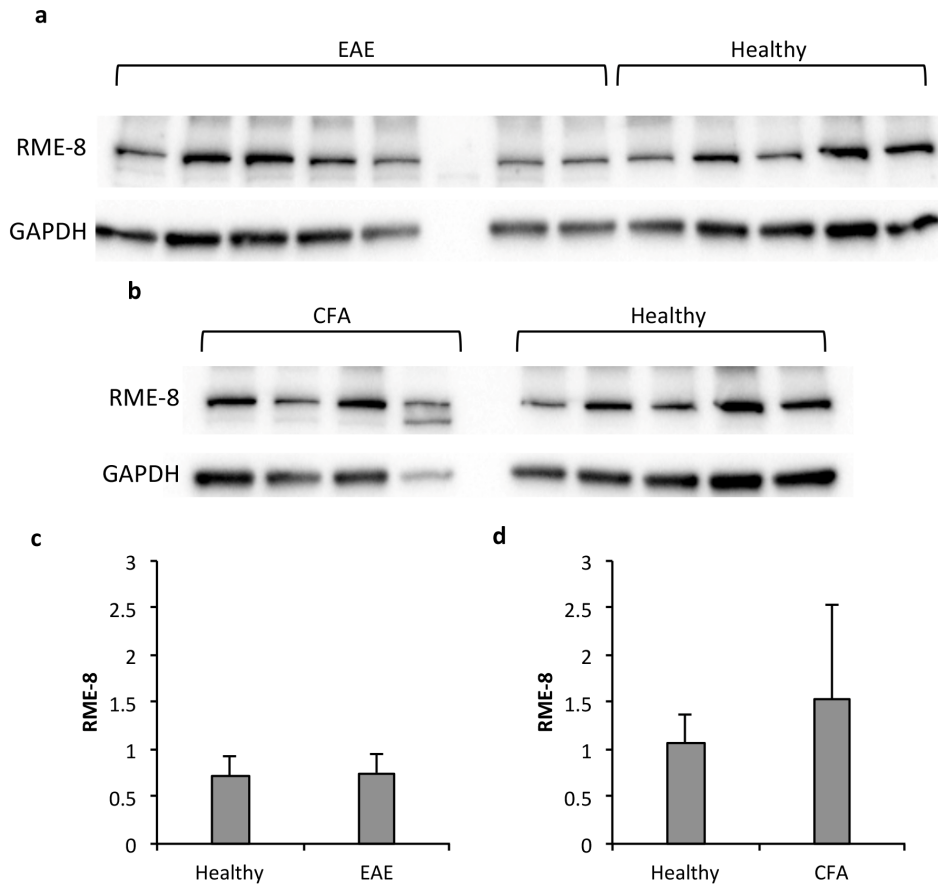


Figure 4.4 No changes in RME-8 expression was seen between healthy, CFA only, and EAE mouse spleens.

(a) RME-8 expression did not change between EAE and healthy spleens or (b) CFA and healthy spleens. (c) RME-8 expression in EAE spleens was not significantly different in healthy spleens. (d) CFA spleens were not significantly different in RME-8 expression in comparison to healthy spleens (Unpaired T test). Average with standard deviation. RME-8 expression was normalized to GAPDH. (n=5 for healthy, n=7 for EAE, and n=4 for CFA spleens)

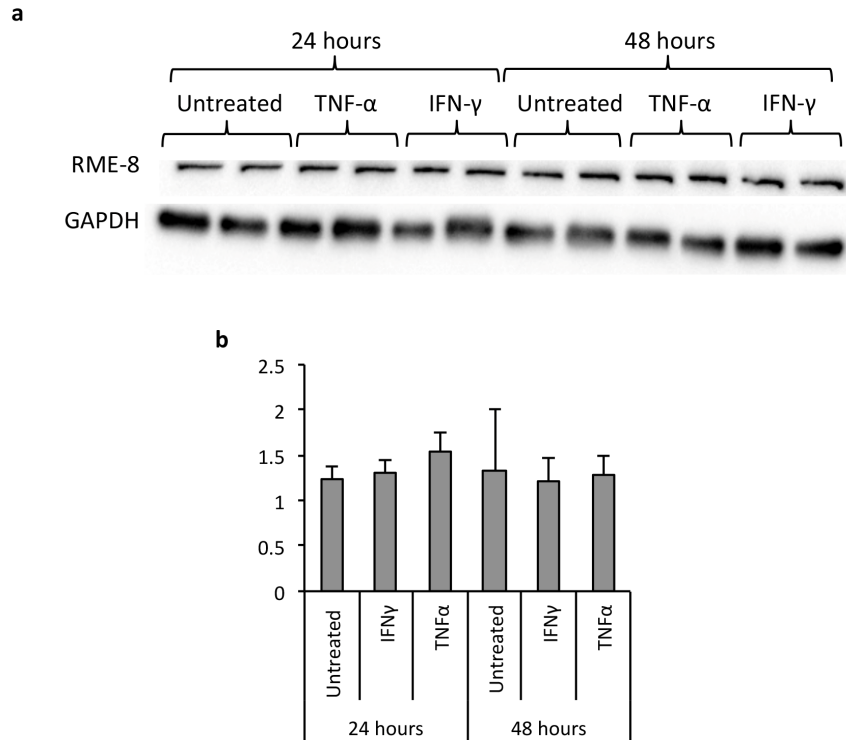


Figure 4.5 Inflammatory cytokines IFN- γ and TNF- α did not alter RME-8 expression in astrocytes. (a) No change in RME-8 expression was seen between astrocytes treated with IFN- γ or TNF- α in comparison to the healthy controls at 24 and 48 hours. (b) At 24 hours, the relative expression of RME-8 was not significantly different between untreated and IFN- γ and TNF- α treated astrocytes respectively. No change in expression was observed at 48 hours across all treatment groups. One-Way ANOVA with Tukey Post Comparison Test. Average with standard deviation. (n=3).

4.3.6 RME-8 mutant mice tend to have less severe clinical disease when immunized for EAE

Heterozygous and homozygous mutant RME-8 knock-ins and wild type mice immunized and induced for EAE had peak disease around day 17 (Figure 4.6). There was no change in day of disease onset between RME-8 knock-in and wild type mice where clinical symptoms were observed roughly around the same time. Heterozygous and homozygous knock-in mutant RME-8 mice appeared to have lower average disease severity with an average disease score of 2.87 and 2.90 respectively in comparison to wild type EAE induced mice that had a score of 3.36. However this study was not sufficiently powered in order to be able to draw conclusions about the significance of the change.

4.3.7 RME-8 is expressed in neurons, astrocytes, and ependymal cells in healthy spinal cord tissue and in CD68 positive immune infiltrates in EAE mice

In healthy mice, RME-8 was expressed in GFAP positive astrocytes (Figure 4.7). RME-8 was also expressed by motor neurons with the majority of the expression being seen throughout the soma. Ependymal cells lining the central canal showed intense staining for RME-8. In a parallel analysis of spinal cords from EAE mice, preliminary results suggest RME-8 expression intensity was increased in astrocytes within the white matter (Figure 4.7f). However, a more quantitative assessment and analysis are required.

CD68 positive cells were not present in healthy mouse spinal cords (Figure 4.8a). In regions of immune infiltrates, RME-8 expression occasionally co-localized with immune infiltrates, specifically CD68 cells (Figure 4.8b).

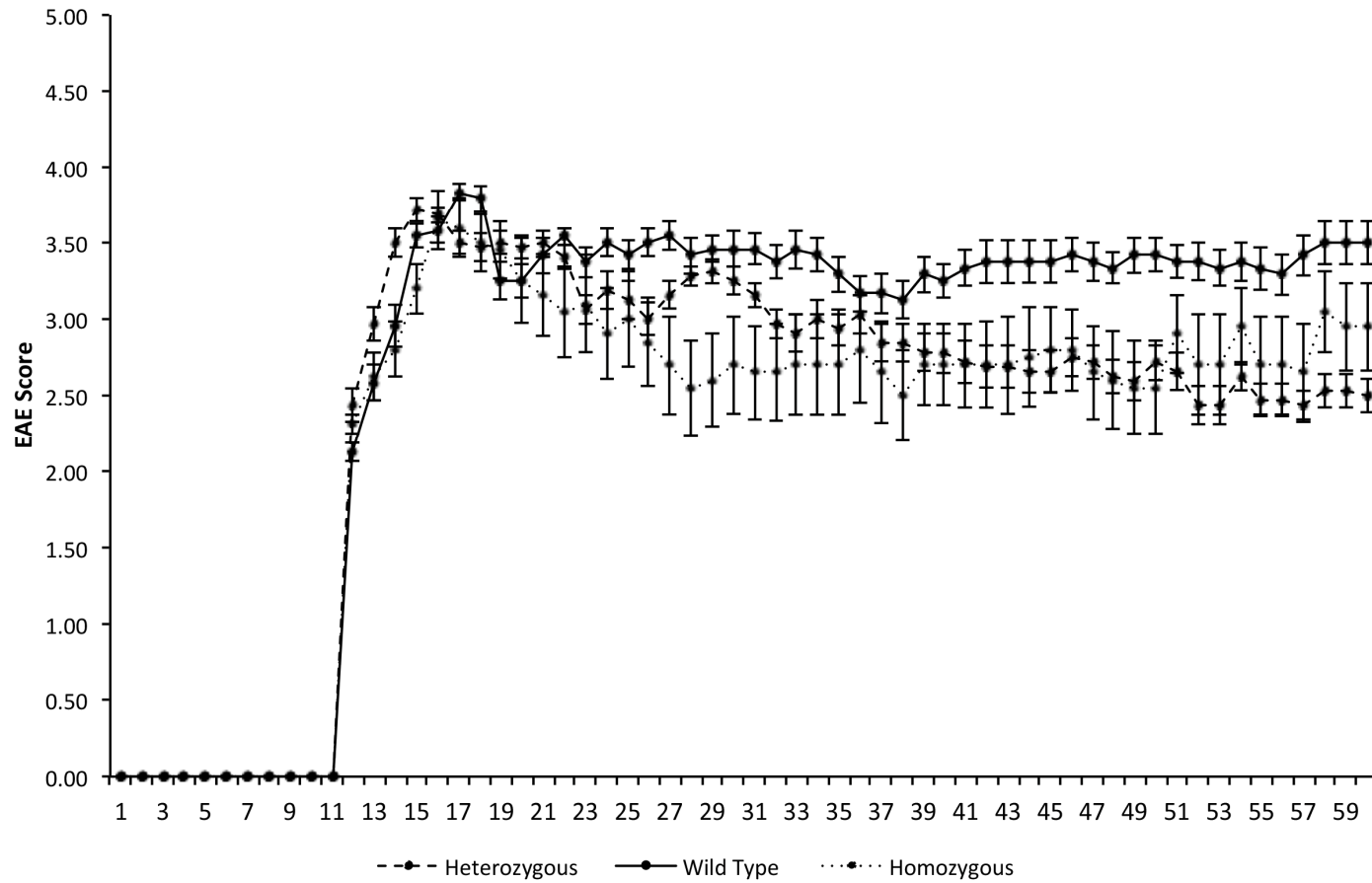


Figure 4.6 EAE disease scores were decreased in RME-8 mutant knock-in mice. Heterozygous and homozygous RME-8 mutant mice tended to have lower disease severity in comparison to wild type EAE induced mice. Wild type mice had an average disease score of 3.36 ± 0.10 , and 2.87 ± 0.09 , and 2.90 ± 0.23 in the heterozygous and homozygous RME-8 mutant mice. Average with standard error of the mean. (n=6 for wild type, n=8 for heterozygous, n=5 for homozygous).

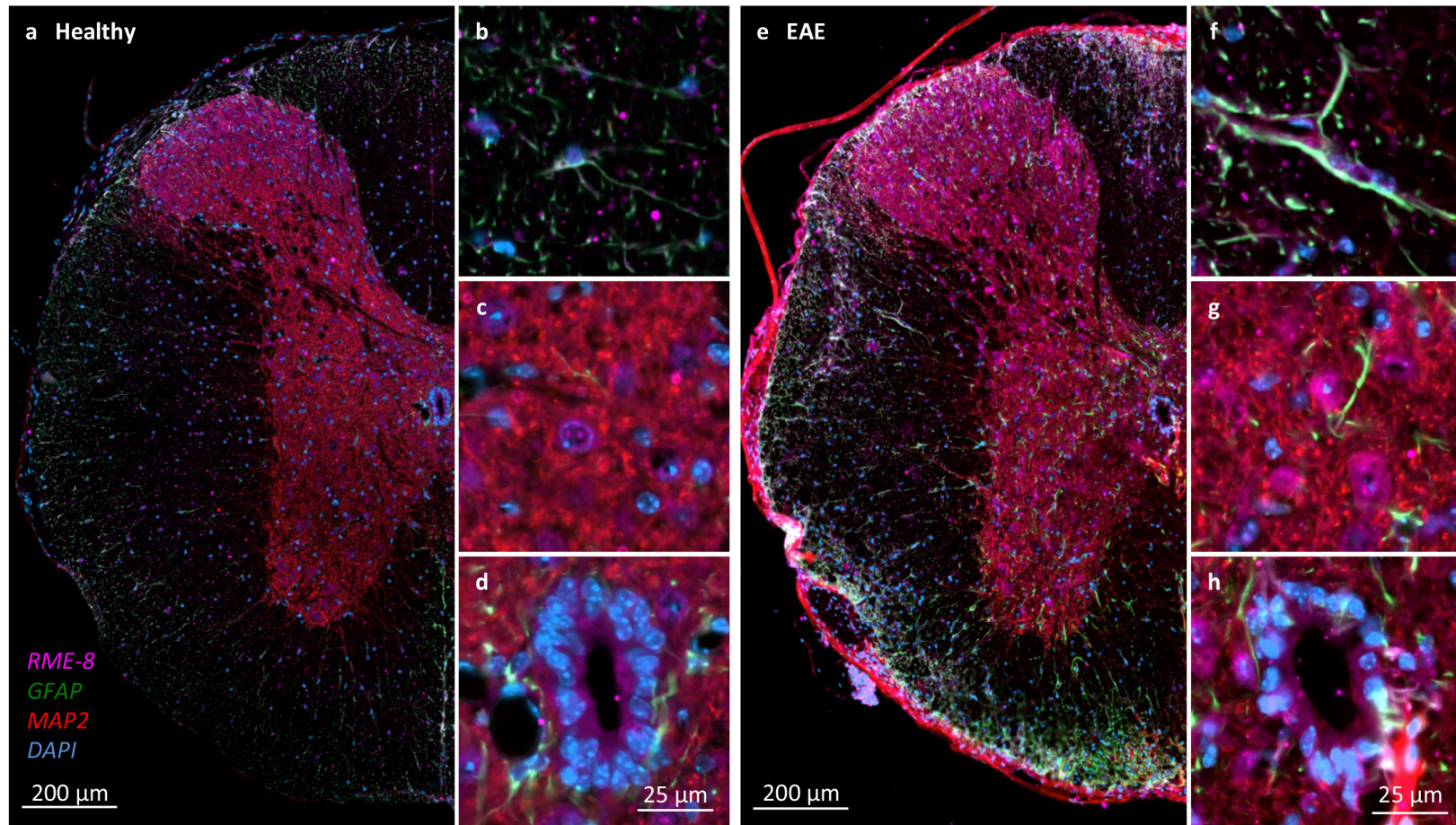


Figure 4.7. Neurons, astrocytes, and ependymal cells express RME-8. (a) RME-8 is expressed by several cells within the spinal cord of healthy mice such as (b) GFAP positive astrocytes (green), (c) MAP2 positive neurons (red), and (d) ependymal cells. (e) RME-8 expression appears to be enhanced in EAE spinal cords in (f) astrocytes and (g) neurons. In mice from each treatment group, one section from each of the cervical/thoracic, lumbar, and sacral region was analyzed. (n=2 for healthy; n=4 for EAE)

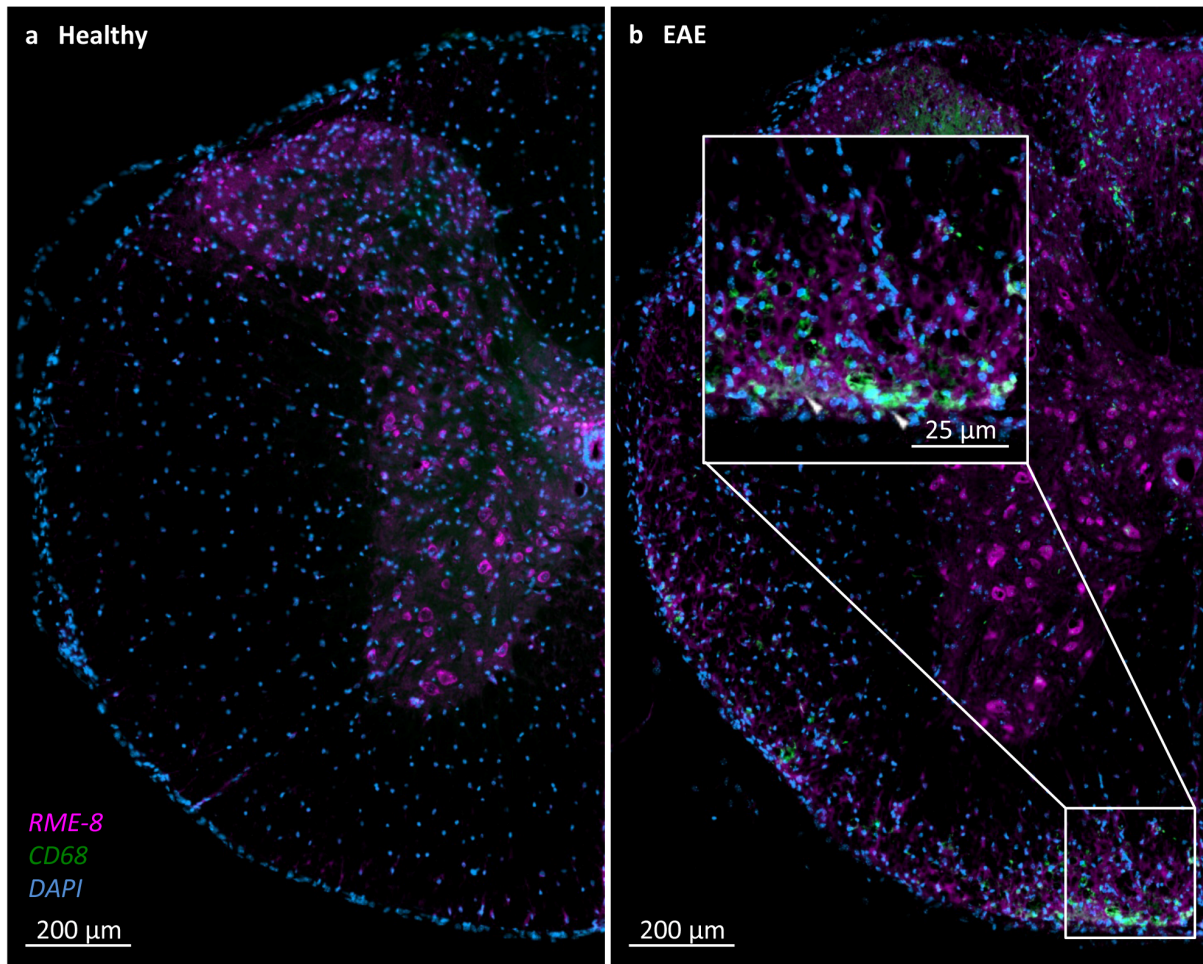


Figure 4.8. CD68 positive cells express RME-8. (a) Healthy spinal cords contained no cells positive for CD68. (b) CD68 positive immune infiltrates localizes with RME-8 expression in EAE mouse spinal cords (white arrows). (n=2 for healthy; n=4 for EAE)

4.4 Discussion

RME-8 has previously been shown to play a role in neurological function where mutations within the *Rme-8* gene resulted in both Parkinson's disease and essential tremor^{120,121}. However, the characterization of this protein in specific cell types of the CNS has yet to be investigated. This study characterized the expression and function of RME-8 in microglia and established the expression in primary cortical neurons, astrocytes, and the hCMEC/D3 cell line. RME-8 was found to be ubiquitously expressed by all primary cells tested, with the highest expression of RME-8 being observed in microglia, followed by astrocytes. This suggests that RME-8 may play a role in functionality of cells within the CNS, especially in glial cells or may simply be influenced by the inflammatory mediators at the time: a functional role as opposed to an association would need to be investigated.

RME-8 mutant microglia show a similar response to wild type microglia when treated with either of the inflammatory mediators tested, LPS and IFN- γ . However, the phagocytosis of Oregon Green® dextran was decreased in homozygous mutant RME-8 knock-ins. This suggests that RME-8 plays a role in phagocytosis in microglia. Dextran is able to be bound by the mannose receptor for its uptake into immune cells^{189,190}. The mannose receptor plays a crucial role in the activation of the innate and adaptive immune systems where the receptor is able to recognize terminal mannose, N-acetylglucosamine and fucose residues on glycans attached to proteins (glycoproteins) found on several bacteria¹⁹¹. The uptake of the mannose receptor and its ligand is determined by receptor-mediated endocytosis¹⁹²⁻¹⁹⁴. Taken together, this suggests that this mutation in RME-8 directly or indirectly impairs the uptake and endosomal trafficking of the mannose receptor. This is consistent with previous studies where endosomal-mediated receptors such as the mannose 6-phosphate receptor or epidermal growth factor receptor, have defective

recycling and uptake when RME-8 is non-functional¹²². This is also consistent with a previous study where RME-8 was found to play an important functional role in macrophage-like coelomocytes¹²⁴.

In preliminary studies using the EAE mouse model, the defined mutation in the RME-8 gene is associated with a trend to decreased disease severity in comparison to wild type mice. However, significance cannot be drawn from the conclusions, as the study was not powered to detect the small differences observed in disease severity. The decrease in EAE score observed could be attributed to a lack of MOG phagocytosis and subsequent antigen presentation during disease induction. MOG is a glycoprotein expressed by oligodendrocytes and is found in myelin¹⁹⁵; and is an essential component in inducing EAE. The development of a T cell response against MOG is essential for MOG EAE requiring sufficient uptake of the protein for antigen presentation and T cell activation. Subsequent myelin uptake via the mannose receptor has been shown in microglia and macrophages¹⁹⁶. Consequently, since RME-8 plays a role in the endosomal trafficking of mannose receptor-mediated uptake, the possible decrease in disease severity observed could be possibly due to the lack of MOG uptake by antigen presenting cells resulting in an attenuated immune response. Since the EAE model requires the generation of myelin-specific autoreactive T cells to help drive disease pathogenesis¹⁹⁷, without adequate antigen uptake and antigen presentation, fewer activated autoreactive T cells would be produced. One must also consider the role microglia play in the process of CNS repair via the uptake and clearance of myelin debris to allow for the remyelination of axons²⁶. A lack of MOG uptake for antigen presentation would translate to a limited disease severity, reducing the need for phagocytosis-mediated repair within the CNS.

Neurons, astrocytes, and ependymal cells in healthy spinal cords expressed RME-8. This suggests that endosomal trafficking by RME-8 of proteins and molecules in and out of the cell is important to the function of these cells. The constitutive expression of RME-8 in astrocytes, neurons, and ependymal cells with a potential increase in RME-8 expression in EAE mice further implicates RME-8 in the CNS response to insult or injury. Ependymal cells line the central canal and are involved in the production and movement of cerebrospinal fluid to clear metabolic waste from cellular interstitial fluid surrounding tissues⁹. Consequently, an increase in RME-8 expression in ependymal cells may illuminate a role for RME-8 in the clearance of toxic metabolites formed from damaged neurons, infiltrating immune cells, and activated microglia and astrocytes. RME-8 expression within neurons may be essential to the shuttling of proteins throughout the axon necessary for neuronal function. Subsequent damage to the axon in EAE mice and the upregulation of RME-8 may suggest a compensatory mechanism to shuttle neurotrophic factors or other proteins needed for axonal function and perhaps even regeneration.

Immune infiltrates were only seen in EAE spinal cords and were frequently CD68 positive with the rest of the cells possibly being T or B cells. CD68 positive cells also co-localized with RME-8 expression. CD68 is expressed primarily by macrophages but is also expressed by microglia^{48,198}. The co-localization of CD68 with RME-8 could suggest the type of function and role that the immune cell has in disease where the phagocytosis of myelin and cellular debris could be enhanced in these RME-8 positive cells.

Our study has shown that alterations in RME-8 can alter the phagocytic potential of microglia. Primary cortical neurons, astrocytes, and the hCMEC/D3 cell line express RME-8. Our *in vivo* study suggests potential differences in disease severity between wild type and RME-

8 mutant mice induced for EAE. Together these studies highlight what may be an important role for RME-8 in the CNS under healthy and inflammatory conditions.

4.5 Limitations

A limitation to this study is that the RME-8 mutation introduced into the mice has yet to be completely characterized for its functionality and whether or not this mutation results in a gain or loss of function and to what degree. Instead, a partial and complete knockdown of RME-8 in wild type microglia using siRNA would be a preferred model to characterize the function of RME-8 for *in vitro* studies.

A cell specific conditional RME-8 knockout mouse would be most effective to see the influence on disease within the CNS in a better-defined setting. As well, if the RME-8 mutant knock-in mice are unable to phagocytose and present the MOG antigen to T cells, the disease severity could vary drastically in comparison to wild type mice. Consequently, this would make studying the effect of the loss of RME-8 function and how this affects the repair process within the CNS under inflammatory conditions difficult if the EAE induction is already limited. A passive model of EAE where T cells are removed and treated *ex vivo* with MOG before being reintroduced back into a naive animal could potentially resolve how the processes of priming versus the effector phases of disease are affected. Another method would be to use an inducible Cre-lox recombination system where RME-8 knockdown could be induced after EAE induction.

4.6 Future directions

We characterized the functionality of RME-8 using RME-8 mutant knock-in mice. For our studies, we used a mutated copy of the RME-8 gene that was already available in the

laboratory of collaborators to investigate the possible role of RME-8 in phagocytosis and associated contributions to EAE. The RME-8 mutation has been previously described as having a loss of function where cytoplasmic accumulations of vesicles are seen in cortical neurons carrying the RME-8 mutation (Milnerwood Lab, Unpublished data). However, another experiment using a complete knockdown in comparison to a partial knockdown of RME-8 using siRNA delivered by nanoparticles, lipofectamine, viral vector, or electroporation would validate and expand upon our data generated using the RME-8 mutant microglia for a true assessment of RME-8 function.

The overexpression of functional RME-8 in microglia and its effect on cell function and response to inflammatory mediators should also be characterized further.

The role of RME-8 in the internalization of the mannose receptor could be confirmed by using fluorescently tagged anti-mannose receptor antibodies to specifically induce the uptake of the receptor in RME-8 knockdown and untreated microglia.

Antigen presentation plays an important role in the EAE model to initiate disease through the uptake and presentation of the MOG peptide on the MHC class II molecule for binding and activation of T cells via CD4 stimulation. This results in the formation of autoreactive T cells and the initiation of inflammation and disease. To test the role of RME-8 in antigen presentation, a co-culture with ovalbumin-specific T cell receptor transgenic OT-I or OT-II T cells could be used to assess the efficiency of antigen presentation by MHC class I and II in microglia respectively with and without a knockdown in RME-8.

Previous studies have shown RME-8 interacts with cell membrane remodeling proteins, which may suggest a possible role for the protein in the formation of lamellipodia. Cell migration

assays using transwell membranes with ATP, a known chemoattractant of microglia, could be used to further assess the importance of RME-8 within microglia.

Our preliminary EAE study suggests the RME-8 mutant knock-in mice had decreased disease severity. However, the study was not sufficiently powered to be able to see a significant change. Therefore, the study could be repeated using a sufficient number of mice. Using the preliminary data set generated, a sample size of 24 mice is required in each sample group in order to reach a power of 80% with a type 1-error rate of 5%. Furthermore, with the mutation in place throughout the induction, priming and effector phases of disease, it was not possible to see whether reduced priming or reduced demyelination may be behind a trend towards reduced disease. Because the peak disease at acute stages was however, rather similar, one is tempted to infer that differences exist at the level of recovery from the acute demyelinating event.

Lastly, although the spleen was analyzed for changes in RME-8 expression in healthy and EAE mice, RME-8 expression and function could still be characterized in other immune cells, most notably, phagocytic cells. As our data suggested that RME-8 plays a role in phagocytosis, peripheral blood mononuclear cells (PBMCs) could be isolated and analyzed for changes in RME-8 expression as peripheral blood contains neutrophils, monocytes, and a few dendritic cells, which are all able to phagocytose.

Chapter 5: Conclusion

5.1 Summary

Microglia play an integral role in the modulation of disease pathogenesis in several inflammatory neurodegenerative diseases including MS. In these diseases, microglial activation and subsequent release of inflammatory cytokines and ROS, along with an increase in phagocytosis, has been thought to play a role in disease severity. However, several studies have shown that the microglia-mediated phagocytosis and clearance of cellular debris by microglia under neurodegenerative conditions is important in the reparative process of the CNS²⁶. Consequently, the study of microglia is important for a better understanding of their role and function in disease, and how experimentally modulating protein expression within these cells can alter their function. This will give a better insight into the characterization of the possible roles for these proteins in influencing microglial contributions to disease onset or progression.

In this study, primary microglial cell cultures were grown using GM-CSF to potentiate the proliferation of microglia from embryonic mouse tissue. The characterization of these cells showed a microglial cell phenotype with a low expression of inflammatory molecules similar to microglia *in vivo* confirming their relevance for use in analyses. Our subsequent studies showed that LPS and IFN- γ stimulation resulted in the upregulation of T cell co-stimulatory molecules CD40, CD80, and CD86. Along with the upregulation of these inflammatory molecules, LPS also increased IL-6, IL10, TNF- α , and CCL2 release. Our untreated GM-CSF cultured microglia were found to be negative for Iba-1 which indicates that our cultured microglia were not activated in nature, making these cells a good model for immune modulating studies. The addition of IL-4 to our cultures with GM-CSF did not significantly change the phenotype of the GM-CSF cultured microglia. This showed that the addition of GM-CSF to our microglia did not

significantly alter their inflammatory profile and that our cells were in a naïve, non-differentiated state comparable to their *in vivo* counterparts.

Using our primary microglial model, we investigated two proteins: the transcription factor ARNT2 and the endosomal trafficking protein RME-8. ARNT2 was expressed in microglia and splenocytes. LPS and IFN- γ were both shown to independently upregulate ARNT2 expression in microglia. In EAE-induced mice, ARNT2 expression decreased in splenocytes of CFA immunized and EAE mice in comparison to healthy control spleens. Taken together, our work suggests that ARNT2 expression is differentially immunoregulated in microglia and also in the immune periphery, but not across all glia, as astrocytes did not respond similarly.

RME-8 was highly expressed in microglia in comparison to other cells of the CNS. RME-8 mutant knock-in microglia showed no change in expression of phenotypic markers CD11b, CD11c, and CD45, and inflammatory markers CD39, CD40, CD80, and CD86 in comparison to wild type microglia. This suggests that this mutation in RME-8 does not seem to influence the inflammatory potential of microglia. However, the receptor-mediated phagocytosis of Oregon Green® conjugated dextran, a ligand of the mannose receptor, was decreased in RME-8 mutant knock-in microglia. This suggests that RME-8 plays a functional role in antigen-uptake and processing in microglia via the mannose receptor.

5.2 Impact

Previously established protocols for culturing microglia relied on a considerable starting amount of nervous tissue in order to yield a relatively small culture of microglia. This considerably hinders the studies that can be conducted using microglia. Our novel method of adding GM-CSF, a growth factor of myeloid derived cells, when culturing primary microglia

overcame these limitations and allowed for large, pure yields of microglia to be cultured. As well, our method for culturing microglia suggests a relatively non-differentiated phenotype in comparison to microglial cell lines. The BV-2 cell line had a constitutively higher expression of CD86 and a low secretion of IL-6 and IL-10 further highlighting the differences in their response to inflammatory mediators in comparison to primary microglia.

We are the first to have characterized the expression of ARNT2 and some means by which it is regulated in glia. ARNT2 expression was significantly enhanced in EAE mouse astrocytes. To our knowledge, our study is the first to describe the expression of ARNT2 in immune cells and how it may be regulated. LPS and IFN- γ increased ARNT2 expression in microglia. In both EAE and CFA treated mouse spleens, ARNT2 expression was decreased in comparison to healthy controls. We found that a few select inflammatory mediators could drive ARNT2 expression, which suggests a role for the protein in immune cell responses to the activation of the adaptive and innate immune systems. IFN- γ is primarily secreted by T_H1 cells, cytotoxic T cells, and NK cells suggesting that IFN- γ mediated upregulation of ARNT2 in microglia is a response to the activation of the adaptive immune system where microglia stimulated secondary to T cell activation¹⁹⁹. LPS, a component of gram-negative bacterial cell walls, would bind directly and signal through TLR-4 of microglia during infections of the CNS, activating the innate immune response²⁰⁰. Targeting ARNT2 and its functional role in transcription could improve the transcription of neuroprotective factors, such as BDNF, important to neuronal health, subsequently improving axonal stability, limiting disease severity, and slowing or halting onset and progression of neurodegenerative diseases.

Similarly, this is the first in-depth study of RME-8 and its role within cells of the CNS. We demonstrated RME-8 plays a role in microglial phagocytosis, and believe the targeting of the

RME-8 pathway could help improve the efficacy of microglial clearance of cellular debris and repair of lesions in various neurodegenerative diseases, traumas, and infections. RME-8 could potentially also play a role in neurodevelopment where synaptic pruning by phagocytosis is crucial for neuronal function^{128,129}.

Microglia and astrocytes are two glial cells that have been shown to play a crucial role in the repair and restoration of the CNS after injury. ARNT2 and RME-8 are two possible neuroprotective proteins that function through the transcription of the neuronal growth factor BDNF and the uptake and regulation of the endosomal pathway respectively. The ubiquitous expression of ARNT2 and RME-8 throughout the CNS suggests an important role for these proteins in cellular function. This study is novel as it is the first to characterize the expression of both proteins in microglia and astrocytes and their possible role in neuroprotection by limiting disease onset and progression *in vivo* and *in vitro*. By furthering our understanding of basic repair processes in the CNS, we are better able to target and enhance these pathways with novel therapeutics to help influence the onset and progression of disease.

References

- 1 Kandel, E. R., Schwartz, J. H. & Jessell, T. M. *Principles of neural science*. Vol. 4 (McGraw-hill New York, 2000).
- 2 Verkhratsky, A. & Butt, A. M. *Glial physiology and pathophysiology*. (John Wiley & Sons, 2013).
- 3 Lawson, L., Perry, V. & Gordon, S. Turnover of resident microglia in the normal adult mouse brain. *Neuroscience* **48**, 405-415 (1992).
- 4 Ginhoux, F., Lim, S., Hoeffel, G., Low, D. & Huber, T. Origin and differentiation of microglia. *Never-resting microglia: physiological roles in the healthy brain and pathological implications*, 6 (2015).
- 5 Alliot, F., Godin, I. & Pessac, B. Microglia derive from progenitors, originating from the yolk sac, and which proliferate in the brain. *Developmental Brain Research* **117**, 145-152 (1999).
- 6 Aloisi, F. Immune function of microglia. *Glia* **36**, 165-179 (2001).
- 7 Dougherty, K. D., Dreyfus, C. F. & Black, I. B. Brain-derived neurotrophic factor in astrocytes, oligodendrocytes, and microglia/macrophages after spinal cord injury. *Neurobiology of disease* **7**, 574-585 (2000).
- 8 Hartline, D. K. What is myelin? *Neuron glia biology* **4**, 153-163 (2008).
- 9 Iliff, J. J. *et al.* A paravascular pathway facilitates CSF flow through the brain parenchyma and the clearance of interstitial solutes, including amyloid β . *Science translational medicine* **4**, 147ra111-147ra111 (2012).
- 10 Hartfuss, E., Galli, R., Heins, N. & Götz, M. Characterization of CNS precursor subtypes and radial glia. *Developmental biology* **229**, 15-30 (2001).
- 11 Zlokovic, B. V. The blood-brain barrier in health and chronic neurodegenerative disorders. *Neuron* **57**, 178-201 (2008).
- 12 Abbott, N. J., Rönnbäck, L. & Hansson, E. Astrocyte–endothelial interactions at the blood–brain barrier. *Nature Reviews Neuroscience* **7**, 41-53 (2006).
- 13 Chung, W.-S., Allen, N. J. & Eroglu, C. Astrocytes control synapse formation, function, and elimination. *Cold Spring Harbor perspectives in biology* **7**, a020370 (2015).
- 14 Dringen, R., Gebhardt, R. & Hamprecht, B. Glycogen in astrocytes: possible function as lactate supply for neighboring cells. *Brain research* **623**, 208-214 (1993).
- 15 Brown, A. M. & Ransom, B. R. Astrocyte glycogen and brain energy metabolism. *Glia* **55**, 1263-1271 (2007).
- 16 Walz, W. Role of astrocytes in the clearance of excess extracellular potassium. *Neurochemistry international* **36**, 291-300 (2000).
- 17 Pekny, M. & Nilsson, M. Astrocyte activation and reactive gliosis. *Glia* **50**, 427-434 (2005).
- 18 Teismann, P. & Schulz, J. B. Cellular pathology of Parkinson's disease: astrocytes, microglia and inflammation. *Cell and tissue research* **318**, 149-161 (2004).
- 19 Eddleston, M. & Mucke, L. Molecular profile of reactive astrocytes—implications for their role in neurologic disease. *Neuroscience* **54**, 15-36 (1993).
- 20 Sofroniew, M. V. & Vinters, H. V. Astrocytes: biology and pathology. *Acta neuropathologica* **119**, 7-35 (2010).

- 21 Ito, D. *et al.* Microglia-specific localisation of a novel calcium binding protein, Iba1. *Molecular brain research* **57**, 1-9 (1998).
- 22 Ferrer, I., Bernet, E., Soriano, E., Del Rio, T. & Fonseca, M. Naturally occurring cell death in the cerebral cortex of the rat and removal of dead cells by transitory phagocytes. *Neuroscience* **39**, 451-458 (1990).
- 23 Davalos, D. *et al.* ATP mediates rapid microglial response to local brain injury in vivo. *Nature neuroscience* **8**, 752-758 (2005).
- 24 Banati, R. B., Gehrmann, J., Schubert, P. & Kreutzberg, G. W. Cytotoxicity of microglia. *Glia* **7**, 111-118 (1993).
- 25 Boje, K. M. & Arora, P. K. Microglial-produced nitric oxide and reactive nitrogen oxides mediate neuronal cell death. *Brain research* **587**, 250-256 (1992).
- 26 Neumann, H., Kotter, M. & Franklin, R. Debris clearance by microglia: an essential link between degeneration and regeneration. *Brain* **132**, 288-295 (2009).
- 27 Mrak, R. E. & Griffin, W. S. T. Glia and their cytokines in progression of neurodegeneration. *Neurobiology of aging* **26**, 349-354 (2005).
- 28 Liu, J. *et al.* Immobilization stress causes oxidative damage to lipid, protein, and DNA in the brain of rats. *The FASEB journal* **10**, 1532-1538 (1996).
- 29 Clark, S. C. & Kamen, R. The human hematopoietic colony-stimulating factors. *Science* **236**, 1229-1237 (1987).
- 30 Williams, G. T., Smith, C. A., Spooner, E., Dexter, T. M. & Taylor, D. R. Haemopoietic colony stimulating factors promote cell survival by suppressing apoptosis. (1990).
- 31 Inaba, K. *et al.* Generation of large numbers of dendritic cells from mouse bone marrow cultures supplemented with granulocyte/macrophage colony-stimulating factor. *The Journal of experimental medicine* **176**, 1693-1702 (1992).
- 32 Heufler, C. *et al.* Interleukin-12 is produced by dendritic cells and mediates T helper 1 development as well as interferon- γ production by T helper 1 cells. *European journal of immunology* **26**, 659-668 (1996).
- 33 Migliore, L. & Coppedè, F. Environmental-induced oxidative stress in neurodegenerative disorders and aging. *Mutation Research/Genetic Toxicology and Environmental Mutagenesis* **674**, 73-84 (2009).
- 34 Ross, C. A. & Poirier, M. A. Protein aggregation and neurodegenerative disease. (2004).
- 35 Varkey, J. *et al.* Membrane curvature induction and tubulation are common features of synucleins and apolipoproteins. *Journal of Biological Chemistry* **285**, 32486-32493 (2010).
- 36 Ermak, G. & Davies, K. J. Calcium and oxidative stress: from cell signaling to cell death. *Molecular immunology* **38**, 713-721 (2002).
- 37 Kujoth, G. *et al.* Mitochondrial DNA mutations, oxidative stress, and apoptosis in mammalian aging. *Science* **309**, 481-484 (2005).
- 38 Beal, M. F. Energetics in the pathogenesis of neurodegenerative diseases. *Trends in neurosciences* **23**, 298-304 (2000).
- 39 Newcombe, J. *et al.* Glutamate receptor expression in multiple sclerosis lesions. *Brain Pathology* **18**, 52-61 (2008).
- 40 Trapp, B. D. & Nave, K.-A. Multiple sclerosis: an immune or neurodegenerative disorder? *Annu. Rev. Neurosci.* **31**, 247-269 (2008).

- 41 Dixit, R., Ross, J. L., Goldman, Y. E. & Holzbaur, E. L. Differential regulation of dynein
and kinesin motor proteins by tau. *Science* **319**, 1086-1089 (2008).
- 42 Hirokawa, N. Kinesin and dynein superfamily proteins and the mechanism of organelle
transport. *Science* **279**, 519-526 (1998).
- 43 Raff, M. C., Whitmore, A. V. & Finn, J. T. Axonal self-destruction and
neurodegeneration. *Science* **296**, 868-871 (2002).
- 44 Thameem Dheen, S., Kaur, C. & Ling, E.-A. Microglial activation and its implications in
the brain diseases. *Current medicinal chemistry* **14**, 1189-1197 (2007).
- 45 Saijo, K. & Glass, C. K. Microglial cell origin and phenotypes in health and disease.
Nature Reviews Immunology **11**, 775-787 (2011).
- 46 Lenzlinger, P. M., Morganti-Kossmann, M.-C., Laurer, H. L. & McIntosh, T. K. The
duality of the inflammatory response to traumatic brain injury. *Molecular neurobiology*
24, 169-181 (2001).
- 47 Ubogu, E. E., Cossoy, M. B. & Ransohoff, R. M. The expression and function of
chemokines involved in CNS inflammation. *Trends in pharmacological sciences* **27**, 48-
55 (2006).
- 48 Lee, Y. B., Nagai, A. & Kim, S. U. Cytokines, chemokines, and cytokine receptors in
human microglia. *Journal of neuroscience research* **69**, 94-103 (2002).
- 49 Lucas, S. M., Rothwell, N. J. & Gibson, R. M. The role of inflammation in CNS injury
and disease. *British journal of pharmacology* **147**, S232-S240 (2006).
- 50 Rogers, J. *et al.* Complement activation by beta-amyloid in Alzheimer disease.
Proceedings of the National Academy of Sciences **89**, 10016-10020 (1992).
- 51 Gay, D. & Esiri, M. Blood-brain barrier damage in acute multiple sclerosis plaques.
Brain **114**, 557-572 (1991).
- 52 Abbott, N. J. Inflammatory mediators and modulation of blood-brain barrier
permeability. *Cellular and molecular neurobiology* **20**, 131-147 (2000).
- 53 Greter, M. *et al.* Dendritic cells permit immune invasion of the CNS in an animal model
of multiple sclerosis. *Nature medicine* **11**, 328-334 (2005).
- 54 Lee, J.-K., Tran, T. & Tansey, M. G. Neuroinflammation in Parkinson's disease. *Journal
of Neuroimmune Pharmacology* **4**, 419-429 (2009).
- 55 McGeer, P., Akiyama, H., Itagaki, S. & McGeer, E. Immune system response in
Alzheimer's disease. *Canadian Journal of Neurological Sciences/Journal Canadien des
Sciences Neurologiques* **16**, 516-527 (1989).
- 56 Faulkner, J. R. *et al.* Reactive astrocytes protect tissue and preserve function after spinal
cord injury. *The Journal of Neuroscience* **24**, 2143-2155 (2004).
- 57 Olah, M. *et al.* Identification of a microglia phenotype supportive of remyelination. *Glia*
60, 306-321 (2012).
- 58 Frohman, E. M., Racke, M. K. & Raine, C. S. Multiple sclerosis—the plaque and its
pathogenesis. *New England Journal of Medicine* **354**, 942-955 (2006).
- 59 Koch-Henriksen, N. & Sørensen, P. S. The changing demographic pattern of multiple
sclerosis epidemiology. *The Lancet Neurology* **9**, 520-532 (2010).
- 60 Orton, S.-M. *et al.* Sex ratio of multiple sclerosis in Canada: a longitudinal study. *The
Lancet Neurology* **5**, 932-936 (2006).
- 61 Thacker, E. L., Mirzaei, F. & Ascherio, A. Infectious mononucleosis and risk for multiple
sclerosis: A meta-analysis. *Annals of neurology* **59**, 499-503 (2006).

- 62 Caillier, S. J. *et al.* Uncoupling the roles of HLA-DRB1 and HLA-DRB5 genes in multiple sclerosis. *The Journal of Immunology* **181**, 5473-5480 (2008).
- 63 Riise, T., Nortvedt, M. W. & Ascherio, A. Smoking is a risk factor for multiple sclerosis. *Neurology* **61**, 1122-1124 (2003).
- 64 Giovannoni, G. *et al.* Infectious causes of multiple sclerosis. *The Lancet Neurology* **5**, 887-894 (2006).
- 65 Marrie, R. A. Environmental risk factors in multiple sclerosis aetiology. *The Lancet Neurology* **3**, 709-718 (2004).
- 66 Olsson, T. *et al.* Autoreactive T lymphocytes in multiple sclerosis determined by antigen-induced secretion of interferon-gamma. *Journal of Clinical Investigation* **86**, 981 (1990).
- 67 Bitsch, A. *et al.* Tumour necrosis factor alpha mRNA expression in early multiple sclerosis lesions: correlation with demyelinating activity and oligodendrocyte pathology. *Glia* **29**, 366-375 (2000).
- 68 Ruuls, S. R. *et al.* Reactive oxygen species are involved in the pathogenesis of experimental allergic encephalomyelitis in Lewis rats. *Journal of neuroimmunology* **56**, 207-217 (1995).
- 69 Sospedra, M. & Martin, R. Immunology of multiple sclerosis*. *Annu. Rev. Immunol.* **23**, 683-747 (2005).
- 70 Benveniste, E. N. Cytokine actions in the central nervous system. *Cytokine & growth factor reviews* **9**, 259-275 (1998).
- 71 Chari, D. M. Remyelination in multiple sclerosis. *International review of neurobiology* **79**, 589-620 (2007).
- 72 Li, H., Newcombe, J., Groome, N. & Cuzner, M. Characterization and distribution of phagocytic macrophages in multiple sclerosis plaques. *Neuropathology and applied neurobiology* **19**, 214-223 (1993).
- 73 Bö, L. *et al.* Detection of MHC class II-antigens on macrophages and microglia, but not on astrocytes and endothelia in active multiple sclerosis lesions. *Journal of neuroimmunology* **51**, 135-146 (1994).
- 74 Satoh, J.-i., Lee, Y. B. & Kim, S. U. T-cell costimulatory molecules B7-1 (CD80) and B7-2 (CD86) are expressed in human microglia but not in astrocytes in culture. *Brain research* **704**, 92-96 (1995).
- 75 Steimle, V., Siegrist, C.-A., Mottet, A., Lisowska-Grospierre, B. & Mach, B. Regulation of MHC class II expression by interferon-gamma mediated by the transactivator gene CIITA. *Science* **265**, 106-109 (1994).
- 76 Goodin, D. *et al.* Disease modifying therapies in multiple sclerosis. *Neurology* **58**, 169-178 (2002).
- 77 Kieseier, B. C. The mechanism of action of interferon- β in relapsing multiple sclerosis. *CNS drugs* **25**, 491-502 (2011).
- 78 Neuhaus, O., Farina, C., Wekerle, H. & Hohlfeld, R. Mechanisms of action of glatiramer acetate in multiple sclerosis. *Neurology* **56**, 702-708 (2001).
- 79 Begum-Haque, S. *et al.* Downregulation of IL-17 and IL-6 in the central nervous system by glatiramer acetate in experimental autoimmune encephalomyelitis. *Journal of neuroimmunology* **204**, 58-65 (2008).
- 80 Rudick, R. A. & Sandrock, A. Natalizumab: α 4-integrin antagonist selective adhesion molecule inhibitors for MS. *Expert review of neurotherapeutics* **4**, 571-580 (2004).

- 81 Gunnarsson, M. *et al.* Axonal damage in relapsing multiple sclerosis is markedly reduced by natalizumab. *Annals of neurology* **69**, 83-89 (2011).
- 82 Polman, C. H. *et al.* A randomized, placebo-controlled trial of natalizumab for relapsing multiple sclerosis. *New England Journal of Medicine* **354**, 899-910 (2006).
- 83 O'Connor, P. *et al.* Oral fingolimod (FTY720) in multiple sclerosis Two-year results of a phase II extension study. *Neurology* **72**, 73-79 (2009).
- 84 Hartung, H.-P. *et al.* Mitoxantrone in progressive multiple sclerosis: a placebo-controlled, double-blind, randomised, multicentre trial. *The Lancet* **360**, 2018-2025 (2002).
- 85 Kleinschmidt-DeMasters, B. & Tyler, K. L. Progressive multifocal leukoencephalopathy complicating treatment with natalizumab and interferon beta-1a for multiple sclerosis. *New England Journal of Medicine* **353**, 369-374 (2005).
- 86 Ghalie, R. *et al.* Cardiac adverse effects associated with mitoxantrone (Novantrone) therapy in patients with MS. *Neurology* **59**, 909-913 (2002).
- 87 Kappos, L. *et al.* Ocrelizumab in relapsing-remitting multiple sclerosis: a phase 2, randomised, placebo-controlled, multicentre trial. *The Lancet* **378**, 1779-1787 (2011).
- 88 Hu, Y. *et al.* Investigation of the mechanism of action of alemtuzumab in a human CD52 transgenic mouse model. *Immunology* **128**, 260-270 (2009).
- 89 Coles, A. J. *et al.* Alemtuzumab for patients with relapsing multiple sclerosis after disease-modifying therapy: a randomised controlled phase 3 trial. *The lancet* **380**, 1829-1839 (2012).
- 90 Hemmer, B. & Hartung, H. P. Toward the development of rational therapies in multiple sclerosis: what is on the horizon? *Annals of neurology* **62**, 314-326 (2007).
- 91 Maghzi, A.-H., Minagar, A. & Waubant, E. Neuroprotection in multiple sclerosis: a therapeutic approach. *CNS drugs* **27**, 799-815 (2013).
- 92 Pender, M. P. Experimental autoimmune encephalomyelitis. (1995).
- 93 Stromnes, I. M. & Goverman, J. M. Passive induction of experimental allergic encephalomyelitis. *Nature protocols* **1**, 1952-1960 (2006).
- 94 Rao, P. & Segal, B. M. Experimental autoimmune encephalomyelitis. *Autoimmunity: Methods and Protocols*, 363-375 (2004).
- 95 Constantinescu, C. S., Farooqi, N., O'Brien, K. & Gran, B. Experimental autoimmune encephalomyelitis (EAE) as a model for multiple sclerosis (MS). *British journal of pharmacology* **164**, 1079-1106 (2011).
- 96 Gold, R., Linington, C. & Lassmann, H. Understanding pathogenesis and therapy of multiple sclerosis via animal models: 70 years of merits and culprits in experimental autoimmune encephalomyelitis research. *Brain* **129**, 1953-1971 (2006).
- 97 Lassmann, H. Axonal and neuronal pathology in multiple sclerosis: what have we learnt from animal models. *Experimental neurology* **225**, 2-8 (2010).
- 98 McCarthy, D. P., Richards, M. H. & Miller, S. D. Mouse models of multiple sclerosis: experimental autoimmune encephalomyelitis and Theiler's virus-induced demyelinating disease. *Autoimmunity: Methods and Protocols*, 381-401 (2012).
- 99 Friese, M. A. & Fugger, L. Pathogenic CD8+ T cells in multiple sclerosis. *Annals of neurology* **66**, 132-141 (2009).
- 100 Huseby, E. S., Huseby, P. G., Shah, S., Smith, R. & Stadinski, B. D. Pathogenic CD8T cells in multiple sclerosis and its experimental models. *The Molecular Mechanisms of Chronic Inflammation Development*, 22 (2012).

- 101 Maisonpierre, P. C. *et al.* NT-3, BDNF, and NGF in the developing rat nervous system:
parallel as well as reciprocal patterns of expression. *Neuron* **5**, 501-509 (1990).
- 102 Lindsay, R. M. & Harmar, A. J. Nerve growth factor regulates expression of
neuropeptide genes in adult sensory neurons. *Nature* **337**, 362-364 (1989).
- 103 Lin, L. F., Doherty, D. H., Lile, J. D., Bektesh, S. & Collins, F. GDNF: a glial cell line-
derived neurotrophic factor for midbrain dopaminergic neurons. *Science* **260**, 1130-1132
(1993).
- 104 Kotzbauer, P. T. *et al.* Neurturin, a relative of glial-cell-line-derived neurotrophic factor.
Nature **384**, 467-470 (1996).
- 105 Sendtner, M., Carrol, P., Holtmann, B., Hughes, R. & Thoenen, H. Ciliary neurotrophic
factor. *Journal of neurobiology* **25**, 1436-1453 (1994).
- 106 Thoenen, H. Ciliary neurotrophic factor prevents the degeneration of motor neurons after
axotomy. *Nature* **345**, 31 (1990).
- 107 Lee, R., Kermani, P., Teng, K. K. & Hempstead, B. L. Regulation of cell survival by
secreted proneurotrophins. *Science* **294**, 1945-1948 (2001).
- 108 Ooe, N., Saito, K., Mikami, N., Nakatuka, I. & Kaneko, H. Identification of a novel basic
helix-loop-helix-PAS factor, NXF, reveals a Sim2 competitive, positive regulatory role in
dendritic-cytoskeleton modulator drebrin gene expression. *Molecular and cellular
biology* **24**, 608-616 (2004).
- 109 Kewley, R. J., Whitelaw, M. L. & Chapman-Smith, A. The mammalian basic helix-loop-
helix/PAS family of transcriptional regulators. *The international journal of biochemistry
& cell biology* **36**, 189-204 (2004).
- 110 Pruunsild, P., Sepp, M., Orav, E., Koppel, I. & Timmusk, T. Identification of cis-
elements and transcription factors regulating neuronal activity-dependent transcription of
human BDNF gene. *The Journal of Neuroscience* **31**, 3295-3308 (2011).
- 111 Hyman, C. *et al.* BDNF is a neurotrophic factor for dopaminergic neurons of the
substantia nigra. *Nature* **350**, 230-232 (1991).
- 112 Stadelmann, C. *et al.* BDNF and gp145trkB in multiple sclerosis brain lesions:
neuroprotective interactions between immune and neuronal cells? *Brain* **125**, 75-85
(2002).
- 113 Linker, R. A. *et al.* Functional role of brain-derived neurotrophic factor in
neuroprotective autoimmunity: therapeutic implications in a model of multiple sclerosis.
Brain **133**, 2248-2263 (2010).
- 114 Jain, S., Maltepe, E., Lu, M. M., Simon, C. & Bradfield, C. A. Expression of ARNT,
ARNT2, HIF1 α , HIF2 α and Ah receptor mRNAs in the developing mouse. *Mechanisms
of development* **73**, 117-123 (1998).
- 115 Drutel, G. *et al.* ARNT2, a transcription factor for brain neuron survival? *European
Journal of Neuroscience* **11**, 1545-1553 (1999).
- 116 Maltepe, E., Keith, B., Arsham, A. M., Brorson, J. R. & Simon, M. C. The role of
ARNT2 in tumor angiogenesis and the neural response to hypoxia. *Biochemical and
biophysical research communications* **273**, 231-238 (2000).
- 117 Miron, V. E. *et al.* M2 microglia and macrophages drive oligodendrocyte differentiation
during CNS remyelination. *Nature neuroscience* **16**, 1211-1218 (2013).
- 118 Napoli, I. & Neumann, H. Microglial clearance function in health and disease.
Neuroscience **158**, 1030-1038 (2009).

- 119 Girard, M. & McPherson, P. S. RME-8 regulates trafficking of the epidermal growth factor receptor. *FEBS letters* **582**, 961-966 (2008).
- 120 Vilariño-Güell, C. *et al.* DNAJC13 mutations in Parkinson disease. *Human molecular genetics* **23**, 1794-1801 (2014).
- 121 Rajput, A. *et al.* VPS35 and DNAJC13 disease-causing variants in essential tremor. *European Journal of Human Genetics* **23**, 887-888 (2015).
- 122 Girard, M., Poupon, V., Blondeau, F. & McPherson, P. S. The DnaJ-domain protein RME-8 functions in endosomal trafficking. *Journal of Biological Chemistry* **280**, 40135-40143 (2005).
- 123 Popoff, V. *et al.* Analysis of articulation between clathrin and retromer in retrograde sorting on early endosomes. *Traffic* **10**, 1868-1880 (2009).
- 124 Zhang, Y., Grant, B. & Hirsh, D. RME-8, a conserved J-domain protein, is required for endocytosis in *Caenorhabditis elegans*. *Molecular Biology of the Cell* **12**, 2011-2021 (2001).
- 125 González, H., Elgueta, D., Montoya, A. & Pacheco, R. Neuroimmune regulation of microglial activity involved in neuroinflammation and neurodegenerative diseases. *Journal of neuroimmunology* **274**, 1-13 (2014).
- 126 Garden, G. A. & Möller, T. Microglia biology in health and disease. *Journal of Neuroimmune Pharmacology* **1**, 127-137 (2006).
- 127 Elkabes, S., DiCicco-Bloom, E. M. & Black, I. B. Brain microglia/macrophages express neurotrophins that selectively regulate microglial proliferation and function. *The journal of neuroscience* **16**, 2508-2521 (1996).
- 128 Paolicelli, R. C. *et al.* Synaptic pruning by microglia is necessary for normal brain development. *Science* **333**, 1456-1458 (2011).
- 129 Huttenlocher, P. R. Synaptic density in human frontal cortex—developmental changes and effects of aging. *Brain Res* **163**, 195-205 (1979).
- 130 Popovich, P. G., Wei, P. & Stokes, B. T. Cellular inflammatory response after spinal cord injury in sprague-dawley and lewis rats. *Journal of Comparative Neurology* **377**, 443-464 (1997).
- 131 Jackson-Lewis, V. *et al.* Blockade of microglial activation is neuroprotective in the 1-methyl-4-phenyl-1, 2, 3, 6-tetrahydropyridine mouse model of Parkinson disease. *The Journal of Neuroscience* **22**, 1763-1771 (2002).
- 132 Barger, S. W. & Harmon, A. D. Microglial activation by Alzheimer amyloid precursor protein and modulation by apolipoprotein E. *Nature* **388**, 878-881 (1997).
- 133 Hall, E. D., Oostveen, J. A. & Gurney, M. E. Relationship of microglial and astrocytic activation to disease onset and progression in a transgenic model of familial ALS. *Glia* **23**, 249-256 (1998).
- 134 Wake, H., Moorhouse, A. J., Miyamoto, A. & Nabekura, J. Microglia: actively surveying and shaping neuronal circuit structure and function. *Trends in neurosciences* **36**, 209-217 (2013).
- 135 Kreutzberg, G. W. Microglia: a sensor for pathological events in the CNS. *Trends in neurosciences* **19**, 312-318 (1996).
- 136 Blasi, E., Barluzzi, R., Bocchini, V., Mazzolla, R. & Bistoni, F. immortalization of murine microglial cells by a v-raf/v-myc carrying retrovirus. *Journal of neuroimmunology* **27**, 229-237 (1990).

- 137 Cheepsunthorn, P., Radov, L., Menzies, S., Reid, J. & Connor, J. R. Characterization of a novel brain-derived microglial cell line isolated from neonatal rat brain. *Glia* **35**, 53-62 (2001).
- 138 Häusler, K. G. *et al.* Interferon- γ differentially modulates the release of cytokines and chemokines in lipopolysaccharide- and pneumococcal cell wall-stimulated mouse microglia and macrophages. *European Journal of Neuroscience* **16**, 2113-2122 (2002).
- 139 De Jong, E. K. *et al.* Expression of CXCL4 in microglia in vitro and in vivo and its possible signaling through CXCR3. *Journal of neurochemistry* **105**, 1726-1736 (2008).
- 140 Horvath, R. J., Nutile-McMenemy, N., Alkaitis, M. S. & DeLeo, J. A. Differential migration, LPS-induced cytokine, chemokine, and NO expression in immortalized BV-2 and HAPI cell lines and primary microglial cultures. *Journal of neurochemistry* **107**, 557-569 (2008).
- 141 Giulian, D. & Baker, T. J. Characterization of amoeboid microglia isolated from developing mammalian brain. *The Journal of neuroscience* **6**, 2163-2178 (1986).
- 142 Cardona, A. E., Huang, D., Sasse, M. E. & Ransohoff, R. M. Isolation of murine microglial cells for RNA analysis or flow cytometry. *Nature protocols* **1**, 1947-1951 (2006).
- 143 Metcalf, D. The molecular biology and functions of the granulocyte-macrophage colony-stimulating factors. *Blood* **67**, 257-267 (1986).
- 144 Fukunaga, R., Ishizaka-Ikeda, E. & Nagata, S. Growth and differentiation signals mediated by different regions in the cytoplasmic domain of granulocyte colony-stimulating factor receptor. *Cell* **74**, 1079-1087 (1993).
- 145 Souza, L. M. *et al.* Recombinant human granulocyte colony-stimulating factor: effects on normal and leukemic myeloid cells. *Science* **232**, 61-65 (1986).
- 146 Labour, M. S. *et al.* Generation of tumor immunity by bone marrow-derived dendritic cells correlates with dendritic cell maturation stage. *The Journal of Immunology* **162**, 168-175 (1999).
- 147 Lu, L., McCaslin, D., Starzl, T. E. & Thomson, A. W. BONE MARROW-DERIVED DENDRITIC CELL PROGENITORS (NLDC 145+, MHC CLASS II+, B7-1dim, B7-2-) INDUCE ALLOANTIGEN-SPECIFIC HYPORESPONSIVENESS IN MURINE T LYMPHOCYTES. *Transplantation* **60**, 1539 (1995).
- 148 Aiga, M., Levinson, J. N. & Bamji, S. X. N-cadherin and neuroligins cooperate to regulate synapse formation in hippocampal cultures. *Journal of Biological Chemistry* **286**, 851-858 (2011).
- 149 Qin, K. *et al.* A much convenient and economical method to harvest a great number of microglia. *Cellular and molecular neurobiology* **32**, 67-75 (2012).
- 150 Moghaddami, M., Mayrhofer, G. & Cleland, L. G. MHC class II compartment, endocytosis and phagocytic activity of macrophages and putative dendritic cells isolated from normal tissues rich in synovium. *International immunology* **17**, 1117-1130 (2005).
- 151 Ford, A. L., Goodsall, A. L., Hickey, W. F. & Sedgwick, J. D. Normal adult ramified microglia separated from other central nervous system macrophages by flow cytometric sorting. Phenotypic differences defined and direct ex vivo antigen presentation to myelin basic protein-reactive CD4+ T cells compared. *The Journal of Immunology* **154**, 4309-4321 (1995).

- 152 Becher, B. & Antel, J. P. Comparison of phenotypic and functional properties of
immediately ex vivo and cultured human adult microglia. *Glia* **18**, 1-10 (1996).
- 153 Zaheer, A., Mathur, S. N. & Lim, R. Overexpression of glia maturation factor in
astrocytes leads to immune activation of microglia through secretion of granulocyte-
macrophage-colony stimulating factor. *Biochemical and biophysical research
communications* **294**, 238-244 (2002).
- 154 Weisbart, R. H., Golde, D. W., Clark, S. C., Wong, G. G. & Gasson, J. C. Human
granulocyte-macrophage colony-stimulating factor is a neutrophil activator. *Nature* **314**,
361-363 (1984).
- 155 Melissa, A. & Lee, S. C. Human Brain Parenchymal Microglia Express CD14 and CD45
and are Productively Infected by HIV-1 in HIV-1 Encephalitis. *Brain pathology* **12**,
442-455 (2002).
- 156 Liu, D. *et al.* Anti-inflammatory effects of fluoxetine in lipopolysaccharide (LPS)-
stimulated microglial cells. *Neuropharmacology* **61**, 592-599 (2011).
- 157 Hanisch, U.-K. & Kettenmann, H. Microglia: active sensor and versatile effector cells in
the normal and pathologic brain. *Nature neuroscience* **10**, 1387-1394 (2007).
- 158 Iglesias, B. M., Cerase, J., Ceracchini, C., Levi, G. & Aloisi, F. Analysis of B7-1 and B7-
2 costimulatory ligands in cultured mouse microglia: upregulation by interferon- γ and
lipopolysaccharide and downregulation by interleukin-10, prostaglandin E 2 and cyclic
AMP-elevating agents. *Journal of neuroimmunology* **72**, 83-93 (1997).
- 159 Mantovani, A. *et al.* The chemokine system in diverse forms of macrophage activation
and polarization. *Trends in immunology* **25**, 677-686 (2004).
- 160 Bosio, C. M. *et al.* Ebola and Marburg virus-like particles activate human myeloid
dendritic cells. *Virology* **326**, 280-287 (2004).
- 161 Rico, M. Á. *et al.* Human respiratory syncytial virus infects and induces activation
markers in mouse B lymphocytes. *Immunology and cell biology* **87**, 344-350 (2009).
- 162 Buelens, C. *et al.* Interleukin-10 differentially regulates B7-1 (CD80) and B7-2
(CD86) expression on human peripheral blood dendritic cells. *European journal of
immunology* **25**, 2668-2672 (1995).
- 163 Wang, T.-F. & Guidotti, G. CD39 is an ecto-(Ca, Mg)-ATPase. *Journal of Biological
Chemistry* **271**, 9898-9901 (1996).
- 164 Braun, N. *et al.* Assignment of ecto-ATPase expression to microglia and vasculature of the brain.
European Journal of Neuroscience **12**, 4357-4366 (2000).
- 165 Färber, K. *et al.* The ectonucleotidase cd39/ENTPDase1 modulates purinergic-mediated
microglial migration. *Glia* **56**, 331-341 (2008).
- 166 Borsellino, G. *et al.* Expression of ectonucleotidase CD39 by Foxp3+ Treg cells:
hydrolysis of extracellular ATP and immune suppression. *Blood* **110**, 1225-1232 (2007).
- 167 Volonté, C. *et al.* Extracellular ATP and neurodegeneration. *Current Drug Targets-CNS
& Neurological Disorders* **2**, 403-412 (2003).
- 168 Khandelwal, P. J., Herman, A. M. & Moussa, C. E.-H. Inflammation in the early stages
of neurodegenerative pathology. *Journal of neuroimmunology* **238**, 1-11 (2011).
- 169 Färber, K. & Kettenmann, H. Purinergic signaling and microglia. *Pflügers Archiv* **452**,
615-621 (2006).

- 170 Okey, A. B., Riddick, D. S. & Harper, P. A. The Ah receptor: mediator of the toxicity of
2, 3, 7, 8-tetrachlorodibenzo-p-dioxin (TCDD) and related compounds. *Toxicology letters*
70, 1-22 (1994).
- 171 Quintana, F. J. *et al.* Control of Treg and TH17 cell differentiation by the aryl
hydrocarbon receptor. *Nature* 453, 65-71 (2008).
- 172 Veldhoen, M. *et al.* The aryl hydrocarbon receptor links TH17-cell-mediated
autoimmunity to environmental toxins. *Nature* 453, 106-109 (2008).
- 173 Drutel, G., Kathmann, M., Heron, A., Schwartz, J.-C. & Arrang, J.-M. Cloning and
selective expression in brain and kidney of ARNT2 homologous to the Ah receptor
nuclear translocator (ARNT). *Biochemical and biophysical research communications*
225, 333-339 (1996).
- 174 Michaud, J. L., DeRossi, C., May, N. R., Holdener, B. C. & Fan, C.-M. ARNT2 acts as
the dimerization partner of SIM1 for the development of the hypothalamus. *Mechanisms
of development* 90, 253-261 (2000).
- 175 Walz, W. & Lang, M. K. Immunocytochemical evidence for a distinct GFAP-negative
subpopulation of astrocytes in the adult rat hippocampus. *Neuroscience letters* 257, 127-
130 (1998).
- 176 Cruz, J. D., Schmidt-Kastner, R., Stevens, J., Steinbusch, H. & Rutten, B. Differential
distribution of hypoxia-inducible factor 1-beta (ARNT or ARNT2) in mouse substantia
nigra and ventral tegmental area. *Journal of chemical neuroanatomy* 61, 64-71 (2014).
- 177 Chavez, J. C., Baranova, O., Lin, J. & Pichiule, P. The transcriptional activator hypoxia
inducible factor 2 (HIF-2/EPAS-1) regulates the oxygen-dependent expression of
erythropoietin in cortical astrocytes. *The Journal of neuroscience* 26, 9471-9481 (2006).
- 178 Miller, R. H. & Raff, M. C. Fibrous and protoplasmic astrocytes are biochemically and
developmentally distinct. *The Journal of neuroscience* 4, 585-592 (1984).
- 179 Abe, K. & Saito, H. Effect of ATP on astrocyte stellation is switched from suppressive to
stimulatory during development. *Brain research* 850, 150-157 (1999).
- 180 Goldman, J. E. & Abramson, B. Cyclic AMP-induced shape changes of astrocytes are
accompanied by rapid depolymerization of actin. *Brain research* 528, 189-196 (1990).
- 181 Hosoya, T. *et al.* Defective development of secretory neurones in the hypothalamus of
Arnt2 \square knockout mice. *Genes to Cells* 6, 361-374 (2001).
- 182 Freeman, C. L., Hesketh, G. & Seaman, M. N. RME-8 coordinates the activity of the
WASH complex with the function of the retromer SNX dimer to control endosomal
tubulation. *J Cell Sci* 127, 2053-2070 (2014).
- 183 Gomez-Lamarca, M. J., Snowdon, L. A., Seib, E., Klein, T. & Bray, S. J. Rme-8
depletion perturbs Notch recycling and predisposes to pathogenic signaling. *The Journal
of cell biology* 210, 303-318 (2015).
- 184 Tanigaki, K. *et al.* Notch1 and Notch3 instructively restrict bFGF-responsive multipotent
neural progenitor cells to an astroglial fate. *Neuron* 29, 45-55 (2001).
- 185 Chambers, C. B. *et al.* Spatiotemporal selectivity of response to Notch1 signals in
mammalian forebrain precursors. *Development* 128, 689-702 (2001).
- 186 Gaiano, N., Nye, J. S. & Fishell, G. Radial glial identity is promoted by Notch1 signaling
in the murine forebrain. *Neuron* 26, 395-404 (2000).
- 187 Weksler, B. *et al.* Blood-brain barrier-specific properties of a human adult brain
endothelial cell line. *The FASEB journal* 19, 1872-1874 (2005).

- 188 Madden, T. The BLAST sequence analysis tool. (2013).
- 189 Kato, M. *et al.* Expression of multilectin receptors and comparative FITC–dextran uptake by human dendritic cells. *International Immunology* **12**, 1511-1519 (2000).
- 190 Hackstein, H., Taner, T., Logar, A. J. & Thomson, A. W. Rapamycin inhibits macropinocytosis and mannose receptor–mediated endocytosis by bone marrow–derived dendritic cells. *Blood* **100**, 1084-1087 (2002).
- 191 Schlesinger, P. H. *et al.* Plasma clearance of glycoproteins with terminal mannose and N-acetylglucosamine by liver non-parenchymal cells. Studies with β -glucuronidase, N-acetyl- β -d-glucosaminidase, ribonuclease B and agalacto-orosomucoid. *Biochemical Journal* **176**, 103-109 (1978).
- 192 Stahl, P., Schlesinger, P. H., Sigardson, E., Rodman, J. S. & Lee, Y. Receptor-mediated pinocytosis of mannose glycoconjugates by macrophages: characterization and evidence for receptor recycling. *Cell* **19**, 207-215 (1980).
- 193 Stahl, P. D. & Ezekowitz, R. A. B. The mannose receptor is a pattern recognition receptor involved in host defense. *Current opinion in immunology* **10**, 50-55 (1998).
- 194 Tan, M. *et al.* Mannose receptor–mediated uptake of antigens strongly enhances HLA class II–restricted antigen presentation by cultured dendritic cells. *European journal of immunology* **27**, 2426-2435 (1997).
- 195 Johns, T. G. & Bernard, C. C. The structure and function of myelin oligodendrocyte glycoprotein. *Journal of neurochemistry* **72**, 1-9 (1999).
- 196 Mosley, K. & Cuzner, M. Receptor-mediated phagocytosis of myelin by macrophages and microglia: effect of opsonization and receptor blocking agents. *Neurochemical research* **21**, 481-487 (1996).
- 197 Kuchroo, V. K. *et al.* T cell response in experimental autoimmune encephalomyelitis (EAE): role of self and cross-reactive antigens in shaping, tuning, and regulating the autopathogenic T cell repertoire. *Annual review of immunology* **20**, 101-123 (2002).
- 198 Holness, C. L. & Simmons, D. L. Molecular cloning of CD68, a human macrophage marker related to lysosomal glycoproteins. *Blood* **81**, 1607-1613 (1993).
- 199 Szabo, S. J. *et al.* Distinct effects of T-bet in TH1 lineage commitment and IFN- γ production in CD4 and CD8 T cells. *Science* **295**, 338-342 (2002).
- 200 Medzhitov, R. Toll-like receptors and innate immunity. *Nature Reviews Immunology* **1**, 135-145 (2001).